Energy Storage System Optimization and Control with Wind Energy

Chad Abbey

Department of Electrical & Computer Engineering
McGill University
Montreal, Canada

October 2009

A thesis submitted to McGill University in partial fulfillment of the requirements for the degree of Doctorate of Philosophy in Electrical Engineering.

2009/10/02

Abstract

This thesis proposes a methodology for planning, scheduling and on-line control of an energy storage system for the integration of wind energy. Using the case study of a remote wind-diesel system, the different time frames of the design and implementation process are detailed. First, a long-term planning approach for rating of the power and energy capacities of the ESS is presented, based on stochastic optimization. The formulation is then adapted into a hourly scheduling approach and results are compared with the expected cost of energy and energy requirements resulting from the planning study. The optimization results are used as training data for an artificial neural network, in an effort to generate an on-line control that captures inherent rules, using artificial intelligence. The ESS is realized as a two-level ESS and a general control structure for on-line operation of multi-level ESS is proposed and adapted for the wind-diesel system, as the first level in a hierarchical control. The system is evaluated in simulation and selected results are validated using a hardware-in-the-loop representation of the system, demonstrating that the proposed controller is realizable.

Résumé

Cette thèse propose une méthodologie pour la planification, l'utilisation et la commande d'un système de stockage d'énergie permettant l'intégration de l'énergie éolienne. Utilisant comme étude de cas un réseau autonome alimenté par un système éolien-diesel, les différentes étapes de la conception et la mise en oeuvre sont détaillées. Premièrement, une étude de planification à long terme pour le dimensionnement de la puissance nominale et de la capacité énergétique du stockage est présentée, basée sur les méthodes d'optimisation stochastique. La formulation est ensuite adaptée à une commande sur une base horaire et les résultats sont comparés, au niveau de l'énergie et de la quantité d'énergie utilisée, aux résultats obtenus dans l'étude de planification. Les résultats obtenus par optimisation du systéme sont utilisés dans l'entrainement d'un réseau de neurones artificiels, afin de produire une commande qui capte les règles inhérentes au système, utilisant l'intelligence artificielle. Le stockage d'énergie est réalisé par un système de stockage à deux niveaux et une structure de commande appropriée à plusieurs niveaux est proposée et adaptée pour un système éolien-diesel, comme premier niveau d'une commande hiérarchique. La performance du système est évaluée par simulation et certains résultats ont été validés avec un banc d'essai. Celui-ci consiste à des convertisseurs électroniques intégrés avec une représentation par simulation temps réel du système. Les résultats obtenus concordent avec les résultats de simulation et confirment que la commande proposée est réalisable.

Acknowledgments

First and foremost I would like to thank my supervisor Professor Géza Joos, who has taught me as much about life, living, professionalism and one's career as he has about engineering and research. He provides the student with myriad opportunities that they can choose to accept or not. Upon accepting any of these endeavors, he is there to offer advice, criticism and suggestions to guide you along the road towards success. In this way the student's potential is limited only by their own drive and determination. One who is sincerely ready to accept the challenge and the proposed method cannot but emerge with the necessary skills to be successful as a researcher and a person. For having given me the opportunity and provided guidance along the way I am forever indebted to him.

I express my thanks and appreciation for financial support through the McGill Majors J.W. McConnell Memorial Fellowship. The financial support, as well as the esteem that accompanies the award, were received with sincere gratitude and honour. The continued research stipend from Prof. Joos, supported through the National Science and Research Council of Canada, is also acknowledged.

I would also like to thank other members of the department for their contributions to the thesis, in particular to members of my committee Profs. Galiana and Giannacopoulos. Special thanks to Prof. Ooi for his constant support and efforts to promote exchange of ideas between different members of the Power Lab. Thanks to Prof. Boulet for his insights into the control problems presented herein. Thanks to Prof. Kabal for making his LaTeX thesis template available. Also, thanks to Donald McGillis and Reginald Brearley for their time spent in helping me with the initial structure of the thesis and the constructive feedback they provided.

Special thanks and appreciation to friend and colleague José Restrepo for the many interesting discussions on our complementary research topics and for his help in the development of the Matlab-GAMS interface that he so graciously put at my disposal. Many of his ideas appear in different forms in this thesis, my only hope is that half as many of mine find their way into his.

With regards to the development of the experimental set-up I must thank Johan Guzman, for really reviving the experimental side of the lab and designing and building many of the components that ultimately found their way into my set-up. Without him, the presence of experimental results would have been unlikely.

Thanks to Kyriakos Giogas, John Chahwan, Loïc Owatta, Jean Morneau, Jonathon Robinson, Carlos Martinez, Mohammed El Moursi, Kai Strunz, and Wei Li, with whom I collaborated on various projects and wrote papers with. You have shaped my thinking on research and these topics.

I am indebted to Michael Ross and Rodrigo Hidalgo Anfossi for having taken the time to proof-read my thesis and in having responded so positively to the offer to collaborate on research with me this early on in their studies. I hope that I have passed some of my knowledge onto them in the process.

Other friends and members of the Power Lab I would like to also thank include François Bouffard, Hugo Gil, Ming Zou, Khalil El Arroudi, José Manuel Arroyo, Nathalia Alguacil, Mohammed El Chehaly, and Sameh El Khatib. Although I did not have the pleasure of formally collaborating with them, they have, together with the others I have mentioned, helped make my Ph.D. studies one of the most rewarding periods of my life.

The Ontario Power Authority and the Kansas Electric Utilities Research Program should also be commended for financing the generation of wind speed and wind power databases and making this information publicly available. This was a vital part of the present research and the availability of this data as a research tool is greatly appreciated.

I would like to extend my special thanks to my employer CanmetENERGY of Natural Resources Canada for giving me the opportunity to supplement my theoretical training with valuable work experience in the industry throughout my studies. Thanks to my supervisor Dr. Lisa Dignard-Bailey for giving me the opportunity, believing in my ability to juggle these two parts of my career, and for all that she has taught me. I also had the pleasure to meet and work with some exceptional people that I benefited from. Special thanks to Farid Katiraei, Dave Turcotte, Michael Ross, and Sylvain Martel for the many fruitful discussions and support during my studies.

My family must be acknowledged for the support that they provided during these past years. My two brothers Josh and Tyler and my sister Chelsea each support me in unique ways and yet we share many common threads. The presence of Tyler in Montréal the past two years and his friendship during that time has made the final leg of the journey easier. Thanks also to Josh's wife Kelley and Tyler's girlfriend Robyn Martin, two amazing women that have given new energy to me and my family. My appreciation to my parents Bonnie and Thomas cannot properly be captured in words. They have instilled in me the fundamental values required to have a good chance of succeeding in life and subsequently

released me to the world. To date, I think things have worked out quite well.

Finally, I would like to thank Valérie Chénard, her parents, Jacques and Sylvie, and our companions William, Julia and Sarah for their love and support. Valérie is an amazing person who I have had the pleasure of accompanying me throughout a significant part of my life, helping me to grow as a person and is responsible in large part for who I am today, perhaps more than she is willing to admit. I certainly would not be the same man had she not been there and for this I dedicate this thesis to her.

Contents

List of Figures

List of Tables

List of Acronyms

AI	Artificial Intelligence
ANN	Artificial Neural Network
ARMA	Auto-Regressive Moving Average
CHP	Combined Heat and Power
DER	Distributed Energy Resources
DLC	Direct-Load Control
DSM	Demand-Side Management
EPRI	Electric Power Research Institute
ESS	Energy Storage System
EU	European Union
HIL	Hardware-in-the-loop
pdf	Probability Density Function
IEEE-RTS	IEEE Reliability Test System
LP	Linear Programming
MILP	Mixed-Integer Linear Programming
MIC	Monitoring, Information Exchange, and Control
NN	Neural Network
RTS	Real-Time Simulation
SOC	State-Of-Charge
VRB	Vanadium Redox Flow Battery
VSC	Voltage Source Converter
WR	Wind Resource
WTG	Wind Turbine Generator

List of Symbols

The following list the most important symbols used in the thesis. Where relevant, boldface is used to denote vectors or matrices.

Indices

i	Index of intrahour time periods running from 1 to I
j	Index of the wind resources running from 1 to J
k	Index of time periods running from 1 to K associated with ESS sliding window control
l	Index of years running from 1 to L
m	Index of two-level storage control modes running from 1 to M
n	Index of energy storage levels running from 1 to N
t	Index of time periods associated with ESS sizing running from 1 to T

Functions

$C_{\mathrm{d}}(\cdot)$	Daily cost of energy served function
$C_{\mathrm{intra}}(\cdot)$	Cost of energy associated with simulation of two-level storage system
$C_{\mathrm{s}}(\cdot)$	Simulated daily cost of energy served function.
$E_{\mathrm{diesel}}(\cdot)$	Diesel energy function in per unit, expressed on a base of total load energy
$E_{\mathrm{dump}}(\cdot)$	Dump load energy function in per unit, expressed on a base of total load energy
$E_{\mathrm{L}}(\cdot)$	Load energy function

$E_{\mathrm{w}}(\cdot)$	Wind energy function in per unit, expressed on a base of total load energy

Parameters

E_{ess}	Energy rating of energy storage system
E_{o}	Initial energy state of energy storage system
n_{d}	Number of days over which the intrahourly resolution simulation is carried out
N_{a}	Length of the project period, in years
P_{ess}	Power rating of energy storage system
P_{min}	Diesel minimum power constraint
r	Discount rate
r_{e}	Rate of yearly average increase in diesel fuel prices
r_{i}	Rate of inflation
$r_{\mathrm{wl,p}}$	Wind installed power penetration level
T_{mt}	Time constant for medium-term ESS device in two-level controller
η	Efficiency of energy storage charging and discharging processes
π_{e}	Price of energy supplied by diesel power, in \$/kWh
$\pi_{\mathrm{ess,e}}$	Cost of storage energy capacity, in \$/kWh/day
$\pi_{\mathrm{ess,p}}$	Cost of storage power capacity, in \$/kW/day
π_{soc}	Penalizing term for ESS state-of-charge, in \$/kWh
π_{w}	Price of energy supplied by wind power, in \$/kWh

Random Variables

$\bar{p}_{\mathrm{res}}$	Average daily residual load
$r_{\mathrm{wl,e}}$	Ratio of daily wind energy to load energy, or also termed daily energy penetration
$\tilde{z}$	Random variable associated with each scenario, relating the probability of a given combination of $r_{\mathrm{wl,e}}$, ρ_{wl}
ρ_{wl}	Hourly correlation coefficient between wind power and load

Variables

$e_{\text{ess,t}}$	Energy state at time, t
$e_{t,k}$	Energy state at time, t, for the k^{th} time step of sliding window operating approach
e_{mt}	Instantaneous energy state of medium-term storage device
e_{st}	Instantaneous energy state of short-term storage device
$p_{\text{ch},t}$	Energy storage charging power at time, t
$p_{\text{diesel},t}$	Diesel generator power at time, t
$p_{\text{diesel,est}}$	Estimated instantaneous diesel power
$p_{\text{diesel,ref}}$	Reference power of diesel plant coming from off-line optimization
$p_{\text{dump},t}$	Dump load power at time, t
$p_{\text{dump,est}}$	Estimated instantaneous dump load power
$p_{\text{dis},t}$	Energy storage system discharging power at time, t
$p_{\text{ess,ref}}$	Reference power of energy storage system coming from off-line optimization
$p_{\text{ess},t}$	Energy storage power at time, t, defined as difference between discharging and charging power
$p_{\text{L},t}$	Load power at time, t
$p_{\text{mt,mod}}$	Modified instantaneous power reference of medium-term ESS device
p_{mt}	Instantaneous power delivered by medium-term ESS device
$p_{\text{res},t}$	Difference between load and wind power or residual load at time, t
p_{st}	Instantaneous power delivered by short-term ESS device
$p_{\text{st,mod}}$	Modified instantaneous power reference of short-term ESS device
$p_{\text{w},t}$	Wind power at time, t
n_1	Number of first-stage decision variables
n_2	Number of hourly second-stage decision variables per scenario
n_{var}	Number of decision variables in the optimization problem
$u_{\text{diesel,ref}}$	Reference diesel plant schedule coming from off-line optimization
$u_{\text{diesel},t}$	Binary variable associated with diesel plant dispatch at time, t
$\mathbf{x}$	Vector of first stage decision variables
$\mathbf{y}$	Vector of second stage decision variables

Chapter 1

Introduction

> A change in the weather is sufficient to recreate the world and ourselves.
>
> *Marcel Proust* (1871 – 1922)

1.1 Background

It could be argued that the human species has reached an impasse—we must decide whether to continue on our destructive path or opt for a more sustainable future. The latter of the choices could more easily be achieved through fundamental cultural change rather than through technology. However, as most signs do not point to significant societal changes, technological change will, at least in the near-term, be looked upon to help curtail the negative impact of a wasteful society.

The power industry is no exception, as we optimistically seek the panacea that will enable us to continue living with our patterns of excess with a clean conscience. The momentum associated with mandates to integrate cleaner forms of electricity generation is compounded with pressures to address the increased frequency of blackouts worldwide [1–3]. Power system engineers must struggle with responding to these cultural and political agendas, while ensuring that traditional tenets of power system reliability are either maintained, or in the best case, enhanced.

Proactively, the electric power supply industry has responded with the Smart Grid

Vision, whose intent is to preserve the integrity of the power network while decreasing dependence on fossil-fuel based generation through the use of new technologies. Its implementation relies on communications and a shift towards a more distributed philosophy for power generation, delivery, and end-use.

1.1.1 The Smart Grid Vision

The environmental crisis, coupled with the pressure to avoid future blackouts has given rise to the Smart Grid: an idealistic vision of the future grid, towards which current systems will evolve [4–7]. This new paradigm came into being with the near-exponential growth of wind in the late 90's, and developed further with the emergence of wide-area control, distributed generation, demand response, and distribution system automation. These developments have not only moderated the generation portfolio but also where power is generated and how it is utilized. This has been complemented in the current decade with initiatives that attempt to render the grid more intelligent, through integration of monitoring, control and communications infrastructure, promoting interoperability and openness, [7,8], helped along by efforts to develop standards that support this emerging culture, [9–12].

While the different preoccupations and inherent characteristics of individual countries shape the specific picture, some general characteristics are ubiquitous—numerous points of information exchange, interoperability of a range of technologies, improved efficiency and performance, and reduced environmental impact through renewable energy such as wind and photovoltaics. If one were given the liberty to draw a parallel to the information technologies (IT) industry, it could be analogous to the revolution in the latter part of the past century, during which telecommunications and the internet revolutionized the way in which people and businesses communicate.

However, the current power system evolution is still nascent and although this eventuality may seem long-term the idea has been refined into R&D initiatives around the globe, that treat one or any number of the elements of the Smart Grid Vision [4–7, 13–15].

1.1.2 Microgrids

A *microgrid* is perhaps the epitome of the move toward distributed power, wherein distributed energy resources[1] (DER) are coordinating to serve the needs of the local distribution network and provide services to the main grid, [16–18]. The term has taken on various meanings in the scientific community and a number of related terms that are related to or synonymous with this concept have also been proposed.

Generally a microgrid refers to a distribution system with distributed energy, that may operate either in parallel with the power system or in isolation, [19]. Also, the microgrid can seamlessly transition between one mode and the other depending on the needs and status of the system. It does not intend to marginalize the importance of the bulk power system but rather attempts to limit dependence on it. Widespread implementation of this concept could permit overall improved system efficiency and reliability, [20]. Demonstration projects have helped viability of the technology, [21]; however, there are a number of interesting research issues that still need resolving.

In microgrids, the planning and operating problem becomes a blend of an isolated power system and a distribution network. DER must be managed appropriately when connected to the main system and perhaps differently when operating in isolation. In addition the challenges associated with the transition between the two modes of operation requires flexibility on the part of the local distribution network, [22–24].

Planning of a distribution system with wind energy for microgrid will be completely different from conventional systems. Uncertainty associated with the mode of operation, the duration of outage, the generation sources, and the load all need to be considered. A hybrid design between remote power systems and active distribution networks is a promising starting point. Remote power systems that include DER represent an interesting case study, to serve as a first step in this process, where renewable energy and energy storage are integrated into an existing power system [25–30].

[1] DER is an umbrella term that encompasses distributed generation, demand response / demand-side management, and energy storage.

Distributed Energy

Distributed energy includes distributed generation and distributed energy storage systems[2,3]. Distributed generation is generation that is connected close to the load and is generally small in size (less than 10 MW). A great detail of research and industry experience on various aspects of DG exists, related to protection, operation, and planning [31–33]. Distributed energy storage, unlike DG, can function as both a load and a generator, depending on the needs of the local network. Both are important components of a microgrid.

It is informative to define *energy reserves*, which will be referred to as additional distributed measures of managing energy use but which are distinct from energy storage in that they are unidirectional (can be seen as an increase in load or an increase in generation but not both). These include curtailing of wind energy (through pitch control, use of a dump load, suboptimal power point operation, or coordinated wind turbine generator shut-down) and load control. The modeling and control of ESS should be applicable to energy reserves, albeit with some modifications to account for the differences. Ultimately, an optimally designed microgrid, remote or otherwise, should balance the use of energy reserves, energy storage, and demand response.

Energy Utilization

As alluded to earlier, loads in the microgrid will not be as inelastic as they have been in traditional networks. This shift will be in part due to the implementation of smart metering but other changes will account for it.

Demand response is a term, which describes load that will curtail itself in response to a given signal, in all likelihood with some form of financial compensation, [6,34]. A particular building may have some loads that respond to this signal while others are deemed more

[2]For the purposes of this thesis, *energy storage* will be defined as the set of technologies that permit the conversion of electrical energy into stored potential energy, for the purpose of its later conversion back into electrical energy for use in the same power system from which the energy was originally provided. This may be in the form of the inertia of a spinning mass, electrochemically through the charging of a battery, or due to gravity by pumping water from a lower reservoir to a higher one. There will always be losses associated with this conversion process; however, this is a tradeoff for being able to control *when* the energy is utilized.

[3]Energy storage systems (ESS) refer to the total infrastructure that allows integration of energy storage with the power system. This includes: energy storage, power conditioning system, protection, control, and monitoring and communication. Energy storage systems that are composed of greater than one energy storage technology will be referred to as either two-level ESS or hybrid ESS.

essential, continuing to behave in an inelastic manner.

1.1.3 Literature Review

In the context of the microgrids and particularly remote microgrids, wind is at present the most important renewable energy source. Its growth has preceded the development of both the Smart Grid and large-scale deployment of energy storage systems, [35–37]. The latter could certainly facilitate more transparent integration of wind energy. However, the merits of these technologies need to be analyzed in terms of how they can aid in mitigating the shortcomings of wind.

Wind integration can be considered on three levels—as part of an interconnected power system, in a isolated power system, and in a microgrid. The role of energy storage in each must be related to its ability to bring value to the system. This means that when considered with equal weighting given to alternatives it provides the greatest overall value. The potential role of energy storage in each of these contexts is described here briefly.

Wind Integration

Engineering of power systems consists of planning and hierarchical control effected over various time frames in order to meet well defined performance criteria. Due to the necessity to balance load and generation in real-time, power engineers are concerned with appropriate scheduling of generation resources, to meet reliability criterion set out by the governing bodies, [38]. The constraints of the electrical infrastructure must be considered in this process to ensure that there are sufficient pathways to transmit the power to the loads. At the distribution level, fine control is invoked to ensure that voltage respects the standard ranges as expected by connected loads.

The integration of wind complicates these different levels of power system planning and operation. The different applications need to be differentiated so as to distinguish local impacts from those that are system-wide. The impacts associated with wind variability can be summarized as relating to the following: generation and reserve scheduling; transmission access; and distribution system operation.

From the global view of the power system, the impact of wind on generation and reserve scheduling is perhaps the most important, since poor planning in this regard could result in degradation of system reliability. However, this is less dependent on location; it is related

more to the total system's installed capacity of wind energy and the ability to schedule other generation in consequence. The impacts are directly related to management of the energy in the system, related to primary regulation and power system reserves[4]. A great deal of research has been conducted on the impact of wind on power system operation and markets [39–48]. Wind introduces a source of uncertainty into this process because it is neither completely predictable nor controllable. The role of accurate forecasting is paramount in minimizing the cost of integrating wind into this procedure.

Construction of new infrastructure has traditionally been employed for point-to-point connections of load and generation or in some cases to improve capacity for reliability improvements. Contrarily, wind plants are not always accompanied by transmission investment. This raises the contentious issue of how to manage constrained transmission access, particularly when wind must compete with central generating units. Again, it is a question of management of energy, only at a much more local level than generation scheduling of the bulk system.

Large amounts of wind is connected directly to distribution systems, and may exceed the local load. This requires analysis of potential impacts on power quality, voltage regulation, and protection coordination, [32, 33]. The power fluctuations can in extreme cases lead to voltage flicker and voltage control issues. If the distribution system is islanded, a separate set of controls for the WTG may be required, [49].

Given that wind turbine generators are generally interfaced using power electronic converters, [36], special provisions have been made to ensure that significant levels of wind do not negatively impact power system security. To avoid loss of numbers of WTG, low-voltage ride through (LVRT) requirements are now imposed to ensure that WTG do not disconnect for normally cleared contingencies, [50, 51]. Also, as power electronic converters that interface generators do not normally contribute to system inertia, future WTGs may need to incorporate this functionality into its controls [52, 53].

Energy Storage

Energy storage is still in its infancy with regards to power system applications. However, mature technologies are now available and while the costs remain high, they are not as

[4] *Reserves* are distinct from energy storage in the sense that they deal more with the scheduling (on multiple time frames) of power delivery from the power system's generation portfolio. Large capacity energy storage may be a subset of what is considered reserves but the two terms are not synonymous.

prohibitive as they once were. Applications include use of storage in shifting load, arbitrage, dynamic voltage support, and balancing power for intermittent generation [50, 54–61].

Power systems research problems associated with storage can be reduced to ESS sizing and value analysis, [59–61], and operation [62–64]. This analysis changes very much depending on the application, as the storage solution will need to fit the characteristics of the particular problem.

As outlined above, wind variability is the most important factor in determination of its integration costs. The problem of balancing power for wind energy is perhaps one of the most challenging in that wind power is a random variable; the cost of energy is relatively low, making the business case for ESS more imposing; and there are a number of competing solutions to achieve the same effect. Some research has considered the inertia of the machine itself as a means of storage, [45, 65, 66]; however, the energy capacity is relatively small, affording power smoothing or frequency regulation only over the short-term.

Research in application of energy storage systems to shape wind characteristics over longer periods considers the scheduling of the ESS to meet some objective of the system, [61–64, 67–69]. While a great detail of good work has occurred in this field, methodologies for design and integration of ESS into various power systems with wind, including microgrids, are somewhat lacking. There is an opportunity to develop approaches for pairing of ESS and wind, sufficiently general that they can be adapted for a given application.

1.2 Problem Definition

Wind energy poses two fundamental problems that negatively impact the reliability and efficiency of power systems: 1) its output power variability and 2) its behaviour during transients. Wind power variability can be further divided into two characteristics that deserve special mention—wind power is uncontrollable[5] and it is not perfectly predictable.

Wind variability, as outlined previously, impacts various levels of power system operation. The type of impact will be a characteristic of the type of application. The two components of wind power variability complicate power system scheduling regardless of whether the power system in question is an interconnection, a remote power system, or a

[5]There are various mechanisms that can be employed to control the output power from wind, such as wind curtailing. However, without exception these imply suboptimal power capture and as a result come at a cost.

microgrid.

Wind Penetration

Within the industry, *wind penetration* is a term used to relate the amount of wind power for the system in question, to either total generating capacity or load. However, when discussing the wind penetration level and possible limits, the context of the problem must be taken into consideration.

Although the whole of wind integration issues cannot be captured in a single metric, wind penetration does serve as a useful tool against which to compare different systems and applications. Formal definitions of wind penetration for each of the levels of system integration will be covered in the ensuing chapters. However, in each case, the definition will be made with respect to the load served.

Cost of Uncertainty

The power system is scheduled in such a way as to respect reliability design constraints, [70], while minimizing costs of supplying the energy. Therefore, if wind introduces uncertainty into the power system and cannot be depended upon to perform basic functions, such as participate in automatic generation control (AGC) or provide reserve capability, then the other power producing units need to be scheduled in consequence, likely resulting in higher costs. Aside from these costs there may be other integration costs that are more location specific. These will need to be included in the problem definition, and follow from formulation of the particular application.

Energy storage provides a mechanism to hedge against the uncertainty of wind power, thereby bringing value to the power system through reduction of otherwise inflated operating costs. However, energy storage also comes at a cost that must be carefully factored into its feasibility assessment.

1.2.1 Thesis Statement

The underlying premise is that any level of wind energy can be integrated into a given power system using appropriate technologies. It is the purpose of this thesis to discern under what conditions wind should be complemented with an appropriately rated energy storage device(s), considered from an economic standpoint. Once the costs associated with

integrating wind exceed those associated with mitigating those costs using energy storage, then the argument for using energy storage for integration of wind becomes viable.

Therefore, the problem can be formulated thusly: given a set of constraints associated with a particular power system and wind energy penetration, what is the optimal energy storage capacity (energy and power rating) and how is the ESS operated. The objective of this thesis is to develop a methodology for design of ESS for use in wind energy applications, which includes two components: sizing and control. The approach is applied to the specific problem of ESS in a remote wind-diesel power system.

The specific issues that this thesis will attempt to address include: at what penetration level can we expect aforementioned problems associated with wind to warrant re-evaluation of the wind park structure and operating strategy, namely the inclusion of ESS in the design; how does the addition of energy storage to a wind park extend the penetration limit for a given system and at what cost; what control approaches and ESS structures are appropriate for real-time ESS control; and how can ESS and their associated application realistically be implemented and tested in a laboratory environment.

1.2.2 Methodology and Tools

Here the specific elements of the problem and the proposed methodologies and tools are outlined.

Energy Storage System Sizing

The sizing component of the design involves two separate steps: (i) pre-feasibility analysis, which acts as a first screening process to determine whether a detailed analysis is warranted or whether the addition of storage is not viable; and (ii) a detailed sizing problem which uses data associated with the system and optimization theory to arrive at the rating of the storage's power and energy components. Pre-feasibility analysis is fairly well covered in the literature and has been used to select the wind-diesel as a suitable case study. A detailed methodology is required to better model the wind power and load dependency, understand the role of key parameters, and to include the operation of the power system. Stochastic optimization is proposed to capture the uncertainty associated with wind and load, together with economic theory to perform the cost-benefit analysis.

ESS Scheduling and Performance Evaluation

Once in place, energy storage systems need to be operated in an optimum manner in order to realize the anticipated benefits predicted by the sizing analysis. Assuming a limited horizon for knowledge of load and wind power, an optimal scheduling approach is required to coordinate flow of energy to and from the ESS. Moreover, results of the ESS operation then need to be contrasted with expected benefits from the ESS sizing study in order to validate assumptions in modeling of the wind and load characteristics. Once this process is complete the adaptation of the scheduling approach to a method that is suitable for on-line control is required. The use of Artificial Intelligence, specifically artificial neural networks (ANN), is proposed to achieve this task.

ESS Control System Design

Scheduling represents the highest level of a hierarchical control whereby hourly averages are used to provide a set-point for the ESS over a given hour. However, dynamics of the wind and load within the hour may justify deviations from the original dispatch either to take advantage of additional opportunities or to respect the ratings of the ESS. In addition, practical limitations may require the pairing of two or more energy storage levels, mandating more elaborate control structures in order to coordinate the different ESS devices. Practical implementation of all or part of these systems is required in order to validate their operation and any assumptions made. To this end, hardware-in-the-loop, real-time simulation will be used to realize, at least in part, the system experimentally.

1.3 Claims of Originality

This dissertation builds on the works of many previous research contributions and adapts fairly well established theories to energy storage systems. Nonetheless, the following can be highlighted as contributions that are, to the best of the author's knowledge, original and distinct:

1. Formulation of the problem of design of power and energy ratings of an energy storage system in order to minimize the cost of energy delivered to a wind-diesel system.

(a) Rigorous definitions of the deterministic and stochastic energy storage sizing problem. Formal definition of the problem for wind-diesel system for continuous diesel operation and permitting shut-down.

(b) Models for characterizing the relationship between wind power and load profiles based on the daily energy penetration and hourly correlation coefficient. Evaluation of different variation of the model and comparison with auto-regressive moving average (ARMA) models.

(c) Sensitivity analysis that considers how the energy storage sizing changes according to wind resource, diesel plant control strategies, and storage device characteristics (efficiency function, costs).

(d) Forecasting of the future role of energy storage based upon different scenarios for evolution of energy prices and capital costs of the technologies.

2. Development of a scheduling algorithm for energy storage system and modifications to capture practical considerations. Development of a methodology for auditing of ESS sizing algorithms.

   (a) Formulation of the continuous and mixed-integer ESS operating problems for the wind-diesel system. Methodology for use of a sliding window to translate the solution of the subproblem to a yearly operating approach.

   (b) Adaptation of the operating approach by inclusion of a penalizing term to modulate ESS energy capacity usage, discouraging low states-of-charge. Guidelines for practical tuning of penalizing term.

   (c) Evaluation of the impact of prediction of wind power and load profile accuracy on operating approach performance.

   (d) Methodology for evaluation of sizing approaches using results generating from yearly operation of the system.

3. Development of an on-line scheduling algorithm for energy storage system based on artificial neural networks. Performance assessment of controllers and comparison with off-line optimization approach.

   (a) Defined a general methodology for translation of off-line ESS optimization results into an on-line control algorithm using ANN, for continuous diesel operation and operation with diesel shutdown permitted.

   (b) Parametric analysis of different ANN architecture and input variables for optimal controller selection.

   (c) General performance assessment of ANN controller through comparison with off-line optimization results over 20 years of operation.

4. Implementation of practical two-level ESS systems in simulation and hardware. Development of a generalized two-level ESS control structure and application to the wind-diesel system.

   (a) Development of generalized real-time control structure for multi-level ESS as part of a hierarchical ESS controller.

   (b) Specification of three control functionalities within the generalized controller framework to meet objectives of dump load minimization, diesel ramp rate limiting and ESS capacity optimization. Definition of six control modes resulting from their combination.

   (c) Development of a hardware-in-the-loop (real-time simulation with power electronic converters) set-up for evaluation of ESS controller performance and prototyping of multi-level ESS.

This thesis provides a methodology for assessing how energy storage systems may be used in the integration of wind energy. It then provides a general hierarchical control structure for scheduling of the optimally designed ESS, to realize the maximum benefit to the power system, while respecting the constraints of the ESS and practical implementation issues.

The claims presented are supported by the fact that portions of the research have already been reviewed and accepted by the research community, in the form of peer-reviewed journals, [50, 71–73]and conference proceedings, [74–76].

1.4 Dissertation Outline

Chapter 2: A Stochastic Optimization Approach for Energy Storage System Sizing

Formulation of the energy storage system sizing problem and its application to the specific case study are presented. The problem is posed first as a deterministic formulation, later extended to a stochastic formulation in order to model the uncertainty associated with the wind resource. The latter considers probabilistic modeling of the wind and load in order to realistically assess the residual load (difference between load and wind power) and its implication on the design. The methodology is applied to the wind-diesel power system and the economic feasibility of ESS is discussed for a representative base case. The dependence of the solution on different parameters, diesel operating scenarios, wind resources, and its sensitivity to different future energy price trends are investigated.

Chapter 3: Optimal ESS Scheduling and Validation of Sizing Methodologies

The chapter first presents an ESS scheduling algorithm based on an extension of the sizing formulation. The detailed formulation for a 24-hour window is presented and its adaptation to a yearly operating approach is explained. The scheduling approach is applied to various wind resources and the actual operating costs are compared with those predicted by the sizing methodology. Practical considerations such as ESS discharge constraints and the accuracy of wind-load prediction are analyzed. Once again different diesel operating strategies are investigated and the important differences are analyzed in-depth.

Chapter 4: On-line Control of Energy Storage Systems

The detailed analysis from the previous chapter is used as training data for a neural network based approach to on-line operation of the storage. The overall rational is presented and various neural network architectures are proposed for continuous diesel operation and operation with diesel shut-down permitted. The optimal NN controller is produced as an output of a parametric analysis whereby performance of different candidates are evaluated using pre-defined performance metrics. The performance of the NN-based controller is compared with the off-line optimization results from Chapter 3 for two different wind resources over twenty years of operation.

Chapter 5: Control of a Two-Level Energy Storage System

The pragmatic issues related to realization of the energy storage system and its real-time control form the basis of this chapter. Special consideration is given to two-level energy storage systems—combination of two complementary energy storage technologies—and their operation on a second-to-second time frame. A general control structure for multi-level ESS is presented and adapted to the specific case of a two-level ESS in a wind-diesel system. A number of control modes are defined using combinations of the different functionalities of the general control structure. The control modes are evaluated for a week of operation of using high resolution wind power data. The simulation results and the ability of the control to work in real-time are validated with the aid of a hardware-in-the-loop, real-time simulation experimental set-up.

Chapter 6: Conclusions

This chapter summarizes the research's main contributions and discusses future research needs in the area. Insight as to how the overall methodology should be modified for different ESS applications and given appropriate data from industry is offered. The extension of the research to microgrid system design and operation is discussed.

Appendices

This dissertation includes a number of informative appendices meant to complement the theoretical developments and presented results. Appendix A provides details of the modeling of the wind power and load profiles used in the ESS sizing methodology of Chapter 2. Appendix B describes the sources of hourly wind power data and data processing that was performed. Appendix C describes high resolution wind speed data and its conversion to wind power to fit the hourly data. Appendix D describes the simulation tools used in the research. Finally, Appendix E provides an overview of the hardware-in-the-loop set-up of the two-level energy storage system and description of the important hardware component and the real-time simulator.

Chapter 2

A Stochastic Optimization Approach for Energy Storage System Sizing

> The most beautiful thing we can experience is the mysterious. It is the source of all true art and science.
>
> *Albert Einstein* (1879-1955)

2.1 Introduction

Sustained growth of wind suggests that it will ultimately become a significant component of generation portfolios of many of the major power systems in the near future. With this expanding role, means to deal with its intermittency will need to be invoked to ensure that the reliability of the system is upheld. Isolated power systems are no exception, as even in remote communities people are turning to wind to help in absolving themselves of, or at least limiting their dependence on, fossil fuels, [28, 29, 77].

This evolution has created a potential role for energy storage technologies, with balancing power for intermittent renewable energy being touted as one of its possible applications. Although in theory this is almost self-evident, the economic justification is not. These technologies remain onerous and therefore, they must be linked to a quantifiable value stream in order to gauge the rating of the energy storage system (ESS) that is required to ensure

a sufficient return. The ESS must be rated both in terms of power and energy capability. Taken together with the fact that wind is a stochastic energy source, ESS sizing represents a challenging, multi-dimensional problem.

ESS sizing has been approached in much of the literature by first considering optimal scheduling of the device and then performing sensitivity analyses to determine the impact of different ratings, [59, 63, 67, 68, 78–80]. In these works, parametric studies have been used either to investigate the impact on reliability indices, [59], or an objective function [67, 68, 78, 79], the latter usually relating to either the profit realized by the installation, or a metric related to the performance of the power system, [63]. These studies are quite useful and can serve as an approach to optimal scheduling of the ESS.

The problem of storage sizing for remote communities has been considered in the context of design of the energy supply mix of the community, with the objective of minimizing the cost of energy served, [69, 81–83]. In each of these references, both operational costs and fixed costs are included in the optimization problem formulation. Databases of monthly energy production from the renewable energy sources (wind and photovoltaics) are used to estimate the contribution from these sources. Reliability design criteria are then imposed through the use of adequacy constraints, which can be met through the inclusion of storage or additional diesel capacity. Although useful as a pre-feasibility assessment for energy storage, each approach neglects intraday operational issues. Also, the different operating schemes of the diesel back-up unit are not dealt with exhaustively, leaving unanswered questions.

2.1.1 Stochastic Optimization in Power Systems

An alternative to a deterministic approach in power system studies is the use of stochastic optimization techniques. These have been successfully applied to various problems in power systems to deal with uncertainties. In [38] Galiana *et al.* presented both the deterministic and stochastic formulations for the problem of scheduling different power system reserves. The scheduling of a hydro plant in a thermal based system was solved using a stochastic formulation of the problem in [84], while in [85], the dispatch of distributed generation units was considered using the same theory.

This chapter will consider the problem of sizing of ESS for isolated wind-diesel power systems using stochastic optimization, an expanded version of the work presented in [71].

The problem is first described and formulated as a stochastic optimization problem to capture the uncertainty associated with the daily energy penetration of the wind and its correlation with respect to the load. The problem is posed firstly with only continuous variables, and then as a mixed-integer formulation that considers unit commitment of the diesel plant. Results are given for the base case, followed by a sensitivity analysis that considers the impact of the wind characteristics, ESS efficiency, diesel plant operating modes, and economic parameters, on the sizing of the ESS and the expected cost of the energy served.

2.1.2 Methodology

The sizing of the ESS must rationalize the costs associated with the installation (both fixed and operating costs) with the monetary benefit that it brings to the system. In many cases there are less tangible benefits that, although real, are not monetized and attributed to the ESS. However, we will concern ourselves only with those where a real revenue (value) stream is in place[1].

Figure 2.1 illustrates the overall proposed methodology to be followed for ESS sizing. The initial steps consist of defining the issues associated with wind integration, identifying costs and potential value streams for storage, and then conducting a prefeasibility study to determine whether a more involved study is warranted. There are a number of readily available programs that could be configured to perform this type of study [86, 87]. This dissertation is more concerned with the final step in the sizing approach—the detailed ESS sizing study. In this step, complete information is required for the analysis, which includes: costs, wind and load data, and any specific contraints asssociated with the power system in question. In the following section, this sizing problem will be formalized and then illustrated using representative data.

The methodology as presented will be applied to the specific case of a wind-diesel system. This example will be retained throughout the dissertation and will form the basis for investigation in subsequent chapters. While all results will be derived for this particular application, one should keep in mind that the overidding approach remains valid for the

[1] *Revenue* stream and *value* stream can be differentiated simply by cases where the ESS receives rumuneration for a service rendered, compared with those where it brings value to a system by reducing costs, respectively. This difference is more a question of ownership and does not greatly affect the overall business case, and thus the two terms will be used interchangeably.

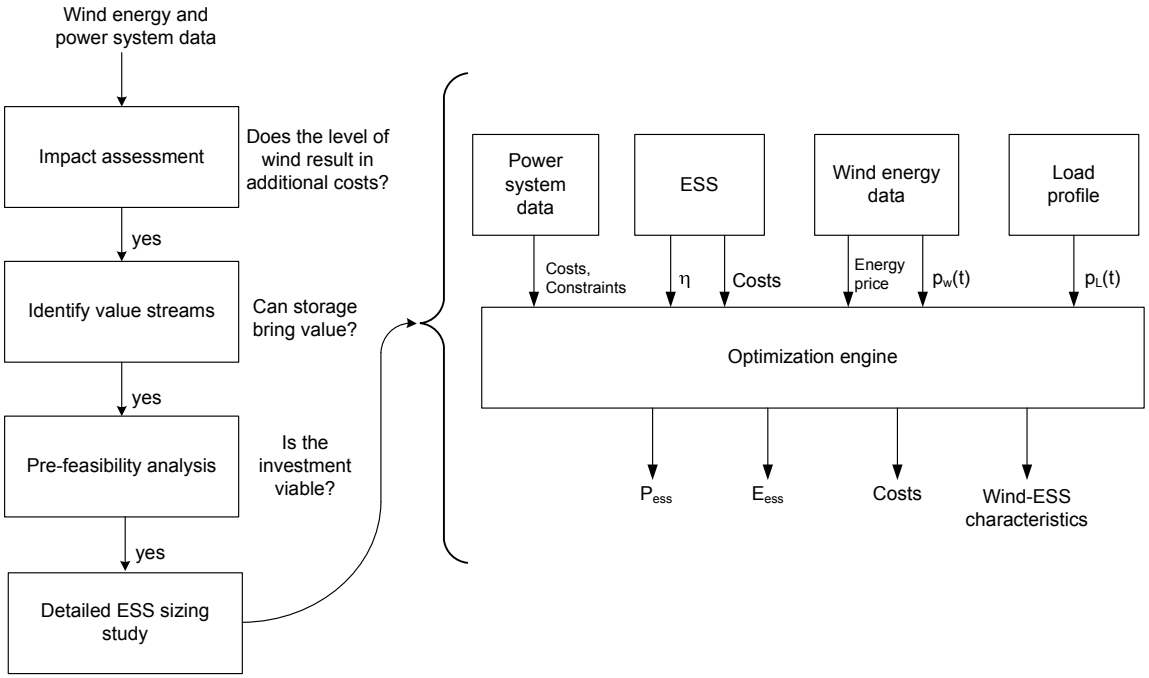

Fig. 2.1 Flow chart of energy storage system sizing methodology for wind integration

general case of wind integration. Also, it is anticipated that some general observations will be gleaned from the results, in such a way that conclusions related to the applicability of storage to wind integration and key parameters that dictate its feasibility can then be made.

2.2 Problem Description

As alluded to in the previous section, the wind-diesel system will be used to illustrate the application of the stochastic optimization approach to ESS sizing. The wind-diesel system is a useful case study due to the fact that electricity prices are much higher than for interconnected power systems, which greatly improves the economic feasibility of energy storage. In addition, the complexity of the system is manageable such that sizing—and in later chapters control issues—can be handled without consideration to power system reserve markets and other operational issues associated with bulk power systems. The author makes no claims as to being an expert in power system markets and has intentionally

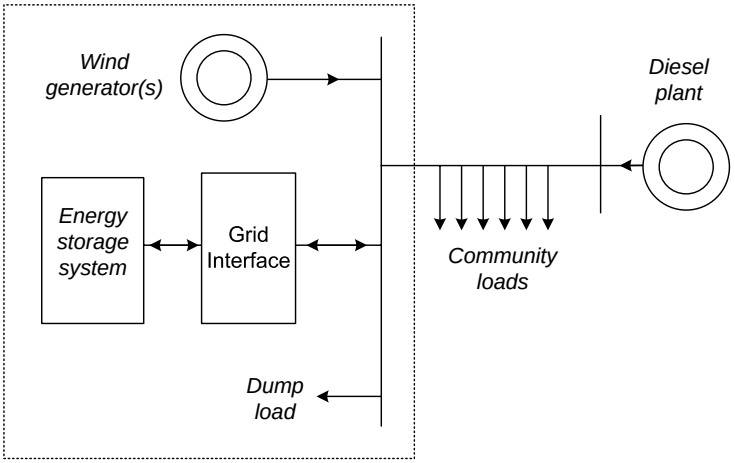

Fig. 2.2 Generic representation of a remote wind-diesel power system with ESS

avoided the use of bulk power systems as a case study. Extrapolation of results to the more general case of interconnected power systems and necessary modifications to the methodology are discussed briefly as part of the concluding chapter.

2.2.1 Wind-Diesel Power Systems

The majority of remote systems consist of a distributed load that is supplied by diesel generators, which serves as the balance of plant. Other elements of the remote power system may include: renewable energy (wind, photovoltaics, small hydro), a dump-load, and possibly one or more ESS technologies, Fig. 2.2. In these systems, the diesel plant is the *de facto* control element for maintaining acceptable frequency and voltage. The dump load is used to regulate the loading on the diesel unit(s), or stated otherwise, manage the wind provided to the community.

This will generally remain unchanged in the presence of an ESS, even though the balance of plant could be shared with the ESS or even accorded solely to the ESS for limited periods. In this thesis, both cases will be considered: the status quo (diesel is always scheduled on) and unconventional operating schemes, including the use of low-load diesels and diesel shut-down.

Diesel Operating Strategies

The operation strategy of the diesel generator will play an important role in determining the magnitude of dumped wind energy and consequently, the sizing of the ESS. Three different diesel operating strategies will be considered, namely: minimum loading; low-load diesel technologies; and diesel unit commitment.

Perhaps the most widespread strategy is the use of a dump load to ensure that the diesel generator is loaded at or above a minimum value (30% of its rated capacity is typical). Generally operation below these levels is avoided as it leads to reduction in lifetime, may lead to fire hazards, and the efficiency generally degrades at low loadings [28, 77, 88]. However, remote communities often have large differences between their peak and minimum loads; even in the absence of wind, diesels may be forced below this threshold.

New diesel generator technologies that utilize electronic fuel injectors can lead to much improved operation, well below 0.3 per unit, as they are able to maintain sufficient engine temperature to avoid the build-up of particulate matter and can selectively reduce the number of pistons in operation, [77, 88, 89]. These units will be modeled by simply relaxing the low loading constraint.

Diesel unit commitment refers to the case where there is sufficient wind power and stored energy (and power capacity) to shut the diesel off during specific intervals. This is modeled using the binary variable, u_{diesel}, which will be designated '1' when the diesel is in operation and '0' when it is shutdown. As will be seen in the next section, these three modes require different formulations of the optimization problem.

2.2.2 Wind-Load Characterization

The diesel constraints provide the foundation for a dump load, which in turn provides an opportunity for ESS. The problem of energy storage sizing is related to tapping into a revenue stream that allows the developer to recover the costs associated with the installation (as well as operational costs). For remote power systems, this revenue is achieved by avoiding the dumping of energy via the dump load by shifting wind energy in time. The degree of dumped wind energy depends on: the diesel operating strategy (and how this impacts the operational constraints of the wind park), the amount of wind energy produced, and its correlation with respect to the community load.

Thus, an important consideration in assessment of the opportunity for ESS is the mod-

eling of the wind and load profiles. Dumped energy is linked to the amount of wind energy that is produced during periods of low load. The diesel plant is lightly loaded during low load and consequently, wind energy produced at these times may invoke the dump load. Large amounts of wind may also require operation of the dump load during even average or peak load but this depends on the relative magnitude of the wind and load. As such, modeling of this relationship is of great importance. One should keep in mind that this information needs to be extracted from data on the wind resource and the load. As well, the complexity of the wind-load model will impact the complexity of the optimization problem.

Definition of Random Variables

An overriding assumption is that the most important cycling of the ESS occurs over daily periods and as a result the relationship between load and the wind resource needs to be established over this interval. To facilitate the modeling of the wind resource and its relationship to the community load, a number of metrics are required. The wind power penetration will be defined as:

$$r_{\mathrm{wl,p}} = \frac{P_{\mathrm{w}}}{P_{\mathrm{L}}} \tag{2.1}$$

where P_{w} is the installed capacity of the wind park and P_{L} is the peak load of the community. The daily energy penetration, which provides a measure of the amount of wind energy produced during a given day compared with the total load energy for the day, will be given by:

$$r_{\mathrm{wl,e}} = \frac{E_{\mathrm{w}}}{E_{\mathrm{L}}} \tag{2.2}$$

And finally, the correlation of the two profiles is vital as it provides an indication of when the peak of the wind power occurs relative to the load peak, given by:

$$\rho_{\mathrm{wl}} = \sum_{t=1}^{T} \frac{(p_{\mathrm{w},t} - \bar{p}_{\mathrm{w}})(p_{\mathrm{L},t} - \bar{p}_{\mathrm{L}})}{(T-1)s_{p_{\mathrm{w}}} s_{p_{\mathrm{L}}}} \tag{2.3}$$

where the subscripts w and l refer to the hourly wind power and load time series; $\bar{p}_{\mathrm{w}}$ and $\bar{p}_{\mathrm{L}}$ denote the average value of the wind and load; $s_{p_{\mathrm{w}}}$ and $s_{p_{\mathrm{L}}}$ correspond to their standard deviations, and $T = 24$.

Wind-Load Models

Here, the approaches used to model the wind-load relationship are discussed, which are intended to test the assumptions of daily variation being the predominant time frame and that the two previously defined random variables capture all important features of the relationship needed for ESS sizing.

The following four wind-load models will be used in the ESS sizing approaches:

(i) Wind modeled as scaled, time-shifted load, 24-hour long scenarios;

(ii) Wind modeled as scaled, time-shifted load, week long scenarios;

(iii) ARMA model of residual load, 24-hour long scenarios;

(iv) ARMA model of residual load, week long scenarios.

The first two models follows directly from the definitions of $r_{\mathrm{wl,e}}$ and ρ_{wl}. In this case, probability density functions are developed from the data for wind power and load. The random variables are calculated assuming a time period, $T = 24$ hours.

In the second case, the validity of the assumption of intradaily variation is investigated by extending the time period to a week, i.e. $T = 168$. The random variables are calculated in the same manner as before only replacing T by this new value in equation A.1.

For the last two modeling approaches an auto-regressive moving average model (ARMA) is used for the residual load:

$$p_{\mathrm{res,t}} = p_{\mathrm{L},t} - p_{\mathrm{w},t} \tag{2.4}$$

which is defined over the corresponding periods. As the details of ARMA models are fairly well established the derivation has been relegated to Appendix A, along with a description on the generation of wind and load profiles from the four models.

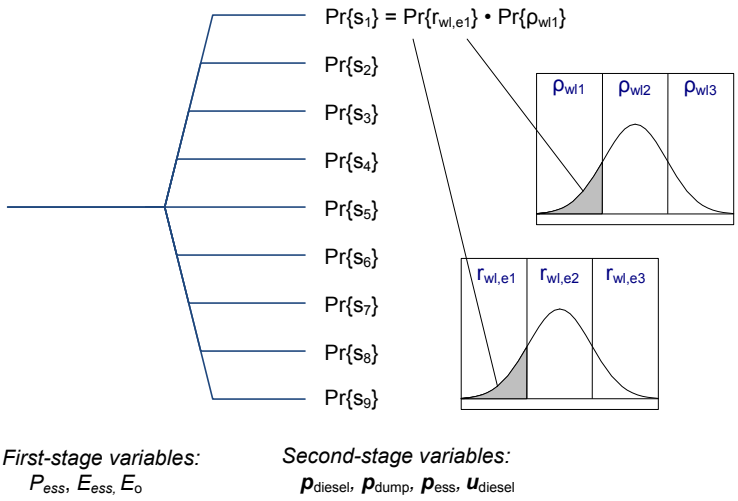

Fig. 2.3 Scenario generation for stochastic optimization approach to energy storage system sizing

Scenario Generation

In stochastic optimization, the probability density functions (*pdf*s) of the random variables characterizing the wind and load resource are used in the formulation to generate scenarios, each weighted with their associated probabilities. In the present case, the optimization problem is solved to determine the optimum sizing of E_{ess} and P_{ess}, for the specified input data. Here, the generation of those scenarios are described for model (i); the overall procedure is valid for all wind-load models, with slight variations depending on the model in question.

Each scenario represents a 24-hour period of wind and load for the community. Each by itself constitutes a deterministic representation of the problem. In the two-stage stochastic formulation [90], the *second stage* variables are specified for each scenario, while the *first stage* variables are common to each. For our problem, the scheduling for each scenario is completely independent of the other—one is not obliged to consider how storage was scheduled the day, week, or month before[2]—whereas ratings must be defined before the installation is constructed, and obviously are shared across scenarios, Fig. 2.3. In addition,

[2]There is actually a link between different days through the stored energy in the ESS at the end of the day, e_{T}. This is accounted for in the formulation by defining a third *first stage* variable E_{o} and a constraint that links it with e_{T}, equation (2.18)

the initial energy state of the ESS, E_{o} has been made a first stage variable. Admittedly, this is more conservative but it was assumed that in general the initial state would be more or less similar across all scenarios, and to limit the dimensions of the problem, it was defined in this way.

The random variable $\tilde{z}$ associated with each of the scenarios, has a probability defined by the probability of a set of wind and load daily profiles having a certain correlation coefficient, ρ_{wl} and energy penetration, $r_{\mathrm{wl,e}}$.

$$Pr(\tilde{z}) = Pr(r_{\mathrm{wl,e}}, \rho_{\mathrm{wl}}) \tag{2.5}$$

Assuming that ρ_{wl} and $r_{\mathrm{wl,e}}$ are independent the probability of $\tilde{z}$ is given by:

$$Pr(\tilde{z}) = Pr(r_{\mathrm{wl,e}})Pr(\rho_{\mathrm{wl}}) \tag{2.6}$$

whose distribution can be plotted through analysis of databases of wind power and load. Obviously, the larger the database, the better; however, it should at least span an entire year to account for seasonal variations of the wind resource and the load.

2.2.3 Problem Formulation

The problem is to determine how much storage capacity is required in order to minimize the supplied daily energy of a wind-diesel plant. Again, the problem is developed assuming the first wind-load modeling approach but is easily adaptable to the other cases.

Before proceeding further, we state the following assumptions:

(i) ρ_{wl} and $r_{\mathrm{wl,e}}$ are independent;

(ii) dumped energy is lost as waste heat, i.e., it is not used to source local heating loads, and;

(iii) direct load control (DLC) or DSM is not considered.

The first is required only to use the simplified equation for calculation of the $Pr(\tilde{z})$, equation (2.6). If it is not true it only slightly complicates the calculation of these probabilities, requiring conditional probabilities. The second makes the ESS sizing case optimistic

as the revenue for avoided dump load is equivalent to the cost of producing that energy. Systems do exist where this is not valid and the formulation would need to be modified in consequence. Demand-side management (DSM) or direct load control (DLC) could also be employed as alternatives to or in concert with ESS; however, they are excluded from the current formulation.

Bearing these assumptions in mind, the problem can be stated formally as:

$$\min_{\mathbf{x},\mathbf{y}(\tilde{z})} \quad \pi_{\text{ess,e}}\, E_{\text{ess}} + \pi_{\text{ess,p}}\, P_{\text{ess}} + \mathrm{E}_{\tilde{z}} \left[\sum_{t=1}^{T} \left(\pi_{\text{e}}\, p_{\text{diesel},t}(\tilde{z}) + \pi_{\text{w}}\, p_{\text{w},t}(\tilde{z}) \right) \right] \tag{2.7}$$

where $\pi_{\text{ess,e}}$ is the cost of ESS energy capacity in \$/kWh/day, E_{ess} is the ESS energy rating, $\pi_{\text{ess,p}}$ is the cost of ESS power capacity in \$/kW/day, P_{ess} is the ESS power rating, π_{e} is the cost of diesel power in \$/kW/day, $\mathbf{p}_{\text{diesel}}(\tilde{z})$ is the diesel power associated with scenario $\tilde{z}$, π_{w} is the cost of wind power in \$/kW/day, and $\mathbf{p}_{\text{wind}}(\tilde{z})$ is the wind power associated with scenario $\tilde{z}$. The operating costs are calculated over all time points, $t \in \mathbb{T}$. The operator $E[\cdot]$ calculates the expected value of the operating costs over the random variable, $\tilde{z}$. The cost associated with wind power is included in the objective function. However, the cost of wind energy has no bearing on the rating of the energy storage system due to the fact that the decision variables can in no way impact the quantity of wind energy produced. The cost of wind energy is only included here to calculate a representative cost of energy served.

The vector of *first stage* variables, $\mathbf{x}$ is given by:

$$\mathbf{x} = \begin{bmatrix} P_{\text{ess}} & E_{\text{ess}} & E_{\text{o}} \end{bmatrix}^{T}, \tag{2.8}$$

which are the rating of the ESS in terms of its power and energy and the initial energy state of the storage device, E_{o}. The *second stage* variables are given by the vector, $\mathbf{y}(\tilde{z})$:

$$\mathbf{y}(\tilde{z}) = \begin{bmatrix} \mathbf{p}_{\,\text{diesel}}(\tilde{z}) & \mathbf{p}_{\,\text{dump}}(\tilde{z}) & \mathbf{p}_{\text{ch}}(\tilde{z}) & \mathbf{p}_{\,\text{dis}}(\tilde{z}) \end{bmatrix}^{T} \tag{2.9}$$

representing the diesel, dump load, and ESS charging and discharging powers for each time interval in the scenario, $\tilde{z}$ with probability $Pr(\tilde{z})$.

The optimization problem is subject to the following constraints:

Power balance

$$\mathbf{p}_{\text{diesel}}(\tilde{z}) + \mathbf{p}_{\text{w}}(\tilde{z}) + \mathbf{p}_{\text{dis}}(\tilde{z}) = \mathbf{p}_{\text{L}}(\tilde{z}) + \mathbf{p}_{\text{dump}}(\tilde{z}) + \mathbf{p}_{\text{ch}}(\tilde{z}) \tag{2.10}$$

Typical distribution losses are small (5%) but may be extreme in some cases (15%). However, the effect in terms of the problem is simply that of additional load. There will be a small effect on storage sizing (slightly reduced rating) but it has been neglected here.

Diesel constraints

$$\mathbf{p}_{\text{diesel}}(\tilde{z}) \geq \mathbf{1} P_{\text{min}} \tag{2.11}$$

In the case where the diesel is allowed to shutdown—this assumes that the balance of plant functionality is performed by the ESS during these periods—equation (2.11) becomes:

$$\mathbf{u}_{\text{diesel}}(\tilde{z})\ P_{\text{max}} \geq \mathbf{p}_{\text{diesel}}(\tilde{z}) \geq \mathbf{u}_{\text{diesel}}(\tilde{z})\ P_{\text{min}} \tag{2.12}$$

This introduces binary variables, which complicates the solution of the optimization problem, requiring mixed integer solvers, such as [91].

Dump load constraints

$$\mathbf{p}_{\text{dump}}(\tilde{z}) \geq \mathbf{0} \tag{2.13}$$

ESS power constraints

$$\mathbf{p}_{\text{ch}}(\tilde{z}), \mathbf{p}_{\text{dis}}(\tilde{z}) \geq \mathbf{0} \tag{2.14}$$

$$\mathbf{p}_{\text{ch}}(\tilde{z}), \mathbf{p}_{\text{dis}}(\tilde{z}) \leq \mathbf{1}\ P_{\text{ess}} \tag{2.15}$$

ESS energy rating limits

$$\mathbf{0} \leq \mathbf{e}_{\text{ess}}(\tilde{z}) \leq \mathbf{1}\, E_{\text{ess}} \tag{2.16}$$

Energy transition

$$e_{\text{ess},t}(\tilde{z}) = \sum_{q=1}^{t} \left(E_o + \eta\, p_{\text{ch},q}(\tilde{z}) - \frac{1}{\eta}\, p_{\text{dis},q}(\tilde{z}) \right) \tag{2.17}$$

Also, as a means of respecting the fact that the storage should not completely neglect the requirements of the following day, a constraint is imposed on the energy at the end of the time series, such that it must be equivalent to the initial energy:

$$e_{\text{T}}(\tilde{z}) = E_{\text{o}} \tag{2.18}$$

This final constraint, although required here in the ESS rating problem need not necessarily be respected by an on-line operating algorithm. For the problem under discussion, this constraint serves to link the different scenarios using the energy in the device at the end (or beginning) of the interval. Another point worth mentioning is that neither E_{o} nor $\mathbf{e}_{\text{ess}}$ appear in the objective function. A modification to the formulation could include these, if it were of interest to penalize certain states-of-charge (SOC), for instance deep discharges. This would require more in-depth knowledge of the characteristics of the ESS technology in question and appropriate costs associated with these specific operating points.

2.3 Case Study

The above developed methodology was applied using a representative wind-diesel system and energy storage data. The objectives of this analysis were to evaluate the value of the stochastic formulation, determine the number of scenarios that were required to sufficiently capture the probabilistic nature of the random variable, and to evaluate the different approaches to modeling the wind-load relationship. The base case data is first introduced before proceeding to analysis of the results.

2.3.1 Base Case

Prior to performing parametric analysis, it is useful to define a base case to serve as a point-of-reference to which other results can be compared. Although its selection is somewhat arbitrary, the base case was selected with an effort to be as faithful as possible to data that is representative of the present situation. The energy prices selected, although realistic, were somewhat biased towards a non-zero ESS rating result, in order for subsequent analysis to be interesting. This also required a high installed wind penetration ($r_{\mathrm{rl,p}} = 0.9$) as illustrated later in the parametric analysis.

Wind and Load Data

In total, 12 separate wind resources (WRs) were used in the analysis but WR 12, from [92], was used for the base case analysis. A description of all 12 WRs is given in Appendix B. The dependence of the design on the wind resource characterisitic is treated in parametric analysis.

For all scenarios considered the IEEE reliability test system (IEEE-RTS) load data was used, [93]. Although it represents load data for an interconnected power system, the approximation was deemed reasonable, in that it follows the typical daily and weekly trends, and is a winter peaking system like the majority of remote systems. Also, suitable remote system data were not available for all hours in the year, making generation of a representative data set problematic, whose accuracy would be only as good as the assumptions made in developing the data.

The impact of using the aforementioned load data is that the results will likely tend to result in smaller ESS capacities. This is due to the fact that remote systems generally have a lower utilization factor (ratio between average and peak load). Therefore, the frequency of low-load-high-wind occurences (and consequently operation of the dump load) will generally be lower using the IEEE RTS data, making ESS sizing more conservative.

Economic and ESS Data

Table 2.1 provides the energy price data (diesel and wind) and diesel constraints. Table 2.2 gives the energy storage system's financial and efficiency data used in the analysis, which was extracted from [56].

Table 2.1 Energy price data and diesel constraints for base case

Project period [yrs.]	Discount rate [percent]	π_{e} [$/kWh]	π_{w} [$/kWh]	$P_{\min}$ [p.u.]
20	8.5	0.60	0.40	0.3

Parameters for storage characteristiscs and energy prices are required as part of the economic calculations. Using the fixed costs from Table 2.1 the daily incremental costs associated with amortization of the investment were calculated using the following rudimentary calculation of annuity:

$$\pi_{\mathrm{ess,e}} = \frac{\pi_{\mathrm{e,fixed}}}{365 N_a} (1+r)^{N_a} \tag{2.19}$$

This converts the incremental capital cost of the energy rating of the ESS, $\pi_{\mathrm{e,fixed}}$, Table 2.2, into a $/kWh/day amount. The project period, N_a, is 20 years and the interest is compounded annually, using a discount rate of 8.5%. The same approach was applied for the incremental capital cost of the ESS power rating. These parameters arise in the objective function as part of the calculation of daily cost of energy served, equation (2.7).

The energy prices associated with diesel fuel and small wind vary significantly in remote communities but the values chosen fall in the set of realistic values, as supported by references [27] and [94], respectively. After establishing a realistic range, the ultimate values for the base case were selected such that the sizing was favorable (as opposed to results where the ESS sizing was zero). This was done to facilitate the analysis but was deemed reasonable as the cost of diesel is expected to rise whereas the cost of wind energy will also rise but at a more moderate rate. As the cost of diesel was varied, the ratio of the cost of wind energy to diesel energy was kept constant at two-thirds.

2.3.2 Comparison of Deterministic and Stochastic Approaches

Stochastic optimization is proposed as an attractive alternative to deterministic analysis, since rather than considering the worst case, or the expected value, one can capture the

Table 2.2 Energy storage system data for base case[1]

$\pi_{\text{e,fixed}}$ [\$/kWh]	$\pi_{\text{p,fixed}}$ [\$/kW]	η
875	213	0.85

1. Typical ESS parameters were taken from [56] and corroborated using [57].

probabilistic nature of random variables using a number of scenarios. The scenarios are each a time series of arbitrary length, representative discrete portions of the probability density functions. Each of the scenarios has an associated probability that is used as a weight in the formulation of the problem. Considering the specific problem in question, this approach can be used to determine ESS ratings in such a way that they are rated non-zero only when there is a sufficient justification considering the shape of the random variable's *pdf*. In contrast, a deterministic approach could result in non-inclusion of the ESS in the design or one that is overrated, becoming an underused asset, due to an overly conservative or optimistic deterministic formulation of the problem.

That being said, without some form of validation of the sizing approach, the degree of goodness of a particular approach can only be evaluated by comparing metrics that result from solution of the problem. These metrics are introduced in the following sub-sections. Also, one should keep in mind that these metrics are only as good as the model's ability to correctly capture the data. While the results presented in this chapter are informative from the point-of-view of comparing different deterministic and stochastic formulations of the problem, their true value can only be established using simulation of the system with the resulting design in place. This analysis will be considered but is deferred to the next chapter.

What follows is a refinement of stochastic formulation before proceeding to the parametric analysis. This includes determination of the appropriate number of scenarios and evaluation of the merits of the different wind-load models.

Table 2.3 Dependence of ESS sizing base case results on number of scenarios, for continuous and mixed-integer formulations

Formulation Type	No. Scen.	P_{ess} [1] [pu]	E_{ess} [pu]	E_{o} [pu]	Expected Cost [$/day]	True [2] Cost [$/day]	Difference [%]
Continuous	1	0.153	0.766	0.193	8951	9874	9.35
	4	0.048	0.448	0.204	9487	9831	3.50
	9	0.110	0.616	0.143	9665	9845	1.83
	16	0.076	0.432	0.044	9686	9824	1.40
	25	0.057	0.376	0.052	9776	9817	0.42
	36	0.055	0.338	0.571	9791	9814	0.23
	49	0.084	0.279	0.041	9820	9833	0.13
	64	0.056	0.320	0.048	9816	9816	-
Mixed-Integer	1	0.131	0.320	0.188	8798	8671	-1.46
	4	0.170	0.485	0.055	8592	8600	0.93
	9	0.157	0.618	0.168	8608	8588	-2.33
	16	0.146	0.545	0.216	8549	8594	0.52
	25	0.142	0.656	0.126	8539	8602	0.73
	36	0.155	0.731	0.278	8514	8582	0.79
	49	0.152	0.682	0.113	8475	8594	1.38
	64	0.159	0.774	0.283	8452	8452	-

1. The base power and energies are 1 MW and 1 MWh, respectively.
2. The true cost is calculated by fixing P_{ess}, E_{ess} and calculating the cost using the maximum number of scenarios, i.e. 64. The value of additional scenarios is given by (2.21).

Number of Scenarios

As parameteric analysis requires repeated solution of an already fairly computationally involved problem, it is first necessary to decide on the number of scenarios required. The goal is to select the number of scenarios that will provide a good tradeoff between accuracy of the solution and the computational effort.

If an equal number of divisions of the *pdf* for the two random variables—$r_{\text{wl,e}}$ and ρ_{wl}—is considered, then the number of decision variables is given by the following:

$$n_{\text{var}} = n_1 + 24 \times n_2 \times n_{\text{scen}} \tag{2.20}$$

where the number of *first stage* variables, $n_1 = 3$, *second stage* variables $n_2 = 4$, and the number of scenarios, n_{scen}, is given by the square of the divisions of each probability density function. For example, if we consider 5 divisions of each *pdf*, the number of resulting variables is $3 + 24 \times 4 \times 5^2 = 2403$. For the formulation allowing diesel shut-down there are an additional 24 binary variables per scenario. Therefore, there is a strong motivation to limiting the number of scenarios. This of course needs to be balanced with an appropriate level of accuracy.

The value of additional scenarios can be approximated considering the difference between the expected cost given by the solution and the cost given by fixing the first-stage variables and solving the problem using the additional scenarios, [90]:

$$\text{Value}\left(n_{\text{scen}} + \Delta n_{\text{scen}}\right) = C_{\text{d}}\left(n_{\text{scen}}\right) - C_{\text{d}}\left(E_{\text{ess}}, P_{\text{ess}}, E_{\text{o}}, n_{\text{scen}} + \Delta n_{\text{scen}}\right) \tag{2.21}$$

The sizing solution was calculated for increasing number of scenarios using the base case data, for both the continuous and mixed-integer formulations of the problem, Table 2.3. As the number of cases is increased, the formulation more accurately represents the combined probability distributions of the two random variables, r_{wl} and ρ_{wl}. The more scenarios, the greater the computational burden and thus a tradeoff must be made at some point.

There are a couple of important observations to make. First, the ratings E_{ess} and P_{ess} both decrease with the number of scenarios and eventually level off once 4 or more slices are used for each distribution (25 scenarios). Also, the true cost of energy[3]decreases in a similar manner as the ratings. This provides a means of assessing when additional scenarios no longer provide additional benefit. Based upon these results it was decided that the 25 scenarios would be sufficient to achieve the degree of accuracy required (less than 1 % error with respect to the case of 64 scenarios). A third observation is that there is a significant difference in cost for the binary and continuous solutions, a fact that will be explored in greater detail later.

In the mixed-integer case, the same trend in reduction of error is not as apparent. This is likely due to the nature of the problem—it is highly nonlinear. With no other results,

[3]This is calculated by fixing the *first stage* variables to the determined optimal for that case and running again using the maximum number of scenarios (81 scenarios). 81 scenarios was selected as the maximum as moving beyond 9 discrete sections of each of the two *pdfs* resulted in memory limitations.

Table 2.4 ESS sizing base case results for various wind-load modeling strategies

Diesel Control Approach	Scenario Length	Number of Scenarios[1]	P_{ess} [pu]	E_{ess} [pu]	Expected Cost [$/kWh]
Continuous	24-hour	25	0.0075	0.0503	0.5802
	week	4	0.2174	3.0382	0.5636
	24-hour	25	no ESS	no ESS	0.5802
	week	4			0.5725
Diesel Shut-down	24-hour	25	0.0924	0.3381	0.5279
	week	4	0.1952	1.1478	0.4919
	24-hour	25	no ESS	no ESS	0.5399
	week	4			0.5387

1. To provide a fair comparison the number of scenarios were selected such that each model would have roughly the same number of *second stage* variables. This accounts for the apparently small number of scenarios for the week long models.

no claims can be made as to the number of scenarios that are required to sufficiently capture the characteristics of the wind. However, as it is the relationship between the number of scenarios and the ability to capture the probabilitic nature of the problem that is under question, it will be assumed that the results from the continuous case suggests that 25 scenarios is satisfactory for this purpose. Validation of these assumptions will be performed using simulation in Chapter 3.

In contrast to the stochastic approach used here, a Monte Carlo approach to the problem would use thousands of deterministic simulations, each coming up with optimal values for the ESS ratings. This would yield a distribution of energy storage ratings, with the expected value being the optimal rating of the device. While it would have been interesting to compare the sizing results with those obtained here, it was simply left as a task for future consideration.

2.3.3 Results for Different Wind-Load Models

The initially proposed wind-load model makes two simplifying assumptions that require further investigation: (i) that the 24-hour scenario is sufficient to capture the most important relationships between load and wind, and (ii) that the wind profile from each scenario

can be generated using a time-shifted, scaled version of a generic load profile. While these two assumptions may be perfectly reasonable, it is worth considering other options. To this end, two variations to the proposed approach for modeling of the wind and load, resulting in an additional three models, were considered, which are recalled briefly here.

The first variation was to simply extend the length of each scenario to one week (168 hours). The rationale for this choice was to relax the stopping constraint, equation (2.18). Using this new formulation the ESS would then be permitted to move energy between days as opposed to only being allowed intraday transfer of energy. Also, it required only slight modifications to the methodology for the 24-hour scenarios.

The second variation considered was to work with the profile of the residual load, p_{res}, or the difference between load and wind generation. The scenarios were then generated using an ARMA of the residual load data, together with the mean value for the corresponding scenario (see Appendix A, for a detailed description of scenario generation). Although ARMA models have been successfully applied in other wind applications (most notably in wind prediction algorithms), it did not produce good results for the present application, resulting in extremely large sizings of the ESS, which following simulation, proved to result in a very high costs of energy. For these reasons, the ARMA approach was discarded and only models (i) and (ii) were retained for further analysis.

The results for the ESS sizing problem for the base case are presented in Table 2.4, for the 24-hour and week long scenarios. There are a couple of trends worth noting. Firstly, the cases with ESS show costs that are equal to or less than those predicted for the cases without ESS. Second, the formulation using week long scenarios results in larger ESS devices, both in terms of the power and energy rating. Also, the cost of energy is lower in the cases using week long scenarios, with and without ESS, and both when diesel shut-down is permitted and when it is not. This is likely due to the fact that with the length of scenarios being longer, there are greater opportunities to shift larger amounts of wind energy further in time. Once again this does not prove that the week long formulation is the superior approach, as the cost of energy is an expected value, considering the model in question. This position cannot be taken until this assertion is supported by simulation results showing operation of the design.

2.4 Parametric Analysis

In this section the impact of the wind resource (both installed capacity and its probabilistic nature), ESS efficiency, diesel operating strategy, and economic parameters on ESS sizing and cost of energy are considered. The problem is solved using the base case values and for two additional cases, when relevant: the case with no ESS and when the capital costs of the ESS are neglected[4]. These latter two cases represent extremes, bounding the overall solution space. This facilitates interpretation of the results and discussion. In the following subsections, the effect of the different parameters previously mentioned are treated in turn.

2.4.1 Wind Resource Characteristics

The wind resource of the wind-diesel system will dictate the relationship between the wind and load profiles, in turn affecting the use of the dump load, which invariably impacts the ESS sizing result. Two sub-components that require further investigation are the penetration level (ratio of installed wind power capacity to peak load, $r_{\mathrm{wl,p}}$) and the actual characteristics of the wind resource (probabilistic features, including capacity factor and correlation of wind peak with load peak, daily and seasonally).

The installed wind capacity is treated in detail using WR 12 in the next sub-section. The results are then repeated for the other eleven WRs in the subsequent sub-section (the WRs are described in Appendix B). The diesel is assumed to be always on-line, shut-down operation is considered later in section 2.4.3.

Installed Wind Capacity

Figures 2.4, 2.5, and 2.6 provide, respectively, the variation of cost of energy, ESS ratings, and expected energies from the various sources (expressed on a base of load energy). Overwhemingly, the results indicate that there is only a very narrow window where ESS can bring value to the system. Even with the ESS fixed costs reduced to 0; a reduction of only 1 cent/kWh is possible at $r_{\mathrm{wl,p}} = 0.9$. In contrast, fixing the ESS rating to an arbitrary value always results in a higher cost of energy, even though dumped energy is lower. A non-zero rating is observed using typical numbers for capital costs; however, the rating of the ESS is very small as is the expected reduction in cost of energy, Fig. 2.4 and 2.5.

[4]ESS sizing was bounded in the case of zero capital costs by setting π_{ess} to 10^{-5}. Efficiency losses also serve to restrict ESS sizing.

One must bear in mind that the overall benefit of reduction of the cost of energy is very marginal—it is dubious that the project would go forward given the associated risks (site access issues, new technology). Reducing the capital costs does make things more attractive. The case where capital costs are neglected in fact give the maximum reduction in \$/kWh possible. The sizing in this case is quite different, as the concern becomes only optimizing the use of energy. The peak sizing with neglected capital costs actually occurs when the real sizing should actually be zero, indicating that the peak sizing does not necessarily coincide with a peak in dumped energy.

Turning to the energies from the various sources there are a number of trends that can be identified as wind penetration is increased, Fig. 2.6. Somewhat obvious, the energy from the wind increases while diesel energy decreases in a similar manner, up to $r_{\text{wl,p}} = 0.6$. At this point E_{dump} becomes non-zero and slightly later the non-zero ESS energy rating is observed over a small range. The total generated energy E_{gen} is simply the sum of 1 and E_{dump}, as expected since all energies are expressed on the base of E_{L}. At high penetration, ESS can no longer contribute value due to the fact that wind energy is too high. While this results in greater opportunity for storage of energy, it also eliminates opportunities to return the energy to the grid—the value stream disappears.

Wind Resource Dependence

In the previous section, WR 12 was used to investigate the variation of the design with installed wind capacity. As the wind power data for WR 12 was generated from wind speed measurement and a wind power curve, it is of interest to compare results with other wind resources, where the powers are generated using a more sophisticated approach (see Appendix B for an explanation of the different WRs). Here the 11 additional WRs were run to generate the cost of energy and ESS ratings versus the expected value of wind energy penetration, $E\,[r_{\text{wl,e}}]$.

The reasoning for using $E\,[r_{\text{wl,e}}]$, instead of $r_{\text{wl,p}}$ is that all WRs were plotted together. Given that each WR has a different capacity factor, this would have resulted in shifted curves had $r_{\text{wl,p}}$ been used, making comparison difficult. Using $E\,[r_{\text{wl,e}}]$ the curves are more or less centered around an optimum energy penetration of about 0.32, where the cost of energy reaches a minimum, Fig. 2.7.

Initial results revealed that a non-zero rating was achieved for only a single WR (other

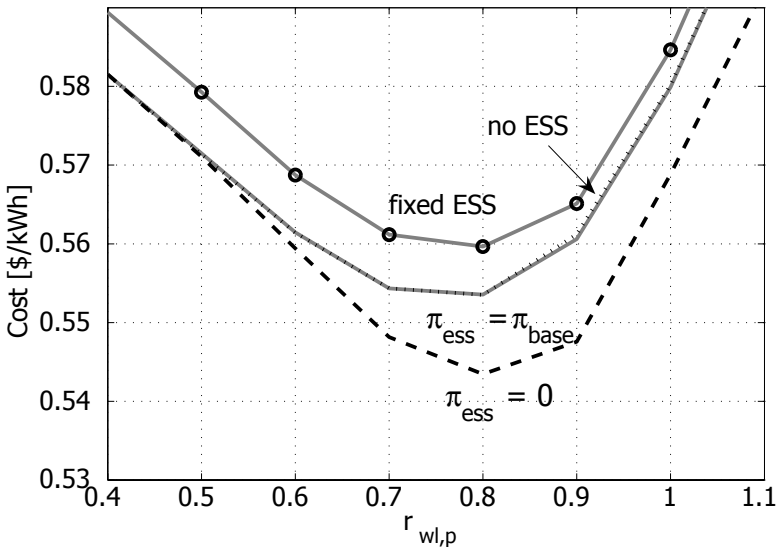

Fig. 2.4 Cost versus wind penetration for: no ESS (dotted line), ESS base case (solid grey line), ignoring the capital cost of ESS (heavy dashed line), and for a fixed ESS rating ('∘').

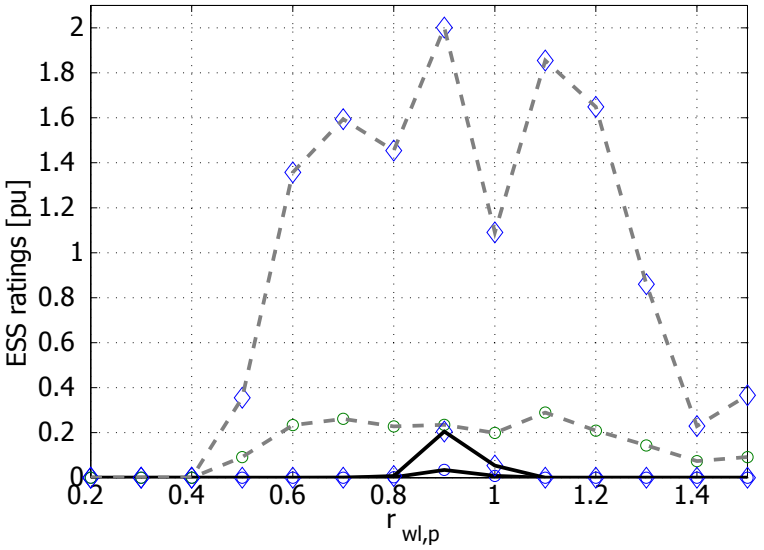

Fig. 2.5 Energy storage power ('O') and energy ('◇') ratings versus wind penetration for base case (solid line) and ignoring capital costs (dashed line).

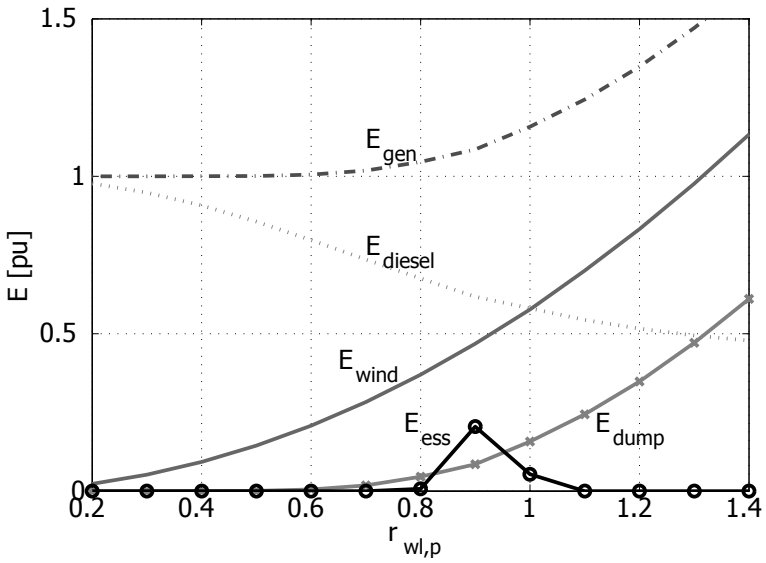

Fig. 2.6 Wind energy, diesel energy generation, total generated energy, dumped energy, and storage energy rating versus wind penetration.

than WR 12, in the previous section)—WR 1 . This bodes the question: what makes wind resources 1 and 12 unique? Due to the fact that the penetration level is increased, the answer must lie in the correlation coefficient, ρ_{wl}. It can be surmised that as ρ_{wl} approaches -1, the case for ESS improves.

The data reveal that the expected value of the daily correlation coefficient for WR 1, $E\ [\rho_{\text{wl}}]$ = -0.08 (see Appendix B). This is average when compared with the other WRs. However, it does have the largest standard deviation. It is important to note that the shapes of the discrete *pdf*s are important—they are not normal—and extreme events with relatively high probabilities can help explain the difference. Recall that 5 slices are used for ρ_{wl} and the standard deviation and mean of this random value only tells part of the story, due to the fact that the distributions for the different WRs are not normal. Also, it should be kept in mind that while WRs 1 and 12 give non-zero ratings, the ratings and cost reduction are quite small. Reducing the fixed costs of storage could indicate whether there is in fact something particular about these two WRs.

To investigate further the different wind resources, the fixed costs of ESS were then reduced by 50%. The cost of energy and the ESS ratings for this condition are given in Figs. 2.7 and 2.8, respectively. Now each of the wind resources gives non-zero sizing,

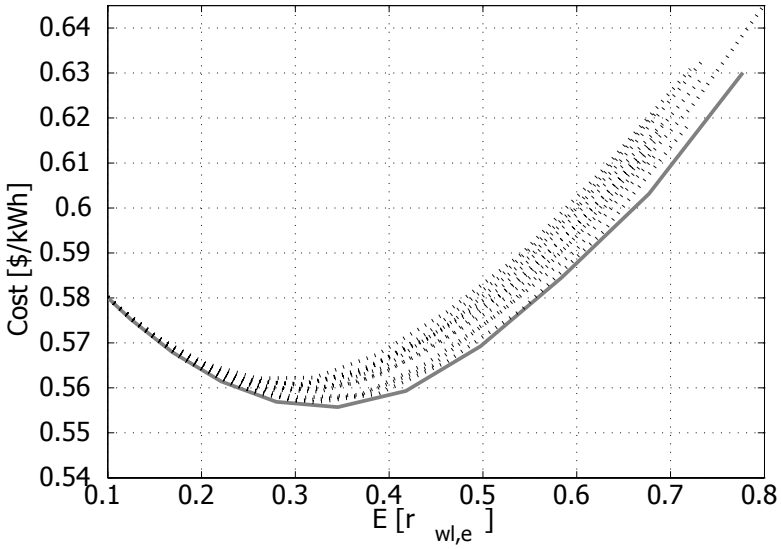

Fig. 2.7 Cost versus versus expected value of energy penetration for various wind resources, for the case of $\pi_{\text{ess}} = 0.5$. WR1 is given by the solid grey line.

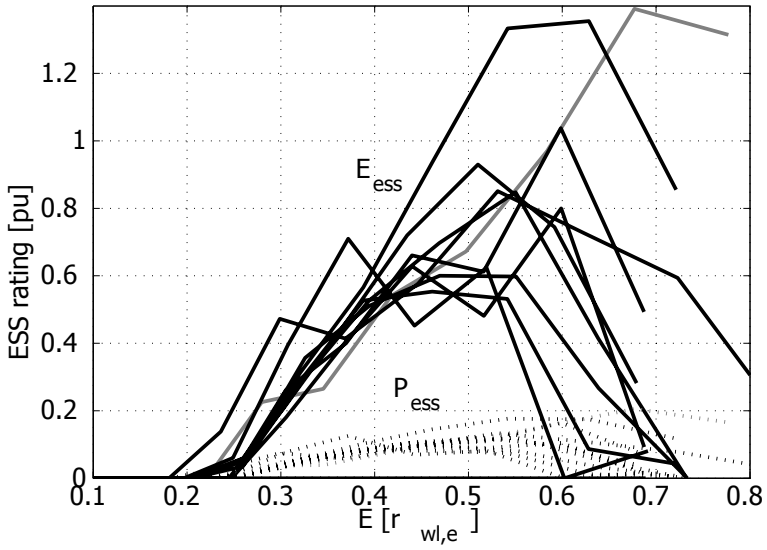

Fig. 2.8 Energy storage power and energy ratings versus expected value of energy penetration for various wind resources, for the case of $\pi_{\text{ess}} = 0.5$. WR1 is given by the solid grey line.

suggesting the earlier differences were in fact a result of slightly different *pdf* for ρ_{wl}. There is a characteristic shape of the cost of energy, which initially decreases (due to the less expensive wind energy contributing a larger share) and then increases (due to large amounts of dump load being required). Again, as was observed in the previous section, the peak rating for ESS is observed at higher penetrations than the minimum cost of energy.

As a final test, the extreme cases for wind-load correlation were considered, by lumping the whole probability of ρ_{wl} either at 1 (perfectly correlated) or -1 (negatively correlated). As load and wind are perfectly matched, the ESS sizing drops to 0, as the dump load is used sparingly, effectively eliminating the value stream. Negatively correlated patterns imply greater use of the dump load, and consequently higher cost of energy but also greater ESS capacity. The relationship between load and wind is critical in identifying sites where the conditions for ESS are favorable.

2.4.2 Energy Storage Efficiency

Considering the case of $r_{\text{wl,p}} = 1$, the role of storage efficiency was then considered. The expected cost of energy and ESS ratings were plotted as a function of efficiency, η. In general, the cost of energy reduces and ESS becomes more viable as efficiency improves, however, the changes are small, particularly when fixed costs are included. An improvement in efficiency from 0.5 to 1 results in less than 0.01\$/kWh gain in cost of energy when fixed costs are ignored, Fig. 2.9. When capital costs are included, the price of energy remains nearly constant, with only a slight reduction as efficiency moves beyond 0.8, due to the zero ESS sizing up to that point.

To some extent greater storage losses associated with poorer efficiency will replace dump load losses. However, efficiency also impacts the discharging process and as a result cost goes up as efficiency drops, even when capital costs are neglected.

The ESS rating results show that for the base case values, storage is not justified for efficiencies below 0.8, Fig. 2.10. Improving the efficiency to $\eta = 1$ results in increased ratings but as seen, only nominal reduction in the cost of energy. The overall rating of the base case changes continuously but never approaches the case with $\pi_{\text{ess}} = 0$ (not shown on the graph). The results only really go to show that with current prices for ESS technologies, capital costs are more of a determining factor in economic feasibility. Higher efficiency is, however, more favourable.

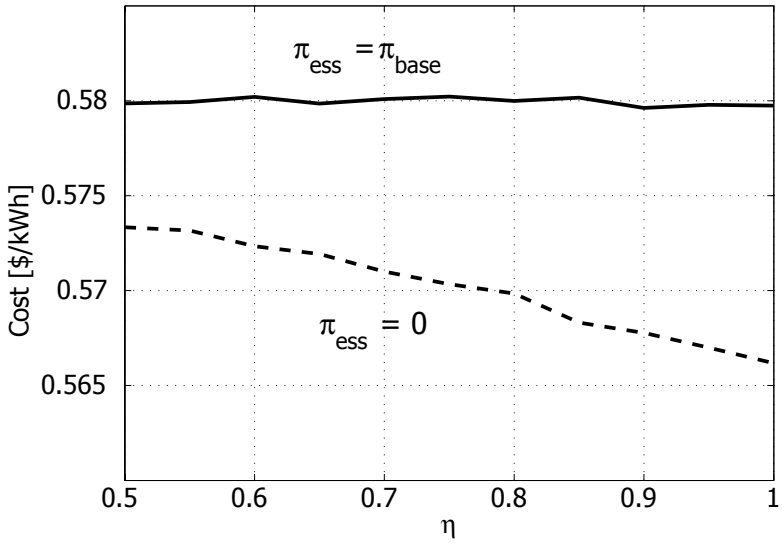

Fig. 2.9 Cost of energy served versus ESS efficiency for: base case ESS (solid line), and ignoring the capital cost of ESS (dotted line).

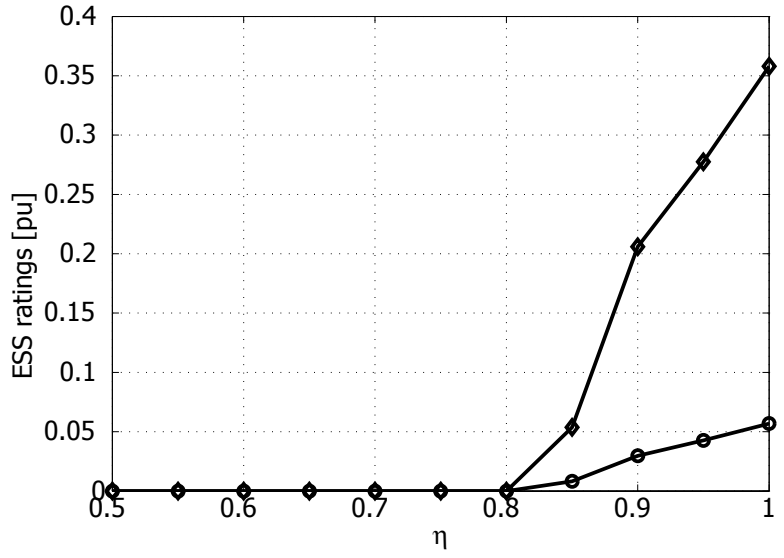

Fig. 2.10 Energy storage power ('O') and energy ('◇') ratings versus ESS efficiency for: base case ESS (solid line).

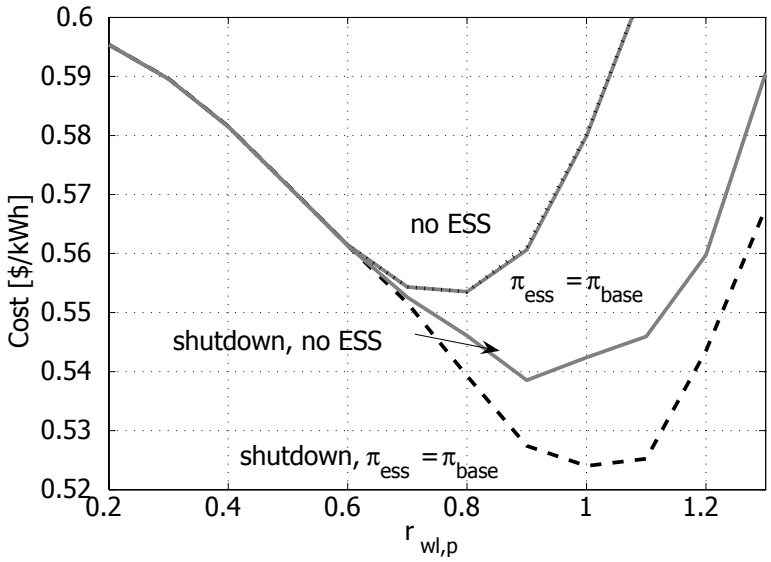

Fig. 2.11 Cost versus wind penetration for: no ESS (dotted line), ESS base case (solid line), and considering diesel generator shutdown (heavy dotted line).

2.4.3 Diesel Operating Strategy

Similar cases as in section 2.4.1 were repeated, only now considering the additional benefit that can be realized by allowing the ESS to replace the diesel as the balance of plant during certain intervals. The results are identical up to the point where storage first becomes justified, beyond which the costs are greatly reduced—at $r_{\mathrm{wl,p}} = 1$ the cost of energy supplied is reduced by nearly 10%, Fig. 2.11. Interestingly, a large component of this reduction is simply due to permitting the diesel to shut-down (roughly 6 %) as demonstrated by the middle curve. Furthermore the optimal penetration level is shifted to the right ($r^{\mathrm{opt}}_{\mathrm{wl,p}} = 1$, compared with 0.8 for continuous operation).

A much greater separation between the curves can be noted. By simply allowing shut-down we can realize large cost reductions. Even greater benefit is realized when storage is used instead of the dump load for establishing the power balance, as a result of energy being supplied back to the grid, later during higher load.

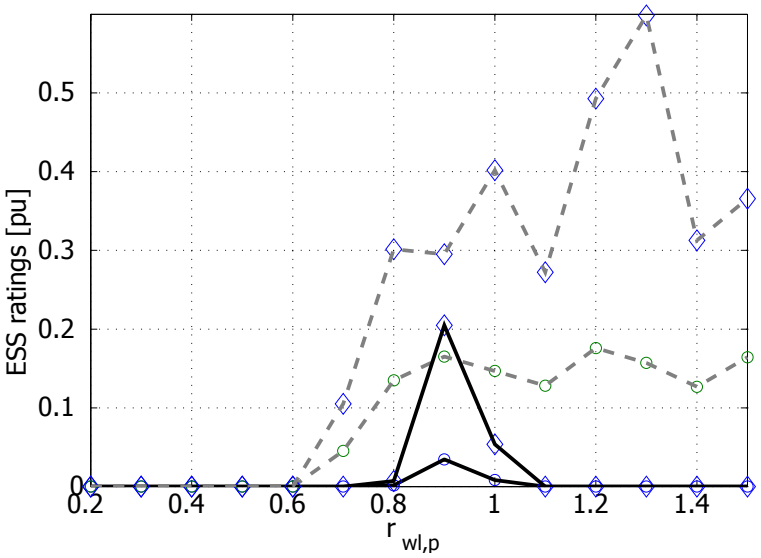

Fig. 2.12 Energy storage power ('O') and energy ('◇') ratings versus wind penetration for base case (solid line) and considering diesel generator shutdown (dotted line).

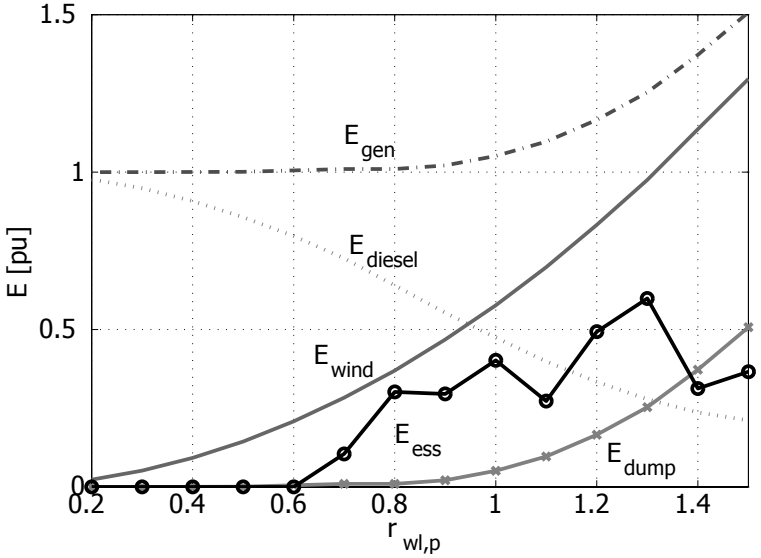

Fig. 2.13 Wind energy, diesel energy generation, total generated energy, dumped energy, and storage energy rating versus wind penetration considering diesel generator shutdown.

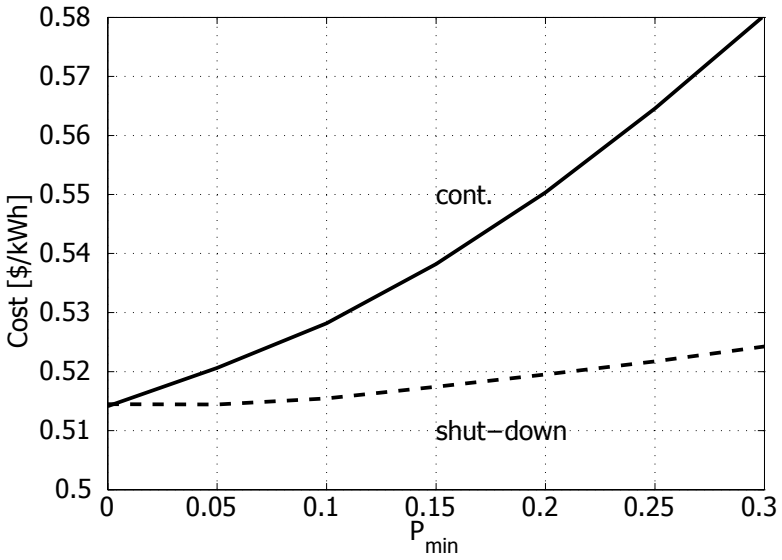

Fig. 2.14 Cost versus diesel minimum loading constraint for base case (dotted line) and considering diesel generator shutdown (solid line).

Considering the ratings of the ESS, Fig. 2.12, it can be noted that the ESS ratings for the case with binary variables are non-zero at lower penetration levels than for the continuous case. The peak rating for the binary case occurs when the rating for the continuous case has returned to zero. Plots of energies, Fig. 2.13, reinforce the observations from these results. The total generated energy actually remains constant (dump load remains zero) up to $r_{\mathrm{wl,p}} = 0.8$. This is reflected in the steep drop in diesel energy used, which is roughly 50 % that of the continous case at the upper end. E_{diesel} decreases even below 0.3, the point corresponding to continuous operation at the minimum loading.

As relinquishing control of the power system's performance to the ESS is still a fairly liberal move, the impact of using advanced low-load diesel was also considered. Relaxing the minimum loading constraint can greatly reduce the cost of energy served. The costs for the base case and diesel unit commitment modes initially start at the same point but as P_{min} increases the two diverge, Fig. 2.14. Increasing P_{min} results in a nonlinear increase in the cost of energy for the continuous case. Costs in the unit commitment case remain nearly constant.

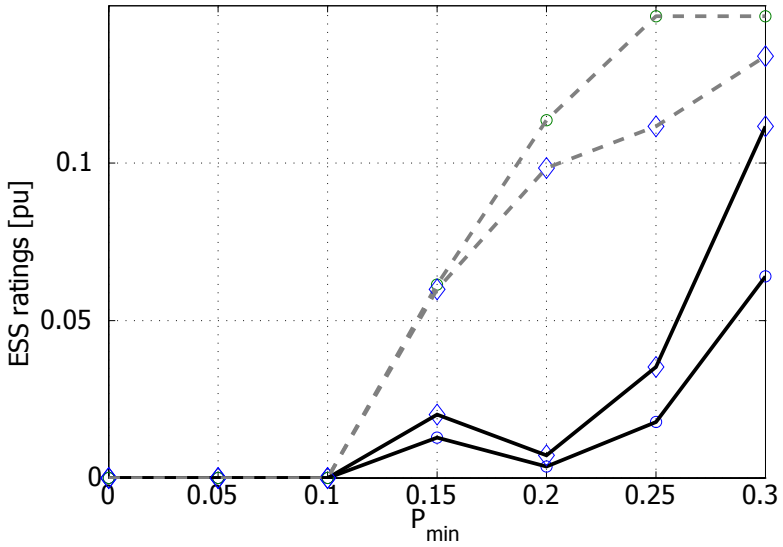

Fig. 2.15 Energy storage power ('O') and energy ('♢') ratings (top) and dumped energy (bottom) versus diesel minimum loading constraint, for base case (solid line) and considering diesel generator shutdown (dotted line).

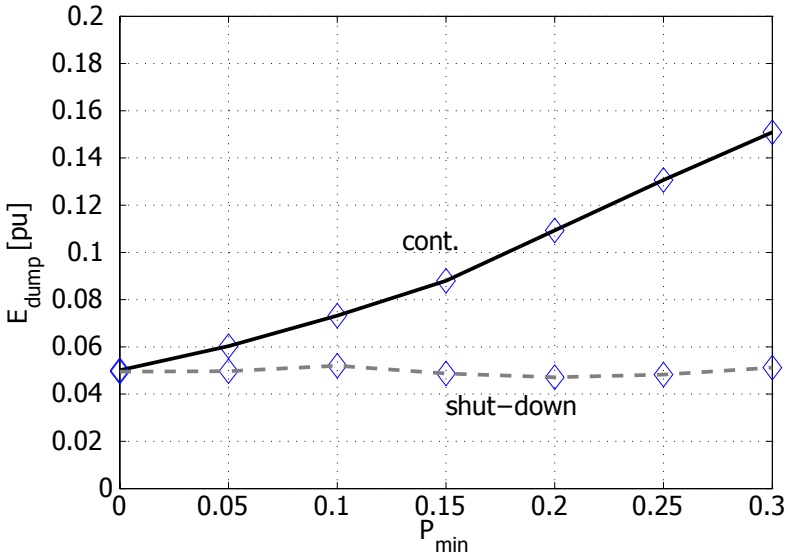

Fig. 2.16 Dumped energy as a function of minimum loading constraint, for base case (solid line) and considering diesel generator shutdown (dotted line).

No ESS is required (no justification can be made) if $P_{\min}$ is below 0.1, Fig. 2.15. The case including shut-down seems to be more constant in that it climbs quickly and then plateaus. $P_{\min}$ really needs to be above 0.2 before it makes sense to include storage in the continuous case. This mirrors the results from the cost of energy in Fig. 2.14.

The dumped energy is maintained constant in the shut-down case, Fig. 2.16. The curves intersect the y-axis at 0.05 due to the fact that p_{w} exceeds p_{L} and as a result dumping is required to maintain the power balance.

Wind Resource Dependence

The analysis from the previous section was repeated for the 11 other WRs, for cost of energy and ESS rating. Regardless of the wind resource, a couple of common trends emerge. First, the minimum cost of energy—in fact the entire curve—is shifted down, Fig. 2.17. The penetration level (again given in terms of $E[r_{\mathrm{wl,e}}]$ for reasons previously stated) associated with the minimum cost of energy is moved to the right, now around 0.55 (Fig. 2.17) compared with 0.32 (Fig. 2.7).

Similar trends noted for WR 12 were observed for the other WRs, considering the ESS ratings. ESS is justified at lower penetrations. The power rating seems to quickly plateau whereas the energy rating increase continuously with energy penetration. Power rating seems to stabilize whereas energy rating stabilizes between $E[r_{\mathrm{wl,e}}]$ of 0.4 and 0.6, followed by another upward trend, Fig. 2.18.

2.4.4 Economic Parameters

The analyses thus far have used typical economic parameters extracted from relevant literature. Because these are subject to change, it is perhaps of greatest importance to analysis the sensitivity of the solution on these paramters. If nothing else this helps to identify the parameters of greatest importance, helping to direct research efforts and facilitate an accurate evaluation of the risks involved.

Energy Storage Fixed Costs

The extremes of the ESS capital costs have already been given, through consideration of the cases $\pi_{\mathrm{ess}} = 0$ and of no ESS (equivalent to the case of $\pi_{\mathrm{ess}} = \infty$). These cases revealed

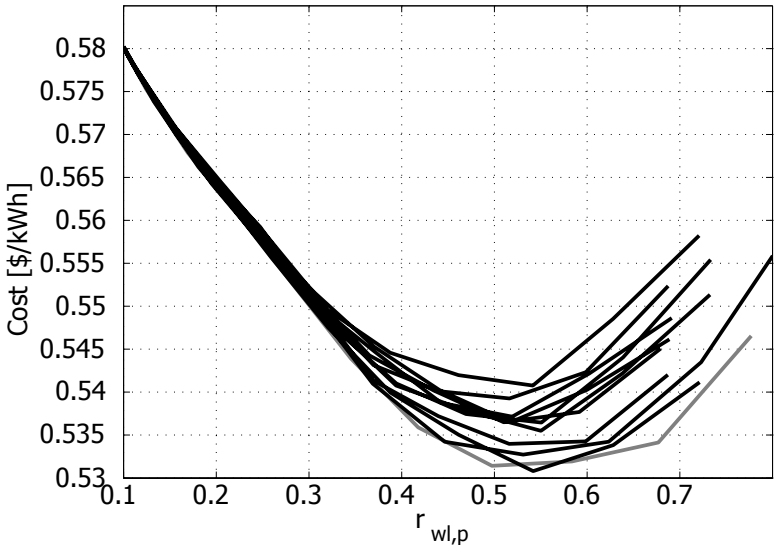

Fig. 2.17 Cost versus versus expected value of energy penetration for WRs 1-11.

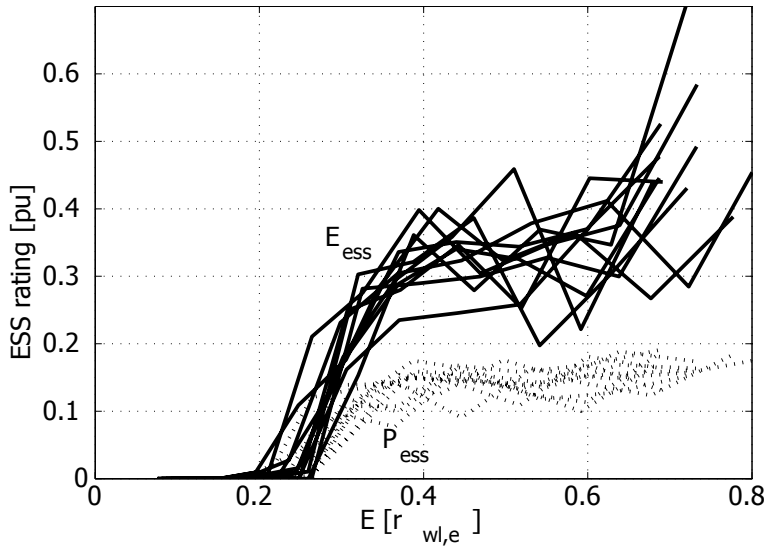

Fig. 2.18 Energy storage power and energy ratings versus expected value of energy penetration for WRs 1-11.

that this is a determining factor. However, it is useful to consider a smooth variation in order to see whether any specific trends present themselves.

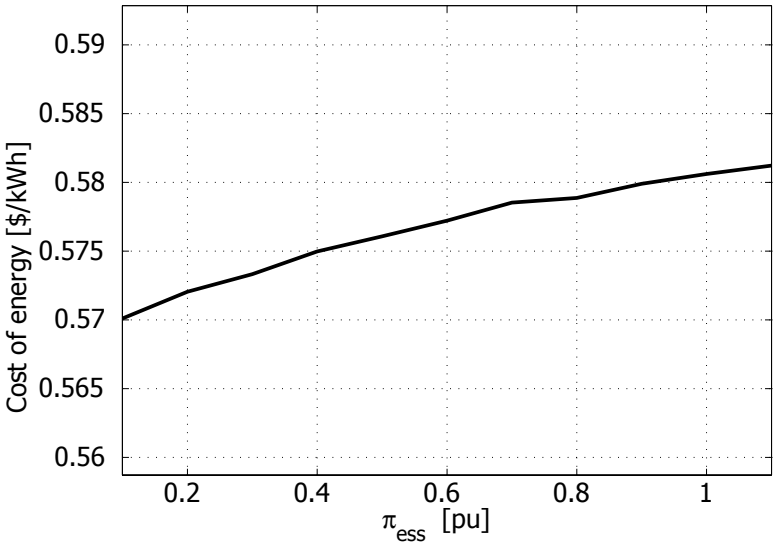

Fig. 2.19 Cost versus ESS incremental capital costs on a base of present prices.

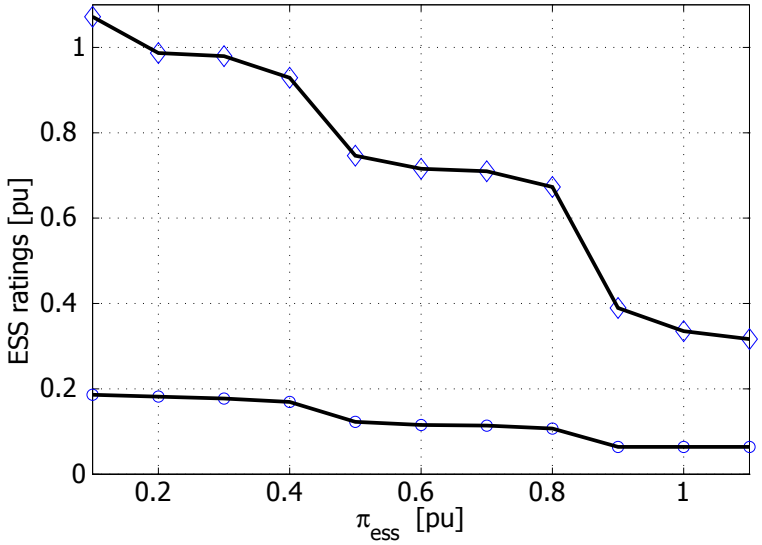

Fig. 2.20 Energy storage power ('O') and energy ('◇') ratings (top) versus ESS incremental capital costs.

Ideally, the results should shed light on the question: What does the price of storage need to be to justify its inclusion given current costs of energy? Reduction in fixed costs by 50% translates to about a 0.005 $/kWh reduction in cost of energy, Fig. 2.19. Storage sizing is sensitive to the parameter whereas energy price is only moderately affected, Fig. 2.20. It really depends what level of cost of energy reduction is required to justify the risk. This can be done by establishing a price reduction target that must be met, or alternatively, risk mitigation could be reflected in the discount rate chosen.

Figure 2.20 demonstrates very nicely what was seen in the wind resource results. For $\pi_{\text{ess}} = 1$, the ratings were very small, almost negligible. Also, as the fixed costs drop, the rating of especially the energy component increases.

Diesel Energy Price Increase

Fuel prices are extremely volatile, particularly in recent history, making prediction of future prices difficult. However, given two well established factors—increasing demand and reducing resources—it is reasonable to expect that the price increase should outpace inflation, possibly by as much as a factor of ten over the next twenty years. Therefore, a number of cases with different yearly average price increases were run, ranging from a rate comparable with inflation to a relatively high rate of 20%.

Table 2.5 provides a sample of the values considered and the equivalent value for π_{e}, using the following equation:

$$\pi_{\text{e}} = \frac{\pi_{\text{eo}}}{N_{\text{a}}} \sum_{j=1}^{N_{\text{a}}} \left(\frac{1 + r_{\text{i}} + r_{\text{e}}}{1 + r} \right)^{j-1} \tag{2.22}$$

where N_{a}, r, r_{i}, r_{e}, and π_{eo}, are respectively the project period, discount rate, rate of inflation, rate of diesel fuel increase, and current fuel price. This assumes that the current price of diesel generated electricity in the community is equivalent to that for wind, 0.4 $/kWh. The base case value considered thus far assume a π_{e} of 0.6 $/kWh, corresponding to an average yearly increase of roughly 10%.

The 10% year over year increase in fuel prices seems to be the break point to making ESS sizing justifiable, Figs. 2.21 and 2.22. This is not conincidental as it has as much to do with initial configuration of the base case than anything else. The value of π_{e} was selected

Table 2.5 Equivalent diesel energy prices for various yearly increases, corrected for inflation

Yearly price increase, r_e (%)	3	6	9	10	12	15	20
Equivalent price of diesel, π_e [$/kWh]	0.323	0.418	0.550	0.605	0.735	0.996	1.689

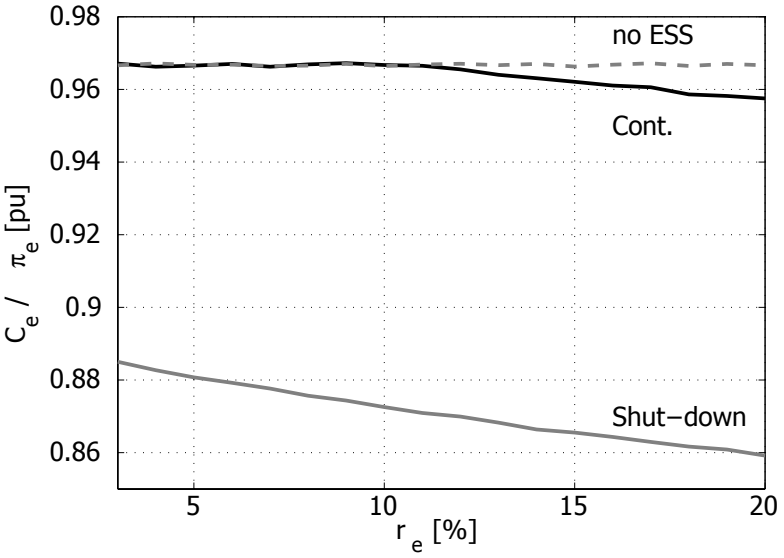

Fig. 2.21 Normalized cost of energy served as a function of diesel fuel price rates (corrected for inflation).

from within the realistic range as indicted by the literature albeit one that resulted in a non-zero ESS rating.

Higher yearly increases make the investment in storage more and more lucrative, with an up to a 1% reduction in the cost of energy (the real cost reduction is in fact much greater since costs are expressed on the base of cost). Considering the real costs, at r_e = 10 %, the cost of energy is about equal to that without storage, or 0.5838 $/kWh. At r_e = 20 %, the cost of energy with ESS is 1.6172 $/kWh compared to the cost without ESS of 1.6299 $/kWh. The case for shut-down is even more interesting, where a nearly linear decrease is observed up to an 11% reduction at the higher end, or 1.4525 $/kWh, almost a 0.18 $/kWh reduction.

Considering the power component stabilizes more quickly whereas the greater the value

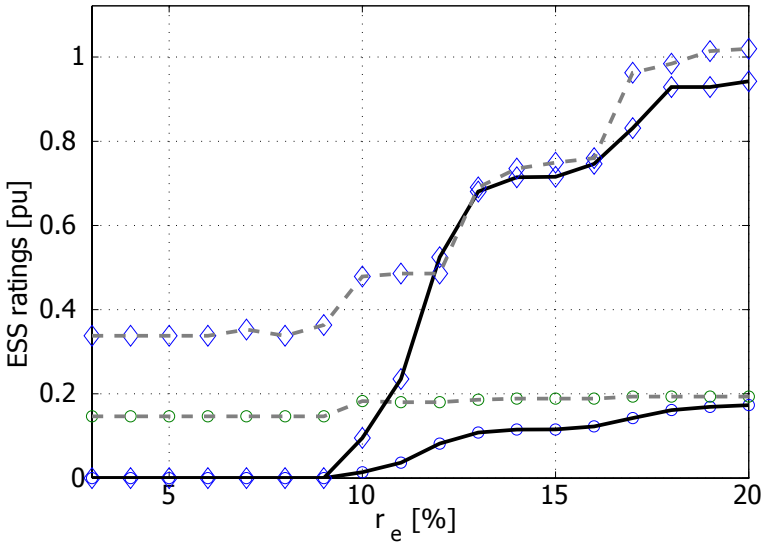

Fig. 2.22 Energy storage power ('O') and energy ('◇') ratings (top) versus ESS incremental capital costs.

of π_e, the larger the energy component ESS is in the design. The shut-down case indicates an almost constant value for the power component, even at low values of yearly increase. The energy rating increases in almost a stepwise fashion. Apparently, a specific cost is required to justify an additional energy rating; once the value is reached a large amount is added rather than in a continuous fashion. This is likely due to the fact that the problem encounters large blocks of potential savings that are eventually realized once the price is sufficiently high

2.5 Conclusions

In the chapter, a methodology for sizing of ESS for wind energy applications was developed and applied. The problem was posed as a two-stage stochastic optimization problem, with the objective of minimizing the cost of supplied energy. It was formulated for the specific case of ESS sizing for a wind-diesel power system. Special consideration was given to the modeling of the wind and load characteristics and various models were proposed. Results were given and analysed for a base case to investigate the differences between the expected costs for the different wind models and for selection of the appropriate number of scenarios.

Base case results showed that the stochastic formulation of the problem resulted in a

two-thirds reduction in ESS power rating and less than half the energy rating compared with the deterministic case (using the expected values). Results showed that roughly 25 daily scenarios were sufficient to capture the probabilitic characteristics of the wind and load relationship. The wind models described by the energy penetration, $r_{\mathrm{wl,e}}$ and the hourly wind-load correlation coefficient, ρ_{wl}, showed the most promising results.

A detailed parametric analysis was then performed to investigate the role of different parameters in determining ESS sizing and energy costs. Parameters investigated included: wind resource characteristics, ESS efficiency, diesel operating strategy, and economic factors. Wind resource characteristics considered included both the installed capacity of the wind plant, as well as the wind resource itself (using different wind data sources). The diesel plant was operating in a continuous mode, using low-load diesel technology (modeled using a relaxed minimum loading constraint), and with shut-down permitted. Economic factors contrasted the impact of ESS fixed costs with different rates of fuel price increase.

The sensitivity analysis revealed that ESS has a role to play in medium to high penetration scenarios but that the expected reduction in the cost of energy served (less than 1%) would not normally be sufficient to justify inclusion of ESS in the design. Storage efficiency does not significantly influence the cost; however, results show a lower bound on one way efficiency can be established, this value being 0.8 for the base case considered. Reduction of ESS capital cost appears to more importantly translate to reduced energy costs than efficiency improvements. Rates of diesel cost increase demonstrated that ESS can be economically viable for moderate to high rates, although uncertainty in future price estimates add too much risk. A variation of the formulation might consider modeling of this random variable in generation of scenarios.

Perhaps the most striking results are the differences associated with various diesel operating schemes, particularly when the diesel is allowed to shut-down and let the ESS serve as the balance of plant. Under this case the cost reduction compared with the base case was up to 11%. Taken together with the reduction of dumped energy, these results suggest that the combination of ESS and innovative diesel operating practices can lead to not only a marketable reduction in cost but also to more sustainable approaches of serving the energy needs of remote communities.

In an attempt to generalize the results, there are a few comments that can be made. The wind-diesel system demonstrates a trend that exists for integration of wind in interconnected systems, in that with increasing penetration wind initially reduces the cost of

energy, but beyond a certain point operating costs attenuate this benefit, possibly even resulting in higher system costs at extreme penetration levels. Although it appears self-evident, energy storage might help in integrating wind but likely only once the maximum cost reduction due to wind integration is realised. In other words, its value will be more in mitigating operational costs, assuming it is the lowest cost technology. As was seen in the diesel shut-down results, it may require pairing storage with innovative operating schemes to realise its full benefit.

In regards to the sizing results presented, there is a caveat that needs mentioning again. All costs of energy obtained are expected values and therefore the ESS sizing and costs of energy obtained are only as good as the models that go into the formulation. This element will be explored in greater detail in the following chapter.

Chapter 3

Optimal ESS Scheduling and Validation of Sizing Methodologies

> Truth, like gold, is to be obtained not by its growth, but by washing away from it all that is not gold.
>
> *Leo Tolstoy* (1828 – 1910)

3.1 Introduction

As alluded to in the previous chapter, it is necessary to validate the ESS sizing results through simulation of the operation of the design. This will permit comparison of the expected cost of energy for a particular ESS sizing with a true cost of energy resulting from its operation with the original time series data. This then provides the best indicator of the quality of the wind-load models used. However, this requires definition of an optimal scheduling that behaves roughly as expected from the ESS sizing formulation.

This chapter is organized as follows. First a description of the optimal ESS scheduling approach and its formulation is provided. This includes the ideal scheduling approach as well as inclusion of variations to the original formulation that may be required for practical reasons. This is followed by a comparison of the ESS sizing results from Chapter 2 with results obtained from running the scheduling algorithm with the full wind-load data set.

The impact of the practical considerations introduced are then investigated. Lastly, sample time domain results are provided for both continuous diesel operation and with shutdown permitted, before summarizing the important results and conclusions.

3.2 Problem Description

The components of the ESS sizing methodology under scrutiny are the choice of random variables, scenario selection, and scenario length. The operating approach has been selected with an attempt to be as faithful as possible to the manner in which the ESS was scheduled for each scenario of the ESS sizing problem. Only in this way can an accurate assessment of the value of the methodology be made.

ESS scheduling formulated as optimization problems has been previously presented in the literature, [58, 63, 67, 68, 74, 79, 84, 95]. Here, the formulation is similar but with slight variation for the specifics of the problem. The operating approach utilized extends from the sizing formulation developed in the previous section. Essentially, the objective function remains identical with the exception that fixed costs are no longer a decision variable, as the rating of the installation is now fixed. The performance of the operating approach should resemble as closely as possible the behaviour expected from the sizing approach. As such, many of the developments that follow include only slight variations to the ESS sizing problem. However, the way in which the input and output data are handled sharply bifurcates the formulation into two distinct problems.

3.2.1 Time Series Data

The wind and load data sources are the same sources used in the previous chapter. However, instead of using the *pdf*s of the two random variables described to generate the time series data, the raw data is used directly for the operating approach. The intent was to determine whether the models used correctly capture the important characteristics required to result in a good balance between fixed costs and reduction of dumped energy. This necessitates going back to the original source for the validation phase.

One important consideration is that while scenarios in the sizing problem were either 24 or 168 hours, the operating approach will be run for an entire year's worth of data, or 8760 hours. This would result in a huge problem if solved as a single problem. Not only would it be untractable using the computing resources available but would also unfairly accord an

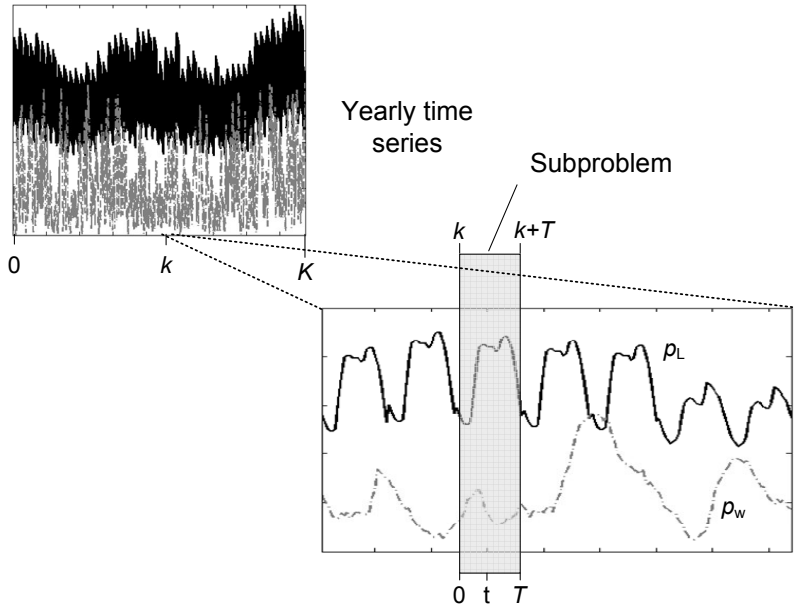

Fig. 3.1 Representation of the structure of the optimal scheduling algorithm and time series data of wind and load

advantage to the operating approach, by providing it with a greater amount of knowledge of the problem. This issue is addressed by considering a series of optimization problems that are solved sequentially. Each problem has a finite horizon of 24 hours, with the individual results being used in the configuration of the subsequent problem. The overall structure is illustrated in Fig. 3.1.

3.2.2 Problem Formulation

The formulation of each subproblem is presented here, followed by issues associated with coordination of the different subproblems. For a decision horizon of T hours, the problem can be stated formally as:

$$\min_{\mathbf{x}} \quad \sum_{t=1}^{T} \left(\pi_{\mathrm{e}}\, p_{\mathrm{diesel},t} + \pi_{\mathrm{w}}\, p_{\mathrm{w},t}\right) \qquad T = 24 \tag{3.1}$$

where $\mathbf{x}$ is given by:

$$\mathbf{x} = \begin{bmatrix} \mathbf{p}_{\text{diesel}} & \mathbf{p}_{\text{dump}} & \mathbf{p}_{\text{ch}} & \mathbf{p}_{\text{dis}} \end{bmatrix}^{\text{T}} \tag{3.2}$$

Note that the optimization problem is now a deterministic formulation; there are no longer *first* and *second stage* variables. The problem is subject to the following constraints:

Power balance

$$\mathbf{p}_{\text{diesel}} + \mathbf{p}_{\text{w}} + \mathbf{p}_{\text{dis}} = \mathbf{p}_{\text{L}} + \mathbf{p}_{\text{dump}} + \mathbf{p}_{\text{ch}} \tag{3.3}$$

Diesel constraints

$$\mathbf{1}P_{\min} \leq \mathbf{p}_{\text{diesel}} \leq \mathbf{1}P_{\max} \tag{3.4}$$

Dump load constraints

$$\mathbf{p}_{\text{dump}} \geq \mathbf{0} \tag{3.5}$$

ESS power constraints

$$\mathbf{p}_{\text{ch}}, \mathbf{p}_{\text{dis}} \geq \mathbf{0} \tag{3.6}$$

$$\mathbf{p}_{\text{ch}}, \mathbf{p}_{\text{dis}} \leq \mathbf{1}\ P_{\text{ess}} \tag{3.7}$$

ESS energy rating limits

$$\mathbf{0} \leq \mathbf{e}_{\text{ess}} \leq \mathbf{1}\ E_{\text{ess}} \tag{3.8}$$

Energy transition

$$e_{\text{ess},t} = \sum_{q=1}^{t} \left(E_{\text{o},k} + \eta \, p_{\text{ch},q} - \frac{1}{\eta} \, p_{\text{dis},q} \right) \tag{3.9}$$

It should be noted that, due to the fact that it is a sliding window, there is no stopping constraint, as existed in the sizing problem. The scheduling algorithm can be as aggressive as possible in deciding how to operate the ESS. This means that if the sizing approach perfectly characterized the problem, one should expect the cost of energy to be slightly less in the simulation of the system, since the stopping constraint has been eliminated. There is no reason to also impose this constraint here; in the sizing problem it was required to provide some link between different scenarios.

When the schedule is completed for the present hour, k, only the schedule for the hour in question is retained. At the next time step another optimization problem is solved, shifted ahead one hour in the wind and load profiles. The initial energy stated is defined by:

$$E_{\text{o},k} = e_{1,k-1}, \tag{3.10}$$

where k is the current time step, and $e_{1,k-1}$ corresponds to the energy state of the first hour, of the $(k-1)^{th}$ time step.

When diesel shutdown is permitted then (3.4) becomes:

$$\mathbf{u}_{\text{diesel}} \, P_{\max} \geq \mathbf{p}_{\text{diesel}} \geq \mathbf{u}_{\text{diesel}} \, P_{\min} \tag{3.11}$$

The approach as presented is somewhat idealized in that it considers that the wind power and load are precisely known over for the time horizon. As well, though not treated here, some specific constraints of the storage's SOC may need to be respected. Although these issues were not considered as part of the sizing problem, they will be introduced in the following section along with other considerations.

3.2.3 Practical Considerations and Limitations

In the ESS sizing methodology, uncertainty in the relationship between wind and load was handled using stochastic optimization and the ESS was modeled essentially as an integrator with efficiency losses. However, in operation is it reasonable to expect that the wind-load relationship is well known for the next 24-hours? Also, in reality should the states-of-charge of the ESS be equally weighted or should certain SOCs be favoured over others? Here these issues are considered, as well as a discussion on how the implementation of the operating approach can be easily realized through a simple adaptation of the sizing problem.

Numerical Implementation

As introduced in the previous section, the optimal operating approach extends directly from the formulation of ESS sizing. A simple realization of the operating algorithm can be developed, assuming a realization of the sizing approach is already in-hand. While this is more of a developmental consideration, it may be informative for some readers.

The operational algorithm can be most easily realized by repeatedly calling the sizing function with the upper and lower bounds of P_{ess} and E_{ess} fixed to the values determined in the sizing analysis. This can be done through the addition of four inequality constraints:

$$P_{\text{ess}} \leq P_{\text{ess,sizing}} \tag{3.12}$$

$$P_{\text{ess}} \geq P_{\text{ess,sizing}} \tag{3.13}$$

Likewise for the energy rating,

$$E_{\text{ess}} \leq E_{\text{ess,sizing}} \tag{3.14}$$

$$E_{\text{ess}} \geq E_{\text{ess,sizing}} \tag{3.15}$$

Modifications to the code are still required, since $E_{\text{o,k}}$ must be fixed (it is no longer a decision variable), according to 3.10, and one must coordinate the input/output data with the position of the sliding window. Also, approached in this way, the formulation requires a dimension that is slightly larger than that required (due to the inclusion of $E_{\text{o,k}}$, E_{ess},

and P_{ess}, and their constraints in the formulation). However, it avoids the need to re-do the entire implementation and may result in time savings.

State-of-Charge Penalizing Term

Research in lead-acid batteries, lithium ion and newer battery technologies suggest that lifetime of the battery is degraded as a result of frequent operation at low SOC, [69,96], As such, it is desirable to incorporate this fact into the operating algorithm. The simplest way of doing this is to re-define the minimum SOC as being non-zero, $E_{\min}$, thereby forbidding operation below that point, assuming this makes sense and is not unduly restrictive.

Although this can be done most easily by imposing a minimum SOC constraint, it would be less restrictive to permit operation at low SOC but discourage these points of operation. Rather than forbid operation beyond a lower SOC limit, the algorithm would then serve to reduce the frequency of operating below a defined lower limit. To this end, it is proposed to incorporate a SOC penalty term into the objective function. The new objective function is then given by:

$$\min_{\mathbf{x}} \quad \sum_{t=1}^{T} \left(\pi_{\text{SOC}}\, e_{\text{ess},t} + \pi_{\text{e}}\, p_{\text{diesel},t} + \pi_{\text{w}}\, p_{\text{w},t}\right) \qquad T = 24,\ \pi_{\text{SOC}} < 0 \tag{3.16}$$

where π_{SOC} is a SOC penalizing term that favours higher SOCs. As it is of interest to penalize low SOC, π_{SOC} should be chosen to be negative. It is difficult to chose its magnitude *a priori* but rather it should be based on specific battery characteristics and extensive parametric analysis. In this chapter, we will consider how this term will impact the ESS's use and cost of energy. In passing, an appropriate penalty term would require consideration of the specific application and the characteristics of the ESS.

Wind-Load Prediction

The above formulation assumes that the wind power and load profile are precisely known over the next twenty-four hour period. While short-term prediction of these quantities is usually fairly accurate, it is not perfect, [97, 98]. As well, some of these methods are extremely involved, relying on large amounts of data, are not at all obvious to the lay person, and may require periodic updates or tuning of the algorithm's parameters. For

these reasons, they may not be suitable for remote applications, where budget and resources are in limited supply.

To investigate the role of this uncertainty on the accuracy of the sizing results, a persistence method can be used as a simple and cost effective means to estimation of the wind and load. Stated formally:

$$\begin{aligned} p_{\mathrm{w},t} &= p_{\mathrm{w},t-24}, & \forall\, t = 1 \ldots 24 \\ p_{\mathrm{L},t} &= p_{\mathrm{L},t-24}, & \forall\, t = 1 \ldots 24 \end{aligned} \tag{3.17}$$

At this point, one might be inclined to question why stochastic optimization is not also used for the operating approach. The short answer is that it could. However, it is important to provide a justification of the value of resorting to a probabilistic approach, which depends on the degree of uncertainty and the cost of *not* modeling that uncertainty. The difference between the results obtained using the idealized operating algorithm (where wind and load profiles are known perfectly over each 24 hour period) and those obtained using a persistence method to prediction, will provide a good measure of the penalty of using a deterministic approach. This in turn, provides an indication of whether the effort of developing a stochastic optimization approach to scheduling is justified.

3.3 Results and Discussion

The optimal scheduling algorithm was used to simulate the operation of the ESS design over the course of a year's worth of data, under different conditions. These results were used in a first instance to compare the cost of energy realized with the expected cost of energy from the various ESS sizing results. Following evaluation of the different sizing approaches, the impact of the SOC penalizing term and the persistence method to prediction of wind and load profiles are then considered. Finally, time domain results are presented for a specific weeks of operation for illustration purposes.

3.3.1 Comparative Analysis with Energy Storage Sizing

A quantitative comparison of the Chapter 2 results with the simulation results requires the use of one or more metrics. The cost of energy will be relied upon as the primary indicator

of performance of a given sizing approach. The dumped energy is a second metric that is used, keeping in mind that it is linked, at least loosely, to the cost of energy (through additional diesel costs). The simulated cost of energy is given by:

$$C_{\mathrm{s}} = \frac{1}{E_{\mathrm{L}}} \left[\frac{K}{T} \left(\pi_{\mathrm{ess,e}} \, E_{\mathrm{ess}} + \pi_{\mathrm{ess,p}} \, P_{\mathrm{ess}} \right) + \sum_{k=1}^{K} \left(\pi_{\mathrm{e}} \, p_{\mathrm{diesel},k} + \pi_{\mathrm{w}} \, p_{\mathrm{w},k} \right) \right] \tag{3.18}$$

This is a sum of the levelized capital costs[1] for the year and the operating costs associated with the wind and diesel energy. As noted, the yearly cost of energy is converted to \$/kWh by dividing the yearly cost by the total load energy. The simulation and sizing results are compared below by: wind-load modeling approach, scenarios selection, wind resource, and diesel operating mode.

Wind-Load Modeling Approaches

Recall that two wind-load modeling philosophies were proposed: one based on the random variables ρ_{wl} and $r_{\mathrm{wl,e}}$, and one using the ARMA model of the residual load. These each included two scenario lengths—24 and 168 hours. As previously mentioned, the ARMA models resulted in very poor results in that the simulated costs greatly exceeded the expected costs, as a result of very optimistic ESS sizing. Consequently, it was decided to omit them from further analysis. The results from WR 12 for the two models using the correlation coefficient and energy penetration, for both continuous and shutdown operation are given in Table 3.1. The results include the case of no ESS, both resulting from simulation of the system and from the different sizing formulations.

The results without ESS are presented for two reasons. First they provide a point-of-reference for the simulation results with storage. If the cost with ESS is higher, this is a clear indication that the sizing methodology was poor, in that the benefit associated with ESS was not sufficient to offset its capital costs, resulting in a higher cost of energy for the community. Second, these results give a good idea of how good a particular model is at predicting costs resulting from time domain simulation, using probabilistic representations of this same data. In the case of continuous diesel operation, the difference between ex-

[1]The term K/T is required to convert the capital cost from a \$/day amount to a dollar amount using the total hours and horizon of the sliding window

Table 3.1 Comparison of ESS Sizing Results with Simulated Costs for Different Wind-Load Modeling Approaches, for WR 12, $r_{\text{wl,p}} = 1.0$

Control Approach	Scenario Length	Number of Scenarios [pu]	P_{ess} [pu]	E_{ess} [pu]	Expected Cost [$/kWh]	Simulated[1] Cost [$/kWh]	E_{dump} [pu]
Cont.	24-hour	25	0.0075	0.0503	0.5802	0.6408	0.2808
	week	4	0.2174	3.0382	0.5636	0.6411	0.2235
	24-hour	25	no ESS	no ESS	0.5802	0.6549	0.2834
	week	4			0.5725		
Shutdown	24-hour	25	0.0924	0.3381	0.5279	0.5469	0.1074
	week	4	0.1952	1.1478	0.4919	0.5410	0.0713
	24-hour	25	no ESS	no ESS	0.5399	0.5669	0.1598
	week	4			0.5387		

1. Simulated refers to the cost calculated after application of the sliding window approach to a the entire year's worth of data.

pected and simulated costs is quite large, whereas the gap is much smaller for the case of shutdown. Nonetheless, it can be seen for all models shown, the ESS sizing approaches all resulted in lower costs for the community.

The 24-hour models resulted in lower realized costs than the week long scenarios for the continuous mode of operation. Contrarily the week long scenarios seems to be the preferred modeling choice in the case of diesel shutdown. The week long scenarios resulted in much larger ESS, whose higher capital costs were offset by the lower dumped energy. The costs for the day long scenarios in Table 3.1 show similar cost for the two models but with the day long scenarios incurring larger diesel costs and the week long scenarios larger capital costs, due to the relative size of the installation. As in the case of no ESS, much better performance was observed in estimating the cost when diesel shutdown is permitted.

Scenario Definition

The ESS sizing methodology employed an equal number of scenarios for each of the two *pdf*s. It was previously observed that the correlation coefficient, ρ_{wl}, was an important parameter in dictating whether storage was economically feasible or not, with systems exhibiting greater tendencies toward negatively correlated wind and load being more conducive to larger ESS capacities. That said, it is worth investigating whether a greater

Table 3.2 Comparison of ESS Sizing Results for Different Scenario, for WR 12

Slices		Scenarios			Expected	Simulated	Diff.
ρ_{wl}	r_{wl}		P_{ess}	E_{ess}	Cost	Cost	%
4	4	25	122.7	746.3	0.5762	0.6395	9.90
5	3	24	170.9	1178.6	0.5739	0.6406	10.41
6	3	28	178.8	1259.1	0.5737	0.6410	10.50
7	2	24	50.6	253.1	0.5752	0.6399	10.11
8	2	27	47.1	294.6	0.5755	0.6398	10.05
9	2	30	29.2	178.3	0.5753	0.6402	10.14
11	1	24	107.9	541.9	0.5733	0.6396	10.37
24	0	25	122.7	825.8	0.5750	0.6396	10.10

1. The above cases were carried out with $\pi_{ess} = 0.5$ to avoid zero ESS sizing for some of the above cases.

number of scenarios placed on one variable or the other might lead to a more accurate assessment of costs and a better design (lower simulated cost).

To investigate the way in which the scenarios were generated, sizing results were generated for different divisions between the two random variables (always maintaining roughly the same number of scenarios) and simulating the resulting designs, Table 3.2. Interestingly, the cost of energy was not greatly affected but the rating of the ESS varies quite dramatically. This suggests that there is a very fine balance between the cost of additional ESS capacity and the potential cost reduction. In the end, an equal number of divisions for the two random variables persevered as the superior approach, indicated by the lowest simulated cost. Although negative correlation of wind and load generally leads to in larger ESS ratings, these results suggest that both variables are equally important in performing a good assessment of the appropriate ESS capacity.

Wind Resources

The other 11 WRs were then analyzed to investigate the dependance of the performance of the sizing approach on the characteristics of the wind resource. As WR 12 came from a different data source and the wind power was derived in a different fashion, it was important to see whether these facts affected the sizing methodology's performance. The results are given in Tables 3.3 and 3.4 for continuous diesel operation and allowing shutdown,

Table 3.3 Comparison of ESS Sizing Results with Simulated Operating Costs for WRs 1-11, $r_{\text{wl,p}} = 0.9$

Wind Resource	P_{ess}	E_{ess}	Expected Cost	Simulated Cost	Diff. %
1	0.1541	0.9696	0.5845	0.5812	-0.568
2	0.1764	1.3334	0.5774	0.5843	1.18
3	0.0816	0.6243	0.5823	0.5802	-0.362
4	0.1207	0.8476	0.5857	0.5830	-0.463
5	0.1196	0.9301	0.5776	0.5802	0.448
6	0	0	0.5806	0.5785	-0.363
7	0.0744	0.5313	0.5898	0.5861	-0.631
8	0.0891	0.4812	0.5844	0.6157	5.08
9	0.1082	0.7259	0.5987	0.5870	-1.99
10	0.0813	0.5977	0.5893	0.5824	-1.18
11	0.1083	0.6123	0.5764	0.5761	-0.0521

1. The above cases were carried out with $\pi_{\text{ess}} = 0.5$ to avoid zero ESS sizing for some of the above cases.

Table 3.4 Comparison of ESS Sizing Results with Simulated Operating Costs for WRs 1-11, with Diesel shutdown Permitted, $r_{\text{wl,p}} = 0.9$

Wind Resource	P_{ess}	E_{ess}	Expected Cost	Simulated Cost	Diff. %
1	0.1445	0.3647	0.5319	0.5397	1.45
2	0.1425	0.3693	0.5308	0.5472	3.00
3	0.1336	0.2530	0.5371	0.5515	2.61
4	0.1355	0.3278	0.5355	0.5476	2.21
5	0.1347	0.4590	0.5365	0.5496	2.38
6	0.1090	0.2581	0.5365	0.5524	2.88
7	0.1178	0.1975	0.5408	0.5518	2.03
8	0.1584	0.3440	0.5393	0.5495	1.86
9	0.1484	0.4117	0.5342	0.5394	0.96
10	0.1392	0.3469	0.5365	0.5469	1.90
11	0.1275	0.3255	0.5340	0.5468	2.34

1. The above cases were carried out with $\pi_{\text{ess}} = 0.5$ to avoid zero ESS sizing for some of the above cases.

respectively. In all cases, the first wind-load model (24-hour scenarios) was used.

Overall, much better agreement between the expected and simulated costs was observed, than with WR 12, particularly with regards to the continuous case. The only exception was WR 8, but even there the percent difference was half that observed with WR 12. Interestingly, an opposite trend was observed here in that the difference in cost of energy was generally larger in the diesel shutdown case, rather than in the continuous case (again WR 8 was an exception).

One possible explanation is the way in which the wind power was generated for WR 12, in that it was a direct application of the wind speed to an equivalent wind power curve. This results in a much more volatile power source as it assumes that each turbine in the plant sees the same wind speed. Consequently, the approximation for each scenario that the wind power be a scaled time-shifted version of the load profile becomes less valid, due to the higher volatility. Closer inspection of the different resources would be required to determine whether this hypothesis does indeed account for the differences observed. A good starting point would consist of analysis of the power density spectrums of the wind power and the load, to determine whether a link can be established between poor performance and the predominant frequencies of variation in the wind and load spectrums.

3.3.2 Impact of Practical Issues

Specific operational issues may degrade the theoretical cost of energy that is possible. Two concerns that will be investigated here are the inclusion of a SOC penalizing term to discourage low SOCs and errors in prediction of the wind and load profiles. Again, the impact on the cost of energy is the key metric that is monitored.

Persistence Approach to Wind Prediction

As introduced earlier, the persistence method is a simple approach to prediction of these quantities; it can be regarded as a single-term auto-regressive (AR) model, [99]. It can be easily implemented by simply retaining the previous twenty-four hours of hourly data for wind power and load. The persistence method was implemented using for the year's worth of data for WRs 1-11. The output of the model was used as the prediction of wind and load to reproduce results for the continuous mode of operation, Table 3.5.

As can be noted from the results, the difference in cost of energy is very small, less than

Table 3.5 Comparison of ESS Sizing Results with Simulated Operating Costs for Different Wind Resources

Wind Resource	P_{ess} [pu]	E_{ess} [pu]	Expected Cost [$/kWh]	Simulated Cost [$/kWh]	Simulated Cost 2[1] [$/kWh]	Diff.[2] [%]
1	0.1541	0.9696	0.5845	0.5812	0.5819	0.120
2	0.1764	1.3334	0.5774	0.5843	0.5851	0.137
3	0.0816	0.6243	0.5823	0.5802	0.5807	0.086
4	0.1207	0.8476	0.5857	0.5830	0.5838	0.137
5	0.1196	0.9301	0.5776	0.5802	0.5808	0.103
6	0	0	0.5806	0.5785	0.5785	0
7	0.0744	0.5313	0.5898	0.5861	0.5865	0.068
8	0.0891	0.4812	0.5844	0.6157	0.6165	0.130
9	0.1082	0.7259	0.5987	0.5870	0.5878	0.136
10	0.0813	0.5977	0.5893	0.5824	0.5830	0.103
11	0.1083	0.6123	0.5764	0.5761	0.5769	0.139

1. The second simulated cost was achieved using the persistence method for predicting the next wind-load profile, i.e. the profile in the next 24-hour period is assumed to be equivalent to the previous 24 hours.
2. The difference quoted here is between the ideal approach, which assumes perfect prediction and the persistence method.

1% in all cases. It is higher for the persistence method in all cases, as expected, due to the fact that there are now errors in the predictions (the case of WR 6 is the same only because no ESS could be justified for $\pi_{\text{ess}} = 0.5$). These results suggest that the persistence method would be quite appropriate for the scheduling of wind and is an argument against a stochastic approach to scheduling of the ESS. If other sources of uncertainty exists in similar applications, this question might be worth revisiting.

State-of-Charge Penalty

Unlike the prediction method consideration, the SOC penalizing term is not a essential requirement of the ESS operating approach. However, as mentioned, battery research has shown that frequent deep discharges (near zero SOC) can greatly reduce the lifetime of the battery. While this may not apply to all energy storage technologies, those that would be most appropriate for the application is question would likely have this as a consideration. While it is difficult to quantify the reduction in lifetime and the associated cost, the impact of the penalizing term on the cost of energy, C_{s}, and the *pdf* of e_{ess} can be obtained. This will provide some insight into the usefulness of its inclusion.

To this end, the results were run again using WR 12, for a number of different penalizing terms. Results are provided for the minimum value of e_{ess}, its average value, and C_{s}, given for both continuous operation and with diesel shutdown permitted, Tables 3.6 and 3.7, respectively. Note that the case of $\pi_{\text{SOC}} = 0$, corresponds to the base case result presented earlier.

Results show that C_{s} is not greatly affected by this penalizing term, whereas even small magnitudes for π_{SOC} result in large increases in the average value for e_{ess}, regardless of the mode of diesel operation. On the other hand, the minimum SOC, $e_{\text{ess}}^{\text{min}}$, requires very large penalizing terms in order to become non-zero. This may not necessarily be a concern, if the interest is in reducing the probability of a deep discharge event, and not in eliminating them entirely.

The usage of the energy storage system can also be visualized using the combination of scatter plots of e_{ess} and p_{ess}, and the *pdf* of e_{ess}. These plots are given for different penalizing terms to illustrate the impact of this term on the manner in which the ESS is utilized, Figs. 3.2 – 3.5.

Figures 3.2 and 3.3 show the ESS power and energy plots, for continuous diesel operation

Table 3.6 Impact of State-of-Charge Penalizing Term on ESS Utilization and Cost of Energy, Continuous Diesel Operation

π_{SOC}	$e_{\text{ess}}^{\min}$	$e_{\text{ess,av}}$	Expected Cost
0	0	0.2856	0.6400
-0.001	0	0.8668	0.6400
-0.01	0	0.8668	0.6400
-0.1	0	0.8668	0.6400
-1	0	0.8668	0.6400
-10	0	0.8672	0.6400
-100	0.2810	0.9549	0.6443
-1000	0.2810	0.9980	0.6511

Table 3.7 Impact of State-of-Charge Penalizing Term on ESS Utilization and Cost of Energy, with Diesel Shutdown

π_{SOC}	$e_{\text{ess}}^{\min}$	$e_{\text{ess,av}}$	Expected Cost
0	0	0.5502	0.5411
-0.0001	0	0.7426	0.5411
-0.001	0	0.7426	0.5411
-0.01	0	0.7426	0.5411
-0.1	0	0.7430	0.5411
-1	0	0.7475	0.5411
-10	0	0.7990	0.5412
-100	0	0.8899	0.5431
-1000	0.5057	0.9842	0.5575

and with diesel shutdown, respectively. Without the penalizing term, the scatter plot shows fairly complete use of the ESS for both continuous operation and with shutdown permitted. In the latter case, the scatter plots show an almost complete coverage of the space occupied. In continuous operation, different points seem to be repeatedly occupied, demonstrated by more deliberate grouping of the points and more white space. This is likely due to the fact that when the diesel is shutdown the ESS must serve as the balance of plant, resulting in more random behaviour.

As the penalty term is increased, the density of operating points shifts towards higher SOCs. At the higher end, the SOC migrates quickly to nearly fully charged and then becomes inactive for continuous operation. In shutdown the operating space is severely limited but some discharging is still observed, indicating that there is greater value associated with operation at those points than the penalty incurred.

There are two portions of the operating space that are never used—the upper right and lower left corners. These can be explained considering that the power term plotted is the power delivered over the hour in question and the energy is the state at the end of that hour. As a result, if one is charging there is a limit to how low e_{ess} can be at the end of the hour (defined by: $\eta\, p_{\text{ch,t}}\, \Delta t$). Likewise, during discharging, there is a limit of how high e_{ess} can be at the end of the hour (defined by: $E_{\text{ess}} - 1/\eta\, p_{\text{dis,t}}\, \Delta t$). These two equations define the valid operating area. The difference in the slopes between the two cases are due to the different ratios of ESS energy to power ratings, E_{ess} / P_{ess}.

Turning to the *pdf* of e_{ess}, these figures translate the density of points in the power and energy plots into probabilities of e_{ess}. The shutdown results initially are more distributed whereas the continuous case is lumped around very low SOCs. In both cases, even small magnitudes for π_{SOC} result in a shift of the probability densities to the right. A small penalizing term is likely sufficient for most applications unless certain low states of charge are to be strictly prohibited. If this were the case, a combination of a non-zero, minimum ESS SOC constraint, $E_{\text{ess}}^{\text{min}}$, together with an appropriate penalizing term could be used to yield the desired performance.

3.3.3 Operating Characteristics

Although time domain results cannot by themselves be used to quantify the value of an approach, it is useful to consider them for illustration purposes. A sample week for WR 12

is used here to give a better sense to the reader of how the system operates and to highlight some of the operational differences between the continuous mode and diesel shutdown.

Figures 3.6, 3.7, and 3.8, provide the operation of the system for the continuous mode, during a representative week. As can be noted, the week includes periods of high and low wind, and low load periods where—particularly during the weekend days—the diesel is operated at its minimum loading, resulting in extensive use of the dump load, Fig. 3.6. The storage device charges during these same periods, at or near full power, to limit the use of the dump load and then discharges once wind power subsides to liberate capacity, Figs. 3.7 and 3.8.

The behaviour of the system is quite different when shutdown operation is permitted, Figs. 3.9, 3.10, and 3.11. The same wind and load profiles now lead to numerous instances of diesel shutdown, predominantly during the weekend, and the dump load is used, but sparingly, Fig. 3.9. No clear pattern can really be discerned from the plots of the ESS power and energy, Figs. 3.7 and 3.8, respectively. The ESS does maintain a higher average SOC in this case than in continuous mode, as was observed in the yearly average. The ESS oscillates between charging and discharging and seems to be mainly active, when the diesel is shutdown or at minimum loading.

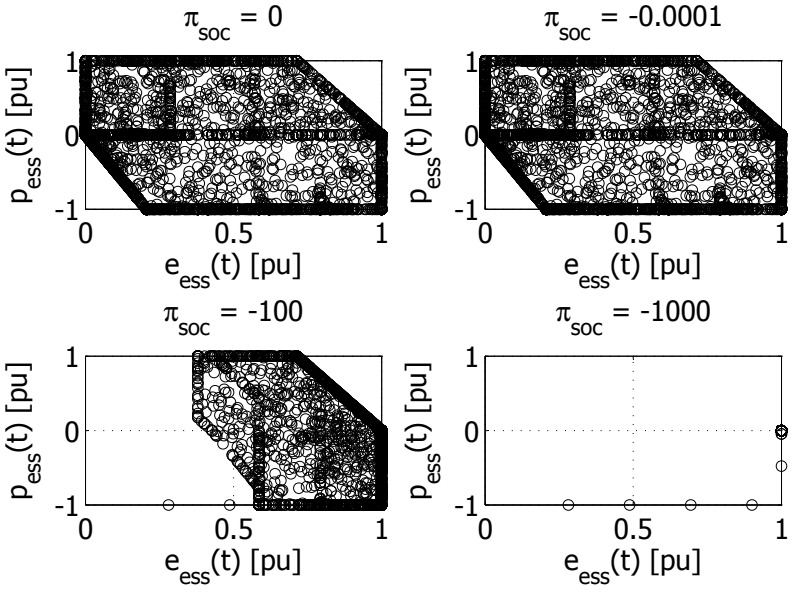

Fig. 3.2 Plot of ESS power and energy states for all hours in the year, continuous diesel operation, given for different penalizing constants, π_{SOC}. $P_{\mathrm{ess}} = 118$ kW and $E_{\mathrm{ess}} = 487$ kWh.

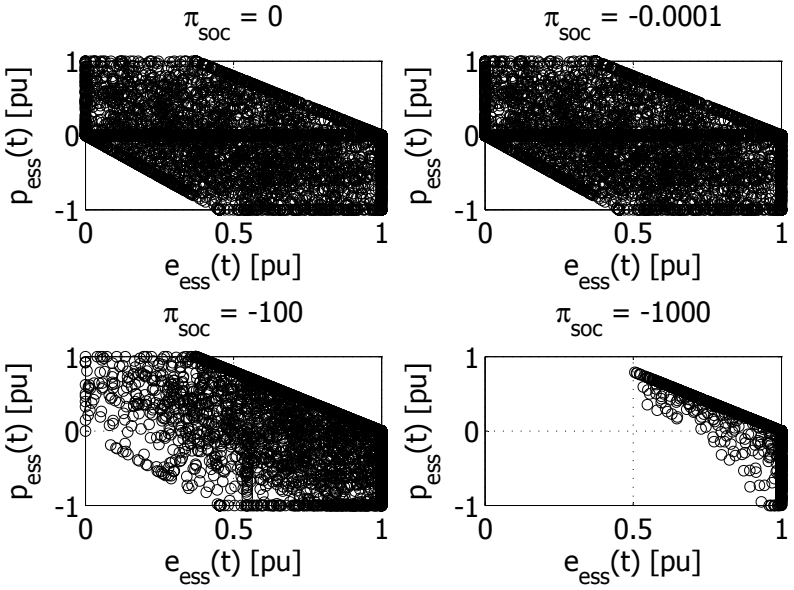

Fig. 3.3 Plot of ESS power and energy states for all hours in the year, given for different penalizing constants, π_{SOC}, with diesel shutdown. $P_{\mathrm{ess}} = 160$ kW and $E_{\mathrm{ess}} = 300$ kWh.

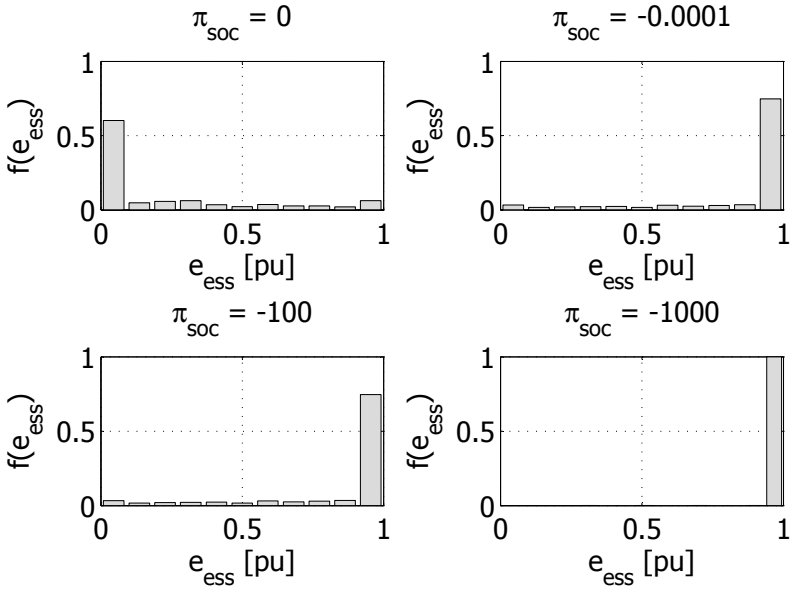

Fig. 3.4 Plot of ESS discrete probability density functions for different penalizing constants, π_{SOC}, for continuous diesel operation.

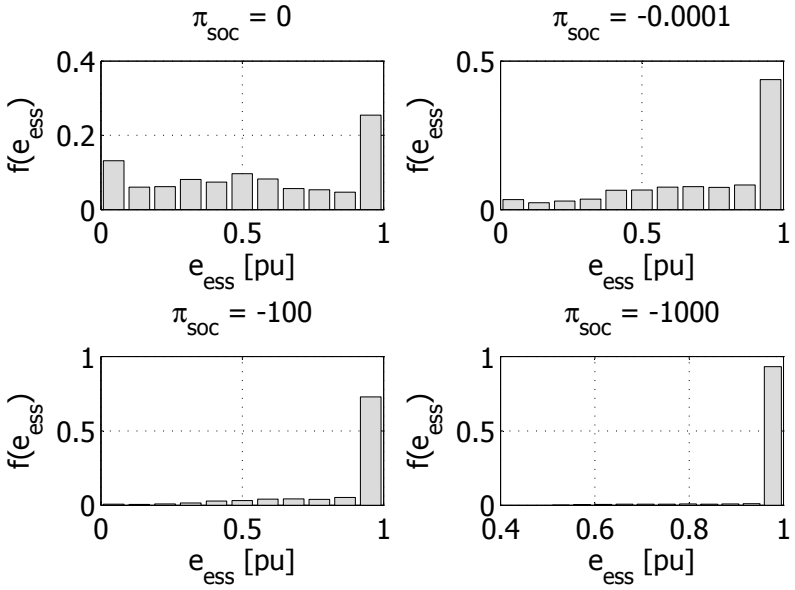

Fig. 3.5 Plot of ESS discrete probability functions for different penalizing constants, π_{SOC}, with diesel shutdown.

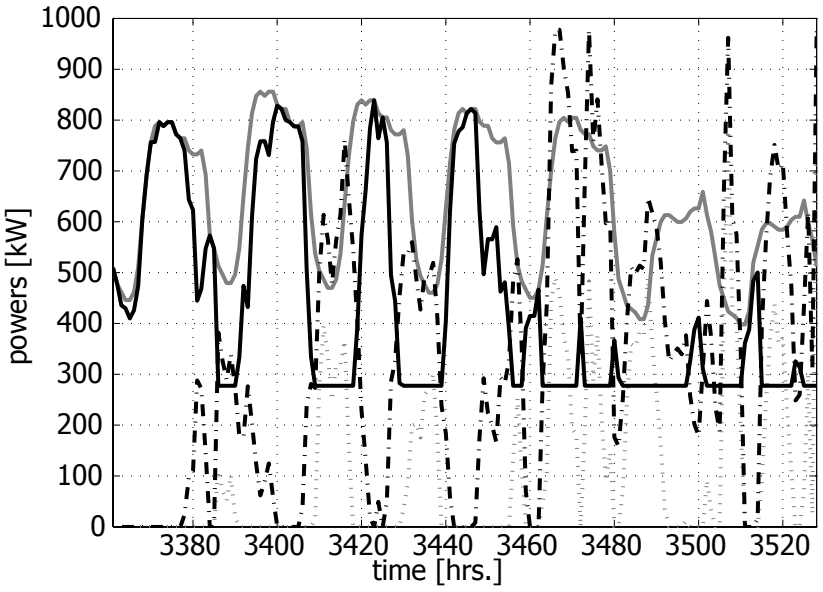

Fig. 3.6 Plot of load (grey), p_{diesel} (solid black line), p_{dump} (grey dashed line), and p_{w} (black dashed line), for continuous diesel operation over a representative week.

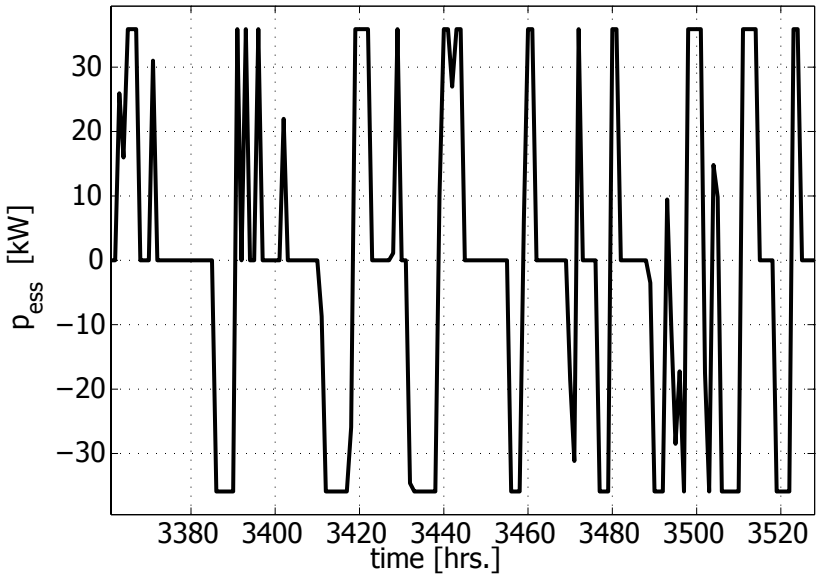

Fig. 3.7 Plot of ESS power, for continuous diesel operation over a representative week.

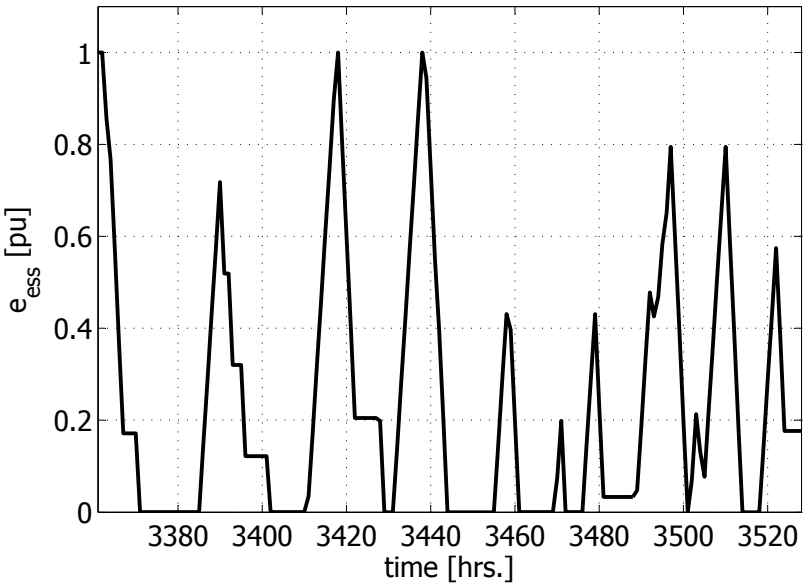

Fig. 3.8 Plot of ESS energy, for continuous diesel operation over a representative week.

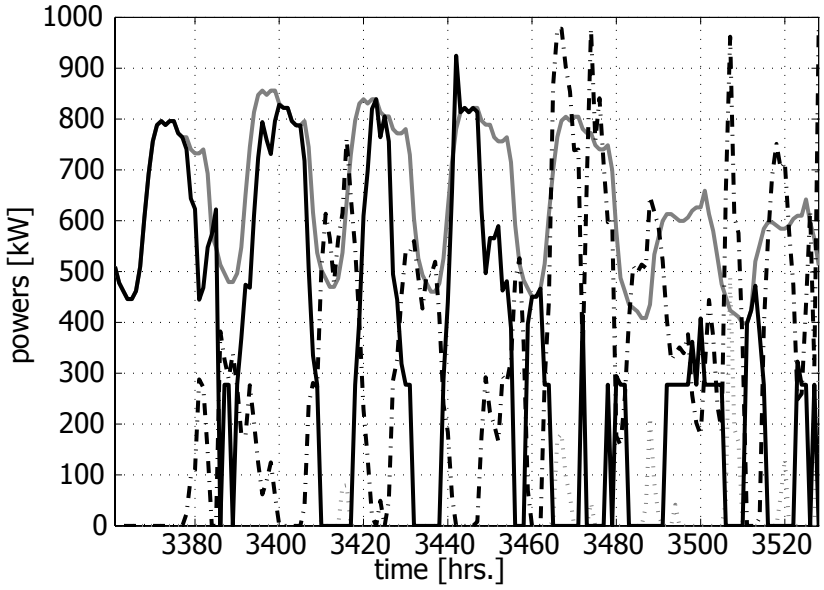

Fig. 3.9 Plot of load (grey), p_{diesel} (solid black line), p_{dump} (grey dashed line), and p_{w} (black dashed line), for diesel operation with shutdown permitted over a representative week.

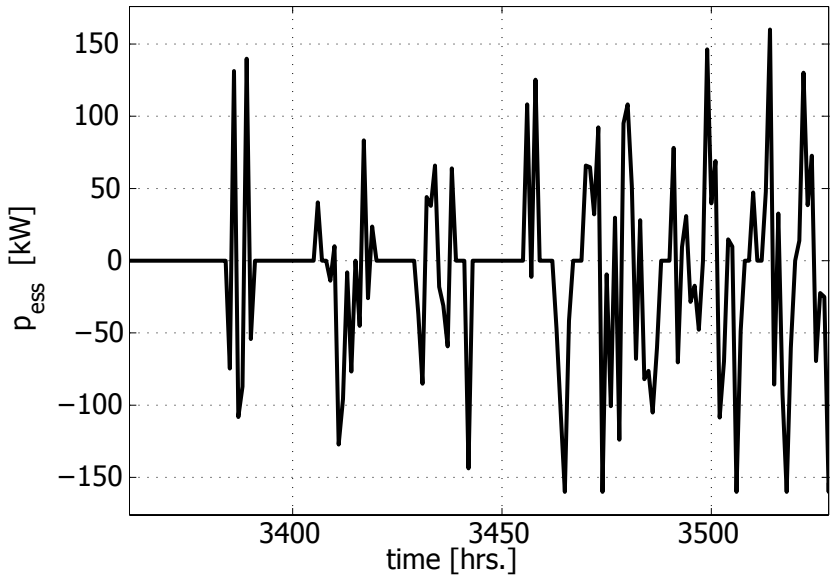

Fig. 3.10 Plot of ESS power, for diesel operation with shutdown permitted over a representative week.

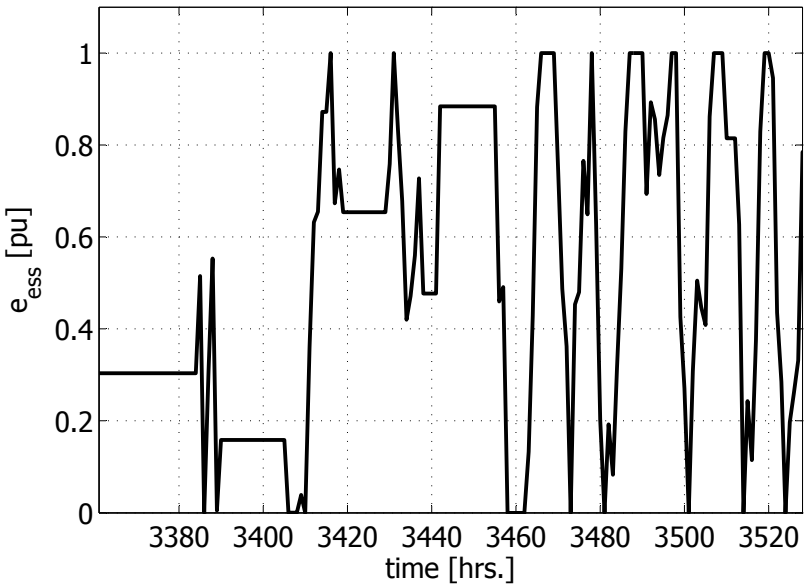

Fig. 3.11 Plot of ESS energy, for diesel operation with shutdown permitted over a representative week.

3.4 Conclusions

In this chapter, evaluation of the wind-load models and other elements of the ESS sizing methodology was performed by simulating the design using an optimal scheduling algorithm that was developed as an extension of the sizing methodology. As well, two practical considerations (limiting deep discharges, and short-term, wind-load prediction errors) were included as part of the analysis to better understand their impact on the cost of energy. Time domain results were also presented to illustrate the operation of the system.

Validation results compared the expected cost of energy, with the simulated cost of energy and dumped energy for different wind-load models considered in Chapter 2. The two random variables proposed—wind energy penetration and wind-load correlation—proved to be superior to ARMA models in characterizing the wind-load behaviour, demonstrated by designs that led to lower costs. The use of 24-hour scenarios led to designs with slightly lower costs of energy for continuous diesel operation whereas week long scenarios proved somewhat better when shutdown was permitted. The ability to correctly estimate the cost of energy using WR 12 was much better for operation with shutdown included.

On the other hand, in the majority of the other wind resources considered, the difference between expected costs and simulated costs was much smaller and the sizing methodology performed better for continuous operation. The specific nature of WR 12—much more volatile—likely accounts for these observed differences. However, more detailed analysis of the relationship between the characteristics of the WR and the performance of the sizing methodology is warranted.

It is important to keep in mind that the main intent of the results was to show whether or not there was good agreement between sizing results and operating results. In most cases, this led to lower costs than without ESS, supporting the fact that the design did bring value to the system. Nonetheless, the results did not provide the *true* optimal design, the design that would result in the lowest simulated cost of energy. This would necessitate performing a parametric analysis: defining a set of ESS ratings and simulating each using the optimal scheduling approach. The minimum cost design could then be obtained, assuming the set of designs was chosen sufficiently large and with a sufficiently high resolution, to include the optimal design. Visually, a three dimensional plot of these results would be revealing. That said, the results confirmed that for the ideal case, the ESS sizing methodology did result in lower cost of energy and wasted diesel fuel for the community.

The practical issues considered did not suggest that they would greatly impact the costs of energy. Errors associated with a persistence method to prediction translated to less than a 0.2 % increase in the cost of energy relative to the ideal case (perfect prediction). As such, it was concluded that neither a stochastic approach to scheduling nor complicated wind-load prediction algorithms were warranted for this application.

Addition of a penalizing term to the objective function is a good means of reducing the probability of low SOC, for negligible increases in cost of energy. If certain low SOC are to be completely avoided the $E_{\text{ess}}^{\text{min}}$ could be increased. Otherwise, a small penalizing term is likely satisfactory for discouraging these operating points. In any practical implementation, lifetime data and operating experience would need to be considered in refinement of the proposed operating strategy.

Time domain results nicely contrasted the differences between the continuous mode of operation and shutdown mode. In continuous mode, the ESS charging is coincident with dump load operation, and discharges in periods of low wind and high load. In shutdown mode, the ESS remains mostly inactive except during periods of shutdown, where it serves as the power balance, alternating between charging and discharging depending on the needs of the system. While these observations may not necessarily be seen for all weeks in the year, we expect that they are representative.

In general, the merits of a probabilistic approach to design can be evaluated by simulation using the same raw data that was used to generate the probability density functions. In ESS sizing for wind-diesel systems, this exercise not only provided an indication of the degree of goodness of the ESS design methodology but also facilitated a deeper understanding of the operational issues associated with this technology, how it is used, and its impact on the other elements of the system. While the optimization approach to ESS scheduling demonstrated good performance, it does impose a significant computational burden. Furthermore, time domain results revealed certain patterns, at least for the week presented, suggesting a rule-based strategy might be a simpler alternative. In the following chapter, we investigate whether the intelligence resulting from these off-line optimization results can be translated into a on-line approach using neural networks.

Chapter 4

On-line Control of Energy Storage Systems

> If both the past and the external world exist only in the mind, and if the mind itself is controllable - what then?
>
> *George Orwell* (1903 – 1950), 1984

4.1 Introduction

Off-line optimization to the ESS scheduling problem can be considered as a benchmark against which a given on-line control algorithm can be measured, much in the same way the ESS sizing methodologies were evaluated in the previous chapter. While powerful as an operating approach, an optimization strategy may not be as amenable to implementation in the field as alternatives. For one, the scheduling algorithm would require an efficient linear programming (or MILP) solver, along with the interfacing to coordinate input and output data. Moreover, the formulation and solution of this problem are generally quite computationally intensive. Even though the costs associated with this are not inordinate, it remains of interest to evaluate other on-line alternatives, if nothing else to again justify a moderately more complicated approach.

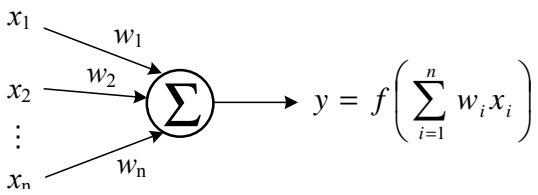

Fig. 4.1 Model of an artificial neuron

Artificial neural networks (ANN) and other artificial intelligent (AI) tools have been used in different areas of power systems, ranging from protection [31], to wind and load forecasting, [98], to electric hybrid vehicles, [100], to energy storage systems, [29, 101–103]. The drawback to use of these tools is that they often fall short in providing an analytical understanding to the problem and too frequently are employed as a quick solution. However, in certain instances, such as when it is desirable to extract patterns from a large amount of data, AI methods—in particular ANN—can be quite useful.

ANN are built from artificial neurons, Fig. 4.1, which serve as the building block for a variety of different architectures. The input-output relationship of a neuron is defined by input weights, $\mathbf{w}$, embedded in a function $f(\mathbf{x})$, which is generally exponential in nature but may be of other related types. This maps a set of inputs $\mathbf{x}$ to an output y. The general structure of these architectures consist of one input layer, one output layer, and one or more hidden layers, with varying numbers of neurons within each, Fig. 4.2. We will not belabour the theory of ANN as it is well treated in a number of texts, for instance [104].

This basic construct will serve as the basis for the ESS on-line control. A number of structures are first presented including different ANN architectures as well as choice of input variables. The proposed controllers are first given for continuous diesel operation and then for diesel shutdown. Results for the proposed controllers are compared with those of the off-line optimization algorithm, the source of the training data. Then, the controllers are tested for the remaining 19 years of data, years that were not included as part of the training set. Once again the performance of the ANN is compared with that of the off-line optimization approach. Finally, ESS operating data is plotted to illustrate how the ESS is utilized in the two cases before presenting the main conclusions from the chapter.

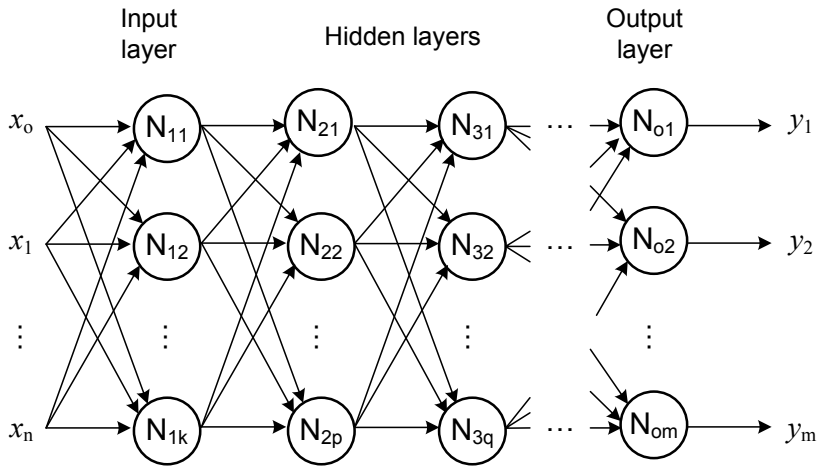

Fig. 4.2 General representation of an artificial neural network

4.2 Controller Design

The general process for ANN design includes: definition of input and output variables; definition of ANN architecture; generation of training data; training; and performance testing, first using the training data set and later using representative input-output data that is independent of the training data. The overall methodology of ANN controller design is illustrated in Fig. 4.3. As can be noted, the first two steps in the process were completed in Chapters 2 and 3, respectively. The present chapter will concern itself mostly with the latter two steps.

The training data for the ANNs comes from the optimum schedules that were obtained for the first year of the different resources. In the first instance, the controllers will be compared with optimal scheduling results by re-simulating the system once again and calculating the various performance metrics, but using the ANNs to determine the schedules. Following refinement of the design, the complete 20 year data set is used to provide a more general assessment of the controller's performance.

4.2.1 ESS Scheduling

In continuous diesel operation, only one decision must be made each hour—how to set the power for the ESS. The information available to the scheduling algorithm is, as before, the

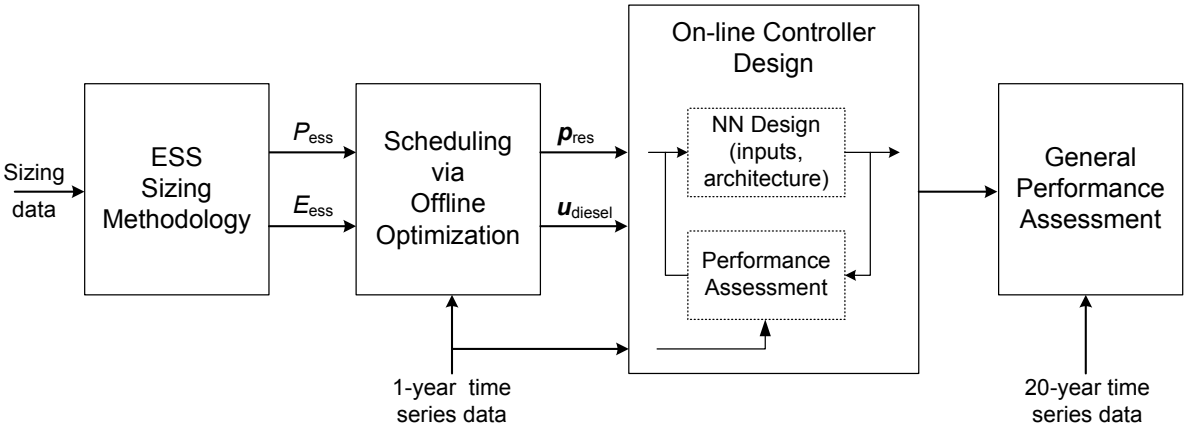

Fig. 4.3 Overall methodology for on-line ESS controller design and performance assessment

anticipated wind and load profiles. Perfect wind-load prediction will be assumed, since as seen, errors in prediction due to the use of the persistence method resulted in only marginally higher costs. As well, it is the difference between the off-line algorithm and the ANN that is of interest and not a global comparison across all methods.

Figure 4.4 shows the two main input-output ANNs considered, where e_k is the ESS energy state in hour k, r_{wl} is the energy penetration over the next 24 hour period, ρ_{wl} is the hourly wind-load correlation coefficient over the next 24 hour period, $p_{\text{res,k}}$ is the residual load in hour k, and $p_{\text{ess,k}}$ is the resulting ESS power schedule for hour k. The ANN architecture is presented generically and will be defined in the parametric analysis. In both cases, the SOC of the ESS is required, in order to capture how the scheduling changes as the ESS approaches its upper or lower bounds. The remainder of the inputs differ for the two cases in the manner in which the wind-load profile is described for the 24-hour horizon.

As the two random variables used in the sizing methodology yielded good results, it was decided to investigate whether good scheduling results could be achieved using only these two additional inputs. The full wind and load profiles for the next 24-hours were used in the second ANN structure, as were used in the off-line optimization results. Regarding the internal architectures of the ANN, different structures will also be investigated to see what combination of layers and neurons within each layer produces results that best match those from the off-line optimization.

Unlike the optimization approach, the ANN may propose a schedule that either exceeds

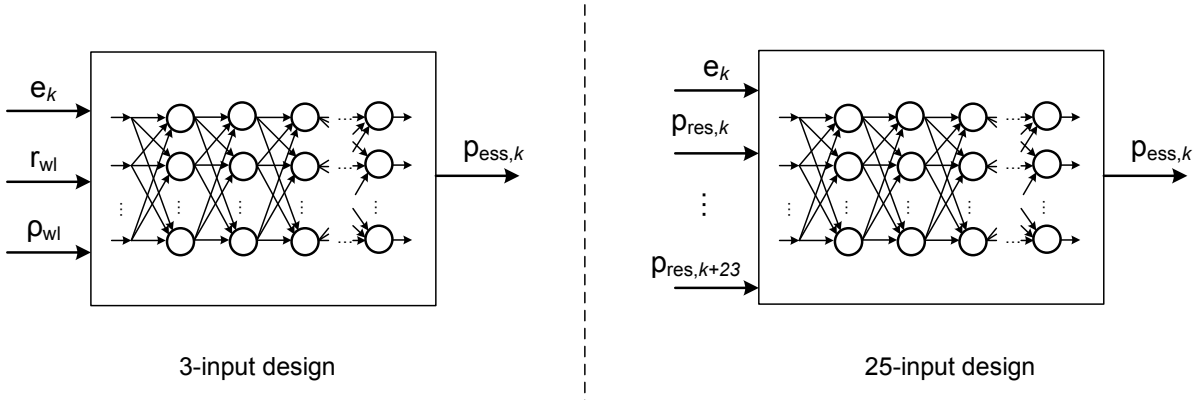

Fig. 4.4 ANN designs for ESS control for continuous diesel operation

the power ratings of the ESS or that would result in the ESS being either completely discharged or overcharged if maintained for the hour in question. This risk would always exist unless the ANN perfectly fits the training data. This is due to the fact that these constraints are not explicitly captured in the ANN but rather are implicit in the input-output relationship it attempts to model. Therefore, various provisions must be made to ensure that the ESS constraints are not violated as a results of the schedule from the ANN.

To this end, the following equations are implemented following the generation of the ANN ESS power reference, $p^{ANN}_{\text{ess,k}}$, for the hour k. First the power rating is checked:

$$p_{\text{ess,k}} = \begin{cases} p^{ANN}_{\text{ess,k}} & \text{if} \quad |p^{ANN}_{\text{ess,k}}| \leq P_{\text{ess}} \\ sgn(p^{ANN}_{\text{ess,k}}) P_{\text{ess}} & \text{if} \quad |p^{ANN}_{\text{ess,k}}| > P_{\text{ess}} \end{cases} \tag{4.1}$$

where $sgn(\cdot)$ is the sign function. In addition, the resulting power reference must be checked to determine whether it leads to over- or undercharging. In the case of charging ($p^{ANN}_{\text{ess,k}} < 0$), $p_{\text{ess,k}}$ is given by:

$$p_{\text{ess,k}} = \begin{cases} p^{ANN}_{\text{ess,k}} & \text{if} \quad E_{\text{o,k}} - \eta\, p^{ANN}_{\text{ess,k}} \leq E_{\text{ess}} \\ -\frac{E_{\text{ess}} - E_{\text{o,k}}}{\eta} & \text{if} \quad E_{\text{o,k}} - \eta\, p^{ANN}_{\text{ess,k}} > E_{\text{ess}} \end{cases} \tag{4.2}$$

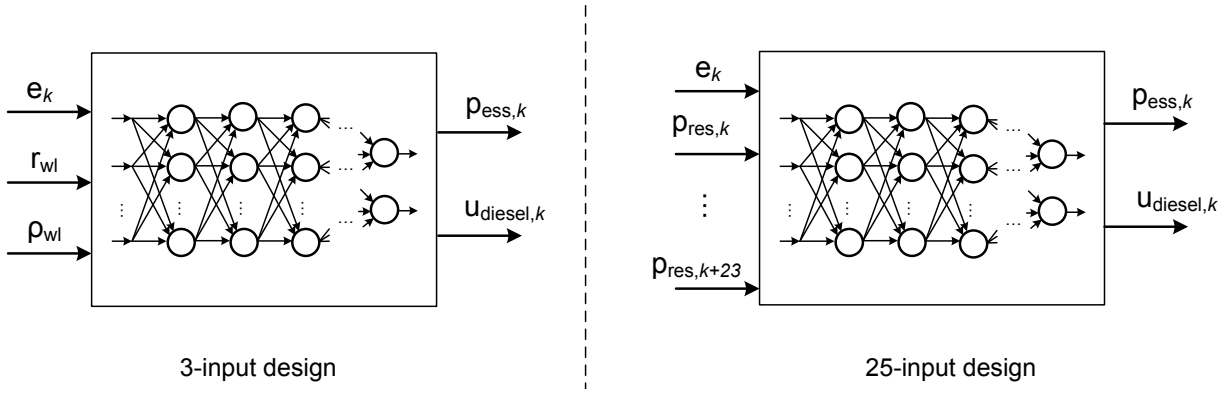

Fig. 4.5 ANN designs for ESS control with diesel shutdown permitted

This redefines $p_{\text{ess,k}}$ to arrive at $e_{\text{ess,k+1}} = E_{\text{ess}}$, if the schedule would have resulted in overcharging. Likewise, the same strategy is employed for the case of discharging, where:

$$p_{\text{ess,k}} = \begin{cases} p^{ANN}_{\text{ess,k}} & \text{if} \quad E_{\text{o,k}} - \frac{1}{\eta}\, p^{ANN}_{\text{ess,k}} \geq 0 \\ \eta\, E_{o,k} & \text{if} \quad E_{\text{o,k}} - \frac{1}{\eta}\, p^{ANN}_{\text{ess,k}} < 0 \end{cases} \tag{4.3}$$

giving $e_{\text{ess,k+1}} = 0$ should there be a risk of undercharging. In the case of diesel shutdown, there are additional conditions that will need to be checked, as will be seen in what follows.

4.2.2 ESS and Diesel Scheduling

In continuous operation, the diesel plant simply follows the residual load (through its load following function) and solicits the dump load only in order to respect its minimum loading. When shutdown is permitted, the on/off schedule must be specified through $u_{\text{diesel,k}}$. This requires a second output from the ANN, one that attempts to extract a pattern for diesel shutdown from the training data. This decision will also impact the scheduling of the ESS and as a result, the two should be somehow coordinated.

Figure 4.5 shows the two main input-output ANNs considered, again with a general representation of the ANN architecture. As in the continuous case, two different structures were considered. The first makes decisions based only on the value of the two random variables while the second considers the residual load profile for the next 24-hour window.

The two outputs originate from the same ANN—as opposed to independent ANNs—and therefore, the schedules of the diesel plant and the ESS will be coordinated. This is less of a concern for the training due to the fact that the goal is to reproduce as closely as possible the input-output relationship. However, when data independent of the training set is used, this fact is likely more important as it facilitates capture of general rules, which might not be possible had two separate ANNs been used.

The schedules arising from the ANN cannot be used directly. As in the case of storage scheduling, diesel shutdown could result in instances where the ESS becomes completely discharged and unable to meet the load. Therefore, the scheduling again needs to be verified to ensure that the ESS constraints are not now violated. In addition to the modifications in equations (4.1)–(4.3) with the diesel on-line, the following conditions need to be checked in the event of shutdown of the plant:

$$p_{\text{ess,k}}^{ANN} = p_{\text{L,k}} - p_{\text{w,k}} \tag{4.4}$$

where $p_{\text{ess,k}}^{ANN}$ is redefined ESS power reference coming from the ANN, if $u_{\text{diesel,k}}^{ANN} = 0$. In other words if the diesel is ordered to shutdown, (4.4) overrides the power reference coming from the ANN. The storage constraints should then be checked for this new condition, and the diesel plant schedule is modified, if necessary:

$$u_{\text{diesel,k}} = \begin{cases} 0 & \text{if} \quad |p_{\text{ess,k}}^{ANN}| \leq P_{\text{ess}} \\ 1 & \text{if} \quad |p_{\text{ess,k}}^{ANN}| > P_{\text{ess}} \end{cases} \tag{4.5}$$

The energy state at the end of hour k must also be checked to ensure that the ESS power given by (4.4) does not result in overcharging or overdischarging. In the case of charging, part of the load is transferred to the dump load to avoid overcharging, according to:

$$p_{\text{ess,k}} = \begin{cases} p_{\text{ess,k}}^{ANN} & \text{if} \quad E_{\text{o,k}} - \eta\, p_{\text{ess,k}}^{ANN} \leq E_{\text{ess}} \\ -\frac{E_{\text{ess}} - E_{\text{o,k}}}{\eta} & \text{if} \quad E_{\text{o,k}} - \eta\, p_{\text{ess,k}}^{ANN} > E_{\text{ess}} \end{cases} \tag{4.6}$$

where the additional load is picked up by the dump load according to:

$$p_{\text{dump,k}} = \begin{cases} 0 & \text{if} \quad E_{\text{o,k}} - \eta\, p^{ANN}_{\text{ess,k}} \leq E_{\text{ess}} \\ p_{\text{ess,k}} - p^{ANN}_{\text{ess,k}} & \text{if} \quad E_{\text{o,k}} - \eta\, p^{ANN}_{\text{ess,k}} > E_{\text{ess}} \end{cases} \tag{4.7}$$

In the case of discharging, an override of the shutdown order must be made if the power given by (4.4) would result in e_{ess} being less than 0. Therefore, the diesel plant schedule is revised according to:

$$u_{\text{diesel,k}} = \begin{cases} 0 & \text{if} \quad E_{\text{o,k}} - \frac{1}{\eta}\, p^{ANN}_{\text{ess,k}} \geq 0 \\ 1 & \text{if} \quad E_{\text{o,k}} - \frac{1}{\eta}\, p^{ANN}_{\text{ess,k}} < 0 \end{cases} \tag{4.8}$$

Likewise, if the diesel plant schedule is revised, the discharge schedule must be modified to avoid e_{ess} from dropping below 0. So, for discharging events during a shutdown request, $p_{\text{ess,k}}$ is given by:

$$p_{\text{ess,k}} = \begin{cases} p^{ANN}_{\text{ess,k}} & \text{if} \quad E_{\text{o,k}} - \frac{1}{\eta}\, p^{ANN}_{\text{ess,k}} \geq 0 \\ \eta\, E_{o,k} & \text{if} \quad E_{\text{o,k}} - \frac{1}{\eta}\, p^{ANN}_{\text{ess,k}} < 0 \end{cases} \tag{4.9}$$

Implementation of these complementary equation together with the ANN yields the on-line controller. The inclusion of these condition will modify the behaviour of the controller but it is the only way to ensure that the ESS ratings are respected. In the following section, the various controllers are simulated to see how their performance fairs with the off-line optimization results.

4.3 Controller Performance Testing

Testing of the developed controller followed the same general procedure as in the following chapter, with some slight modifications. The ANN controllers were simulated using the year's worth of data used as input training data. For simplicity only WRs 1 and 12 were considered. The controllers were compared using the previously defined metrics—cost of

Table 4.1 Impact of the number of neurons in input and hidden layers on ANN performance for continuous diesel operation

Wind Resource	Input Layer Neurons	Hidden Layer Neurons	Expected[1] Cost [$/kWh]	Simulated[2] Cost [$/kWh]	Expected E_{dump} [pu]	E_{dump} [pu]
1	— no ESS —		-	0.5658	-	0.0507
	5	5		0.5735		0.0505
	5	50	0.5666	0.5735	0.0345	0.0502
	5	30		0.5735		0.0502
12	— no ESS —		-	0.6223	-	0.2308
	5	50		0.6262		0.2311
	10	50	0.6213	0.6262	0.2200	0.2312
	5	30		0.6262		0.2312

1. *Expected cost* refers to the cost of energy obtained using off-line optimization, or stated otherwise, the cost of energy if the NN fit the data perfectly.
2. *Simulated cost* refers to the cost of energy resulting from simulation of the system using the NN based controller.

energy and dumped energy—recalling that the off-line optimization results represent the highest level of performance possible, for the horizon considered. Thus, good agreement between the off-line optimization results and the ANN controller is taken to be synonymous with good performance.

A number of different ANN controllers were simulated and compared to the off-line optimization results. Different architectures were compared by varying the number of layers and neurons within each of the layers. This was done for the two types of input variable definitions presented above, for the two diesel plant control modes investigated. The best performing controllers were then selected and run in parallel with the off-line optimization for the twenty years using WR 1.

4.3.1 Neural Network Architecture

There is no universally accepted methodology for definition of ANN architectures; it more or less follows a trial-and-error process to determine the optimal design. There are a few guidelines, [104], which have been abided by here. The following subsections present the results of a parametric analysis of different ANN architectures, whereby only the top performing controllers were retained.

Continuous Operation

A number of ANN architectures were considered, for the 3-input, 1-output ANN, including those with a single hidden layer and those with two hidden layers. The number of neurons were increased in each, up to a maximum of 50 neurons per layer, in steps of 5. The exception was the output layer, which was limited to a single neuron, due to there being only one output. The ANNs were implemented and trained using the MATLAB Neural Network toolbox. Each node was represented by a *tansig* function and the network was trained using the Powell-Beale Restarts Conjugate Gradient method (*traincgb*). Each ANN was trained until the mean squared error performance function was less than 10^{-2} or 250 epochs was reached, which ever arrived sooner.

Results are presented for the preferred architectures resulting from this parametric study along with the results from the off-line optimization (indicated by Expected Cost and Expected E_{dump}) and the case with no ESS, Table 4.1. The results are not very promising in that cost of energy and the dumped energy are not only significantly higher than in the off-line optimization results, but C_{s} is also higher than in the case with no ESS.

It must be conceded that the improvement in C_{s} is quite marginally; performance that does not precisely replicate the optimization results can easily result in higher costs due to the capital costs of the ESS. However, one would still hope that an on-line method preform better than the system without storage, otherwise what is its point. In the case of WR 1, the point is that the dumped energy is somewhat lower but likely not enough to lobby for merits of this controller.

The shortcomings of the ANN controller aside, it can also be noted that the optimization also results in a higher cost of energy than without ESS for WR 1. For cases where the expected benefit of the ESS is small, the ESS project would likely not go ahead. Some margin should also be built into the sizing methodology to also account for reductions in this benefit associated with the use of ANN operating schemes, if relevant. Taken together, these results reinforce the main conclusion from the ESS sizing chapter—inclusion of ESS in the wind-diesel design is only feasible if the right economic signals are present and shutdown of the diesel plant is permitted.

Table 4.2 Impact of the number of neurons in input and hidden layers on ANN performance with diesel shutdown permitted

Wind Resource	Input Layer Neurons	Hidden Layer Neurons	Expected[1] Cost [$/kWh]	Simulated[2] Cost [$/kWh]	Expected E_{dump} [pu]	E_{dump} [pu]
1	— no ESS[3]—		-	0.5591	-	0.0395
	5	10		0.5608		0.0346
	50	10	0.5456	0.5609	0.0042	0.0346
	5	5		0.5609		0.0347
12	— no ESS[3]—		-	0.5611	-	0.1287
	5	50		0.5534		0.1077
	10	50	0.5354	0.5535	0.0617	0.1079
	5	30		0.5536		0.1082

1. *Expected cost* refers to the cost of energy obtained using off-line optimization.
2. *Simulated cost* refers to the cost of energy resulting from simulation of the system using the NN controller.
3. The numbers presented here assume that diesel shutdown is still permitted. In these instances the dump load is used to meet the power balance equation.

Diesel Shutdown

In the ESS sizing and optimal scheduling results, diesel shutdown permitted sizable gains once ESS was integrated into the system. In an effort to see whether these gains could be also realized using the proposed on-line controller, another parametric analysis was performed. Once again the number of hidden layers and neurons within each layers were varied and only the most promising candidates were retained.

Table 4.2 presents the results for the selected ANN controllers for WRs 1 and 12, along with the results for the off-line optimization and with no ESS. The savings realized with the ANN controller fall short of those from the off-line optimization results. However, it could be argued that the results are more favourable than in the continuous case. The dumped energy is now consistently lower than the case without ESS, and in the case of WR 12, the ANN realizes a lower cost of energy. Nonetheless, it would be hoped that the gap between the cost of energy for off-line optimization results and the ANN controller could be reduced. The size of this gulf can, in part, be attributed to the fact that the ANN controller uses significantly less information in making its decision than the optimization algorithm.

Table 4.3 Comparison of ANN performance for different wind-load modeling approaches as input variables, continuous diesel operation

Wind Resource	Wind-load Inputs	Expected[1] Cost [$/kWh]	Simulated[2] Cost [$/kWh]	Expected E_{dump} [pu]	E_{dump} [pu]
1	no ESS	-	0.5658	-	0.0507
	$r_{\text{wl,ek}}$, $\rho_{\text{wl,k}}$	0.5666	0.5735	0.0345	0.0505
	$\mathbf{p}_{\text{res}}$		0.5702		0.0420
12	no ESS	-	0.6223	-	0.2308
	$r_{\text{wl,ek}}$, $\rho_{\text{wl,k}}$	0.6213	0.6262	0.2200	0.2311
	$\mathbf{p}_{\text{res}}$		0.6229		0.2242

1. *Expected cost* refers to the cost of energy obtained using off-line optimization.
2. *Simulated cost* refers to the cost of energy resulting from simulation of the system using the NN controller.

4.3.2 Input Variables

The ANN controller in the previous section used only three inputs in continuous operation in order to make a decision regarding the scheduling of the ESS. Even after extensive parametric study for selection of the architecture, the performance was very poor, underperforming even the case without ESS, for WR 1. Here, rather than limiting the number of inputs to the ANN, the same information is provided to the ANN as was provided to the off-line optimization algorithm, in an effort to yield a better fit of the training data.

Continuous Operation

The parametric analysis was re-run but this time using the residual load over the next 24-hours as the input to the ANN, instead of the two random variables for the same period ($r_{\text{wl,ek}}$ and $\rho_{\text{wl,k}}$.) The simulated cost and dumped energy is provided along with the results for the ANN using $r_{\text{wl,ek}}$ and $\rho_{\text{wl,k}}$ as inputs, and for the off-line optimization results and for no ESS, Table 4.3.

The 25-input, 1-output ANN performs better than the 3-input, 1-output ANN but it still results in higher cost of not only the off-line optimization results but also of the case with no ESS. More encouraging is the fact that the dumped energy is now consistently lower than the case of no ESS, which should be a minimum performance requirement for

Table 4.4 Comparison of ANN performance for different wind-load modeling approaches as input variables, diesel shutdown permitted

Wind Resource	Wind-load Inputs	Expected[1] Cost [$/kWh]	Simulated[2] Cost [$/kWh]	Expected E_{dump} [pu]	E_{dump} [pu]
1	no ESS[3]	-	0.5591	-	0.0395
	$r_{\text{wl,ek}}$, $\rho_{\text{wl,k}}$	0.5456	0.5608	0.0042	0.0346
	$\mathbf{p}_{\text{res}}$		0.5567		0.0260
12	no ESS[3]	-	0.5611	-	0.1287
	$r_{\text{wl,ek}}$, $\rho_{\text{wl,k}}$	0.5354	0.5534	0.0617	0.1077
	$\mathbf{p}_{\text{res}}$		0.5411		0.0864

1. *Expected cost* refers to the cost of energy obtained using off-line optimization.
2. *Simulated cost* refers to the cost of energy resulting from simulation of the system using the NN controller.
3. The numbers presented here assume that diesel shutdown is still permitted. In instances of shutdown—only possible when $p_{\text{w}} > p_{\text{L}}$—the dump load is used to meet the power balance equation.

any ESS controller. Due to the fact that the cost savings associated with even the off-line optimization approach are fairly small, this controller shows greater promise. As well, given that E_{dump} is now consistently lower than the case without ESS indicates that it is better at managing energy than when only 3-inputs were used.

Diesel-Shutdown Permitted

Table 4.4 gives the results for the 25-input, 2-output ANN controller resulting from parametric analysis of ANN architectures, together with results for the 3-input, 2-output ANN controller. Again, results from the off-line optimization and without ESS are included to facilitate easy comparison.

As in the case of continuous diesel operation, the use of $\mathbf{p}_{\text{res}}$ in place of $r_{\text{wl,ek}}$ and $\rho_{\text{wl,k}}$ as inputs, results in improved performance for the ANN controller. The cost of energy and E_{dump} are lower than in the case without ESS, for both WRs. The improvement as a result of changing the input variables is greater for this mode of diesel operation than that seen in continuous mode of operation, perhaps because there are a greater number of opportunities for reducing dump load.

4.3.3 General Performance Assessment

As in the training of persons, one of the best measures of an ANN's performance is not in repeating a certain task that has been rehearsed numerous times but to subject the ANN to a new set of conditions that are representative of, but unique from, the original data source. Only in this way is it possible to ascertain whether the ANN has extracted knowledge from the training set and can apply it in a general sense. The performance of the ANN relative to the off-line optimization algorithm should remain constant. Should implicit operating rules in the training data exist, and the ANN has extracted them rather than being overtrained to the specific data, it will be clear in its performance with the new data set.

To this end, the ANNs were simulated using the full 20 year data set for WR 1, using only the 25-input ANNs. In addition, the off-line optimization approach was provided the same data set in order to establish the minimum values for cost of energy and dumped energy. This was performed for both continuous operation and diesel shutdown.

Table 4.5 ANN controller and off-line optimization performance for future years

Operating Approach	Period[1]	Expected[2] Cost [$/kWh]	Simulated[3] Cost [$/kWh]	Percent Error [%]	Expected E_{dump} [pu]	Simulated E_{dump} [pu]
Continuous	1	0.5666	0.5702	-0.64	0.0345	0.0420
	1 to 5	0.5655	0.5710	-0.97	0.0446	0.0560
	6 to 10	0.5671	0.5721	-0.88	0.0412	0.0514
	11 to 15	0.5673	0.5723	-0.88	0.0422	0.0525
	16 to 20	0.5670	0.5720	-0.89	0.0428	0.0532
	1 to 20	0.5667	0.5719	-0.90	0.0427	0.0533
shutdown	1	0.5456	0.5567	-2.03	0.0042	0.0260
	1 to 5	0.5394	0.5547	-2.83	0.0060	0.0367
	6 to 10	0.5429	0.5568	-2.55	0.0058	0.0338
	11 to 15	0.5427	0.5572	-2.67	0.0060	0.0351
	16 to 20	0.5424	0.5568	-2.65	0.0066	0.0356
	1 to 20	0.5419	0.5563	-2.68	0.0061	0.0353

1. *Period* refers to the year or range of years over which the controller's performance was evaluated.
2. *Expected cost* refers to the cost of energy obtained using off-line optimization.
3. *Simulated cost* refers to the cost of energy resulting from simulation of the system using the ANN controller.

The results are presented for the training data, in periods of five years, and for the comprehensive results, Table 4.5. Comparing the training data set with those for other periods, it can be seen that there is only a small increases in the percent error, indicated that although the ANN is not perfectly tuned to the training data, it performs almost equally well in future years—it captures well the rules for operation of the ESS and adapts well to other conditions. Assuming a new structure could yield better agreement with the training set, there is also the risk of overtraining, whereby the performance is seriously degraded for other years.

Considering the results more generally, the characteristics vary slightly from one period to the next but overall the cost of energy and dumped energy remain relatively constant. This suggests that a years worth of data is a good size for ESS sizing analysis in that it likely captures the main characteristics of the wind and load resource.

4.3.4 ESS Usage Comparison

To visualize how the scheduling commands from the ANN controller affect the usage of the ESS, the power and energy scatter plots and the *pdf* of e_{ess}, were generated for year 2 of operation, Figs. 4.6 and 4.7, respectively. Plots are given for both continuous and shutdown modes of operation, for the off-line optimization results and for the 25-input ANN controller.

The results indicate that the off-line optimization approach makes much better use of the overall operating area, with scatter plots reminiscent of those presented in the previous chapter. The slope defining the boundaries of operation are once again clear, as defined by the relative ratings of the power and energy components. These edges are visible for the ANN controller as well, but are much less well defined, due to the smaller degree of scatters of operating points. The ANN controller does exhibit a fairly wide spread in terms of e_{ess}, the distribution is actually quite similar as the case of the off-line results. However, considering p_{ess}, one can note that the values are grouped near zero power, using predominantly small charging/discharing rates. The total ESS power capacity is rarely used throughout the year.

This suggests that the ANN based control approach is much more conservative, and although the decision to charge or discharge may be in line with the off-line approach, the magnitude is only a fraction of its value. One way of possibly circumventing this problem

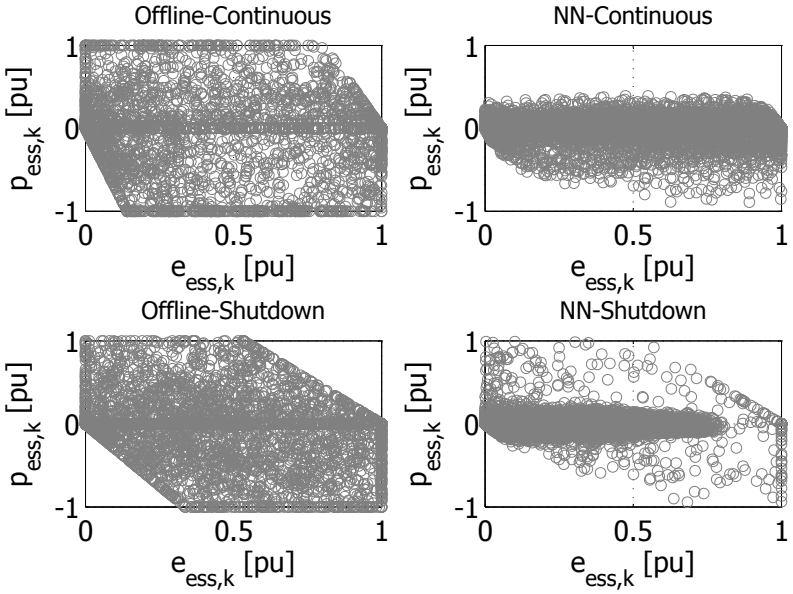

Fig. 4.6 Plot of ESS power and energy states for all hours in year 2, for off-line optimization and ANN controller, with and without diesel shutdown.

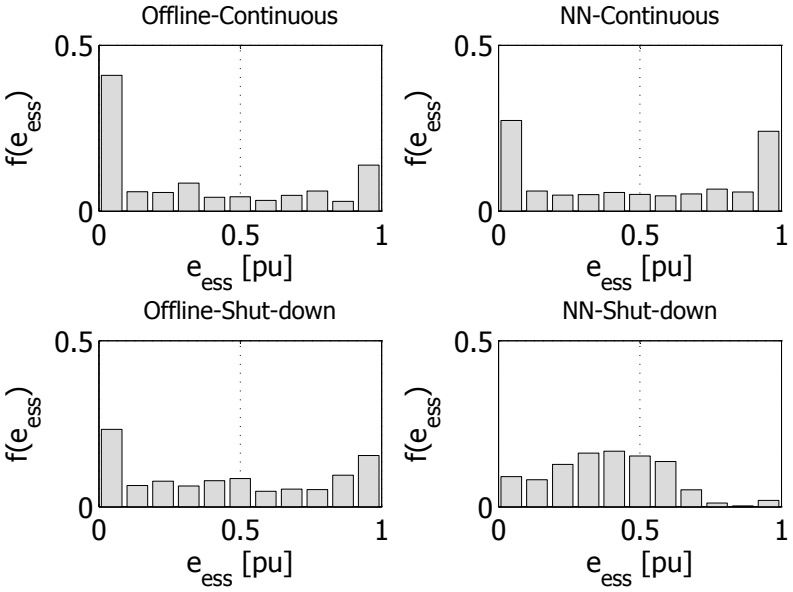

Fig. 4.7 Plot of ESS discrete probability functions for all hours in year 2, for off-line optimization and ANN controller, with and without diesel shutdown.

could be to apply a scaling factor to the output of the ANN controller. However, this presumes that the sign of p_{ess} is the same as that in the off-line optimization. A likely consequence of this intuitive countermeasure would be very high charging and discharging rates, possibly degrading performance, if the sign during a significant number of cycles is non-ideal. A more analytical based solution would be preferable in that it could be invoked more generally and would lead to better understanding of the problem.

Figure 4.8 provides greater insight into the relationship between ESS scheduling and the diesel operating point for each case. For continuous operation, ESS charging only takes place when the diesel is at its minimum loading for the ideal case, a rule that the ANN failed to fully capture. In diesel shutdown, the ESS may charge with the diesel at higher loadings. Likely these cases are soon followed by a shutdown period; the ESS charges to be able to meet future load for the anticipated shutdown. The graphs reinforce the fact that the ANN fails to use its entire power capacity. A better understanding of the relationship between the diesel and ESS could be useful for arriving at a more viable structure for the ANN.

The power density function of the diesel power was also plotted in order to compare how the diesel is being used with each of the two controllers, Fig. 4.9. Interestingly, for continuous operation, the frequency of operation of the diesel at its minimum loading is actually higher in the case of the off-line optimization approach, which is somewhat unexpected given that the cost of energy was lower in this case. These occurrence would have to have been linked with periods of ESS charging in place of the dump load, as implied by Fig. 4.8. This is reflected in lower diesel energy in the ideal case, resulting in the lower costs, all other things being equal (wind energy operating costs and storage fixed costs are the equal).

In the case of diesel shutdown, the distributions are very similar, only that the off-line optimization approach has a greater number of shutdown periods. This is consistent with what is expected since lower cost of energy and dumped energy is realized with less diesel fuel. The higher frequency of shutdowns results in lower total diesel energy, translating into a lower cost of energy.

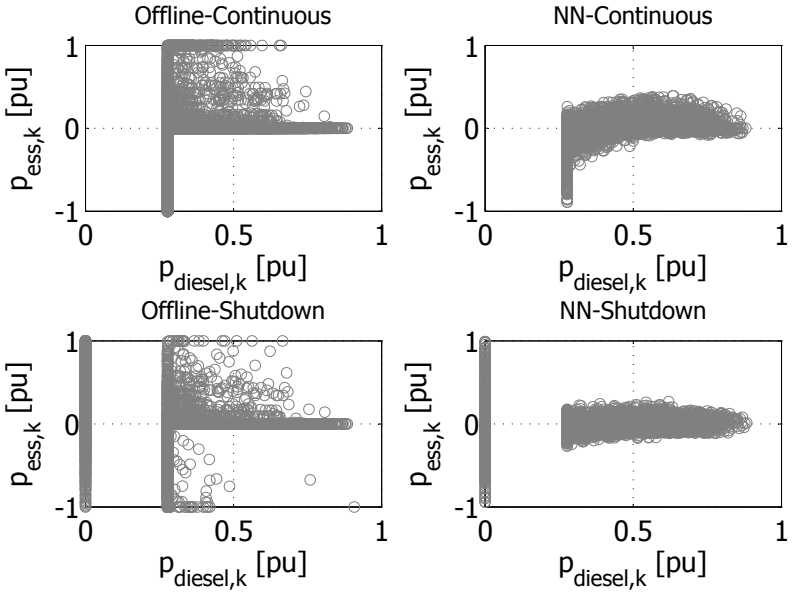

Fig. 4.8 Plot of ESS and diesel powers for all hours in year 2, for off-line optimization and ANN controller, with and without diesel shutdown.

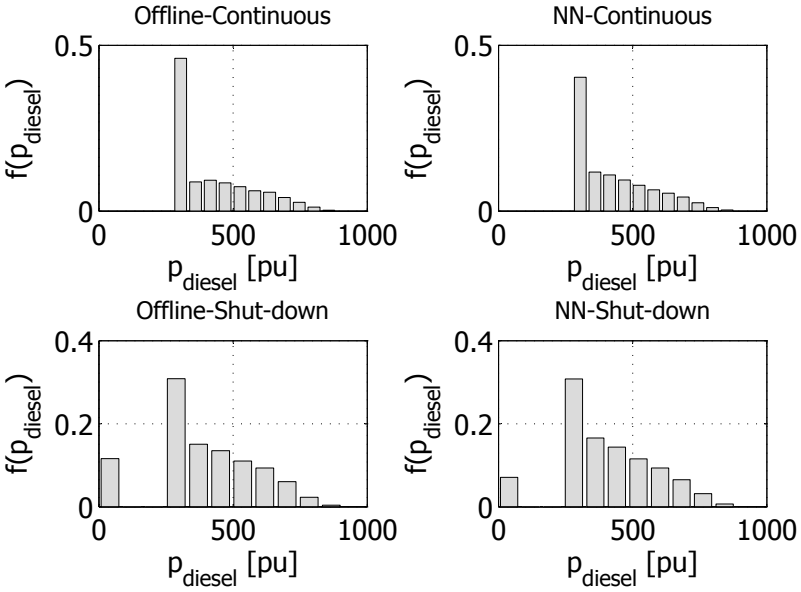

Fig. 4.9 Plot of diesel power discrete probability functions for all hours in year 2, for off-line optimization and ANN controller, with and without diesel shutdown.

4.4 Conclusions

In this chapter, the results from the off-line optimization approach were used as training data for an ANN based controller, suitable for on-line operation. Two different input-output structures were considered for each of the diesel plant operating modes, and a number of ANN architectures were evaluated. The best performers were selected from the set of different controllers and were compared with the off-line approach over the twenty years of available data for WR 1. The usage of the ESS was compared using power and energy scatter plots and *pdf*'s of the SOC and diesel power.

The ANN consisting of one input layer, two hidden layers and an output layer proved to be the preferred structure. The optimal number of neurons in each layer was respectively, 5, 10, 10, and 1, although the optimal number of hidden layers depended on the WR and the mode of operation. The 25-input structures were greatly preferred to the 3-input structure. Although simpler, the latter resulted in very poor performance, generally exhibiting higher costs than the case without ESS, and in certain cases higher dumped energy.

The 25-input structure yielded greatly improved performance; however, it still lagged significantly behind the off-line optimization results. In order to be a viable operating strategy, further investigations would be required to see if the performance of the off-line optimization approach can be more closely reproduced. Some ideas worth consideration include consideration of other input parameters (such as: past schedules, estimated dump load without storage, separating load and wind into two variables rather than using the residual load) or attempting other ANN architectures outside the set considered. Scatter plot results suggested that the power component of the ESS was greatly under used, and the use of a scaling factor might help to render the controller more aggressive, but more careful adjustment would likely lead to greater gains.

The eventual ANN designs arrived at were tested for future years, to establish whether or not the controller would give similar performance for wind and load data independent of the training set. The relative performance (measured with respect to the off-line optimization results) decreased only slightly, indicating that the controller did well at extracting the implicit rules from the off-line optimization results.

As mentioned the usage plots showed that the ANN controller was much more conservative than the off-line optimization results, particularly in terms of the ESS's power capacity. The energy capacity was fairly well used as illustrated by the *pdf*. The diesel

power distributions were similar for the two approaches but with the off-line optimization had a higher frequency of operation at minimum loading and of shutdowns, in the case of the two diesel operating approaches. This resulted in lower diesel consumption and the associated lower cost of energy. Perhaps the most revealing were the scatter plots of the diesel and ESS powers. These showed that especially for continuous operation, there were specific operating rules that the ANN failed to properly capture. Revisions to the ANN structure should pay particular attention to these results in deciding on alternate input variables.

The gap in performance observed between the off-line optimization and AI approach to ESS scheduling forces one to re-evaluate the pros and cons associated with the two methods. If an optimization approach to scheduling is sufficiently affordable and is capable of computing the solution in the time required, it might be preferable to forego further consideration of alternatives. However, if through modifications to the above structure or complementing ANN with other AI techniques (data mining or fuzzy logic) one can succeed in extracting general operating rules from the data, then an AI approach might be possible and even preferred. The exercise would likely lead to greater insight into how the ESS is used and might permit definition of a generic controller, should the resulting rules be sufficiently general to work across different WRs. If one is allowed to be ambitious, one might even imagine creating structures that might be applicable across different ESS applications.

Chapter 5

Control of a Two-Level Energy Storage System

The devil is in the details

Gustave Flaubert (1821 – 1880)

5.1 Introduction

Up to this point, the scheduling of the ESS has been considered on an hourly basis. We have not concerned ourselves with the behaviour of the system within each hour, rather choosing to represent load, wind and ESS by their hourly averages. From a practical point of view this was necessary, since for sizing or operational studies that consider numerous years it would have been far too involved to consider higher resolution data, data storage requirements aside. Moreover, the results would not necessarily have provided greater clarity without high fidelity, sampled at high frequency, over a full 20 years. Any attempt to construct such a data set would have produced results that would only have been as good as the assumptions made in producing data.

That said, this chapter will consider the control issues and performance of the ESS on a second-to-second time frame. This time frame is of interest to understand how the diesel behaves, particularly during highly volatile wind; what benefits ESS can provide in terms of reducing fluctuations seen by the diesel; and to see how the ESS behaves during shutdown periods. Furthermore, practical issues such as the response time of the ESS call

for more sophisticated designs than the simplified storage model considered thus far. These topologies will need to be considered in the intrahour simulations.

Multi-level storage systems, generally limited to two levels, may be used to circumvent the problem associated with response time limitations of batteries and other high energy rated devices, [105–108]. In these arrangements, a fast-acting ESS, typically with a much smaller energy rating, is paired with a slower responding but larger energy capacity ESS. A general representation of a two-level ESS system for wind energy applications is shown in Fig. 5.1. Here the combined ESS power reference is sent from a high level control to the two level controller, which is tasked with allocating the reference power between the two levels. The problem becomes how should this be done over the hour and in particular what should be done around boundary conditions, such as when the SOC of either storage level is nearing its upper or lower limits, or when the ESS power reference can no longer be met.

This chapter will present the details of the two-level ESS system as it relates to the wind-diesel system treated thus far. Specific issues that will be covered include: the hierarchical control structure, the response time of the ESS and hardware components, comparison of hourly and intra-hour performance, and implementation of the system in a real-time, hardware-in-the-loop simulation. The bulk of the analysis is performed using a simulation model of the system. A hardware-in-the-loop (HIL) set-up is used to validate the real-time implementation of the controller and compare with the simulation results for a selected hour. Taken together this will place the other chapters into perspective and allow summary of the overall contributions of the body of work.

5.2 Two-Level ESS Control

Because of the large capital investments, the operation of energy storage with wind systems would need to be intelligently managed, as much on a intrahourly basis as on hourly intervals. Any deviations from a constant dispatch over the hour in question that might translate to additional gains are worthwhile endeavours. These delineations from the dispatch may also be required due to changes revealed by higher resolution data. For instance, large variations in wind power from the hourly average over the short-term may justify action of the ESS even though the scheduling using hourly data may not. The higher the probability of these large variations, the greater the need for a control algorithm that adjusts the operation of the ESS in consequence.

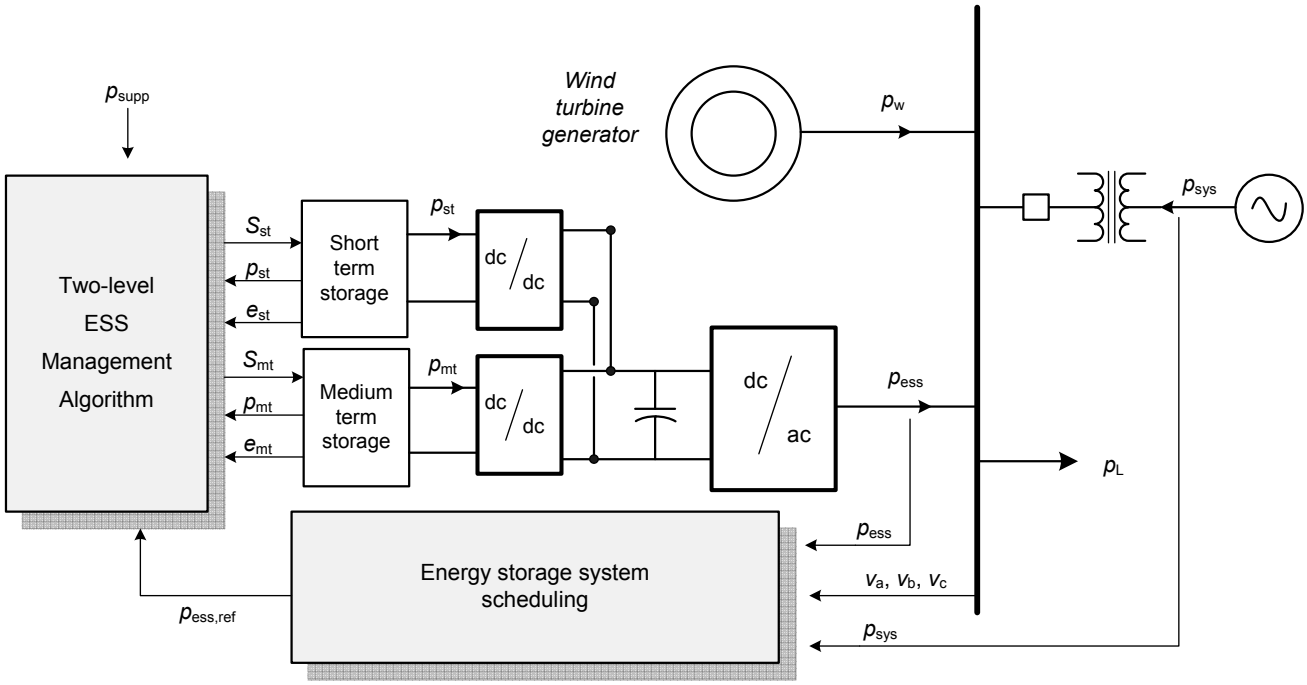

Fig. 5.1 Two-level energy storage system and its associated control

The use of AI approaches to short-term scheduling of storage have been considered in various publications, [50, 72, 102, 103, 106], likely due to the fact that, particularly fuzzy logic can be used to mathematically capture intuitive rules. In these cases, the focus is primarily on modifications to the power references at ESS energy limits. In [105, 109], the rules consider the response times and the energy states of the storage levels to make a decision about how to modify the power reference, and are coded as $if/else$ statements.

The problem of storage scheduling is further complicated when two ESS technologies are combined—the two-level ESS introduced in Fig. 5.1. The issue then becomes how to schedule the individual devices to provide a combined reference and to determine what action should be taken during limiting operation. In [106], fuzzy logic was used to respect the limits of the short-term device but it was not coordinated with the battery storage. In the rule-based method of [105], a short-term storage device is used to compensate for fast power fluctuations while a long-term storage device assists in following long-term trends. Again, these methods work well to quickly adapt intuition to controllers.

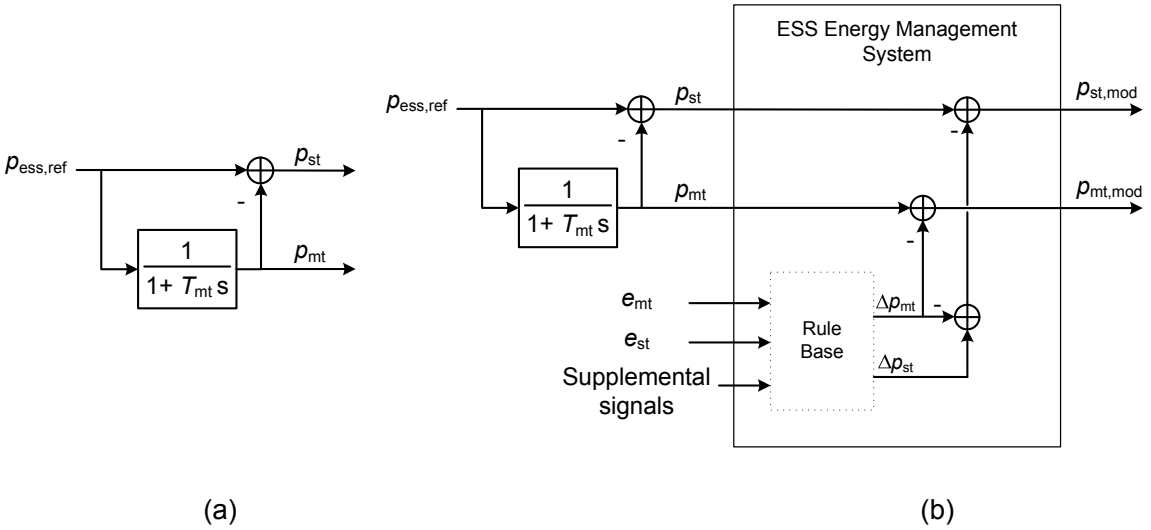

Fig. 5.2 Generic two-level energy storage system controller

Here the generic controlled structure given in Fig. 5.2 is proposed, which will be adapted to meet the specific needs of the wind-diesel system. This structure consists of a low-pass filter, where the lower bound of its time constant is set by the response time of the medium-term[1] device, and whose output generates the initial power reference for the slower ESS. The short-term ESS power reference is then generated by the difference between the ESS power reference and that of the medium-term device. These power references are then either directly sent to their respective ESS controls, Fig. 5.2 (a), or they may be further modified by a rule base that considers the SOCs of the two levels and possibly other supplemental signals, which would be characteristic of the specific application, Fig. 5.2 (b).

5.2.1 Generation of ESS Power Reference

The two-level ESS controller's role is allocation of the power reference between the two-levels. This power reference is assumed to be provided from some higher level energy management system. In this way, the control presented here is the base control in a hierarchical structure. The output signals from this controller are provided as references to the ESS power electronic converter controls, such that they are delivered to the system.

[1] *Medium-term* ESS, device or level will refer to the high energy capacity ESS, whereas the qualifier *short-term* will refer to fast-acting low energy capacity ESS

In the case of the wind-diesel system, this ESS power reference comes from either the optimization results or ANN controller that define the hourly schedules for the ESS and unit commitment of the diesel plant, if shutdown is permitted. The two-level control must then attribute a portion of this reference to each of the levels, and if necessary, make modifications to the schedule. The first stage in this process is the low-pass filter used in defining the initial power reference of the medium-term ESS.

5.2.2 Medium-Term Time Constant Selection

The first component of the algorithm simply divides the power reference signal, $p_{\text{ess,ref}}$, into two separate signals: p_{st} and p_{mt}, corresponding to the short-term and medium-term power references, respectively. The latter of the two signals is generated by passing $p_{\text{ess,ref}}$ through a low-pass filter with time constant, T_{mt}, such that:

$$p_{\text{mt}}(s) = p_{\text{ess,ref}}(s)\frac{1}{1+T_{\text{mt}}s} \tag{5.1}$$

The short-term output power is then calculated to ensure that the output power reference is maintained,

$$p_{\text{st},i} = p_{\text{ess,ref,i}} - p_{\text{mt},i} \tag{5.2}$$

While there is a lower limit on the value of the time constant, T_{mt} (dictated by the response time of the medium-term storage), it is interesting to consider the impact of its value on the required power and energy ratings of the two levels. To this end, a 1-hour wind speed profile, sampled at 5 Hz, with wind speeds varying between the cut-in and cut-out speeds, was used, [110].

The system was scheduled to deliver the average output power resulting from application of the wind speed profile to the generator characteristic given in [65]. The analysis was run for different values of T_{mt}, and the rated power for each of the storage levels was determined, taking the infinity norm of the power time series:

$$P_n = \|\mathbf{p_n}\|_\infty, \qquad n \in [st, mt] \tag{5.3}$$

where $\mathbf{p_n}$ is the vector of storage powers, for level n, corresponding to the time series, $\mathbf{i}$. The energy rating was determined by the maximum deviation of energy over the interval,

where the energy state for level n at time i is given by:

$$e_{ni} = E_{no} + \sum_{q=1}^{i-1} p_{nq} \triangle i \tag{5.4}$$

Where $\triangle i$ is the time step of the time series and E_{no} is the initial energy state, which was chosen to be 0.5 per unit. This allowed the generation of plots of the energy and power ratings, expressed as a function of T_{mt}, Figs. 5.3 and 5.4, respectively.

ESS sizing should be conducted along the lines of the methodology proposed in Chapter 2. However, these results assume that the power and energy ratings are predetermined and are meant to illustrate how the inclusion of the time constant will inflate these ratings. Before proceeding to the specific case of the wind-diesel system, a few remarks are made:

Remark 1: The segregation of storage into two distinct levels will result in a total storage energy capacity that is greater than or equal to energy rating resulting from a single level. This is due to the fact that at certain times one level is charging while the other is discharging.

Remark 2: The optimum T_{mt}, if based upon minimization of the total energy rating alone, is zero. However, the response time of the medium-term device will impose a lower limit on the value of T_{mt}. This fact should somehow be incorporated into the ESS sizing methodology, perhaps in terms of a scaling factor on the fixed costs to account for the fact that a higher rating is required for practical realization.

Remark 3: Although the sum of the two power ratings increase with T_{mt} this does not imply that the power rating of the ac interface converter increases. The reference power of the ESS is unchanged and as a result, the two levels are not supplying their rated power conjointly. The power rating is defined by the greater of the two-levels over the period, or equivalently, to the maximum of the high level ESS power reference (see eqn. (5.3)).

Again, this is not a suitable sizing approach as it considers only a single hour—it does not replace the methodology presented earlier. Rather, it serves to provide an estimate of how the ratings resulting from a sizing study translates into the two levels, for a given T_{mt}.

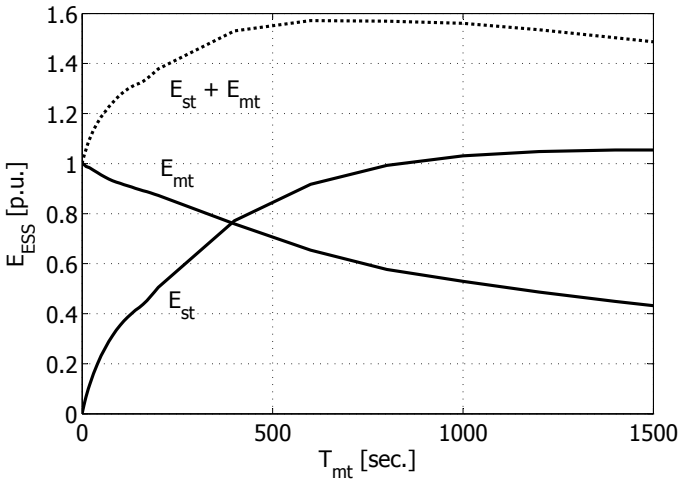

Fig. 5.3 Variation of minimum energy rating with T_{mt}

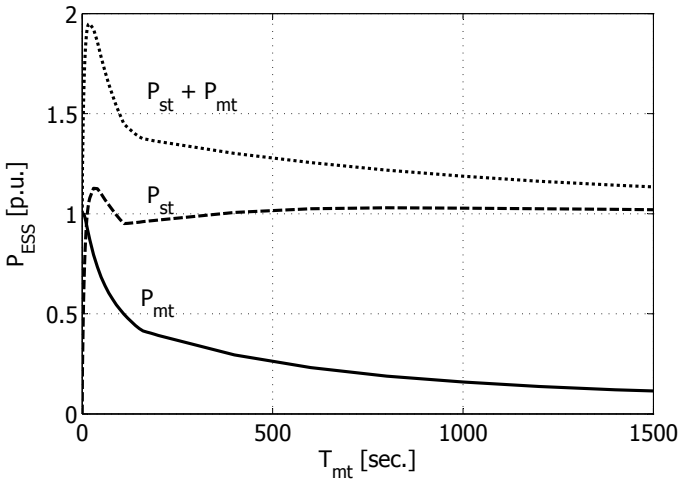

Fig. 5.4 Variation of minimum power rating with T_{mt}

5.2.3 Application to Wind-Diesel Systems

The basic structure presented must now be adapted to the specific application considered thus far. Each application will likely require supplemental signals to those given in Fig. 5.2. These will depend on the characteristics of the problem but it is hoped that the process followed here will provide some guidance.

Figure 5.5 gives the overall hierarchy of the two-level ESS control for the wind-diesel

system. The reference power for the two-level system is provided each hour according to the means outlined in previous chapters. The exception to this rule is when the diesel is shutdown, in which case the ESS power reference equals the difference between the instantaneous load and wind power, or residual load, $p_{\text{res,i}}$. This signal is then divided between the two-level using the low-pass filter and the resulting power references are provide as inputs to ESS energy management system. The general structure is given in Fig. 5.5, whereas details of the generation of the energy management system outputs are provided in Fig. 5.6.

In addition to the power references for the two ESS levels, the instantaneous energy states of each ESS level and the estimated dumped energy are also given as inputs. The dump load is estimated according to the original schedule from the high level control. This is done considering the instantaneous wind and load profiles, $p_{ess,ref}$ (defined as $p_{\text{ess,k}}$ in previous chapters), and the minimum loading constraint.

In the event it is desirable to maintain the diesel at is scheduled level, for instances to limit the up/down rates of the diesel, this can also be incorporated into the ESS power reference. The estimated deviation of the diesel plant from its schedule is given comparing the estimated schedule with $p_{\text{diesel,ref}}$ ($p_{\text{diesel,k}}$). In this way, the ESS absorbs the majority of the fluctuations about the hourly average, assuming of course it has sufficient capacity. This and other variations to the general control structure will be considered in the simulation of the system.

Unless the ESS is grossly overrated, limiting conditions will invariably occur, when the ESS is forced to either its upper or lower limits. This can be due to intrahour fluctuations or variations to the control structure that cause the ESS to behave somewhat differently than that expected by the hourly scheduling control, or simply because maintaining the schedule $p_{\text{ess,k}}$ leads to incomplete discharge or charging of one or both levels. The component that handles these conditions, and modifies the powers to respect these limits is detailed below.

Energy Management Rule Base

The ESS energy management system (EMS) consists fundamentally of a rule base that takes various system variables as inputs and provides changes to the power references as outputs. It essentially consists of a table of modifications to the output powers for different set of input conditions. An initial structure was put together by identifying limiting condi-

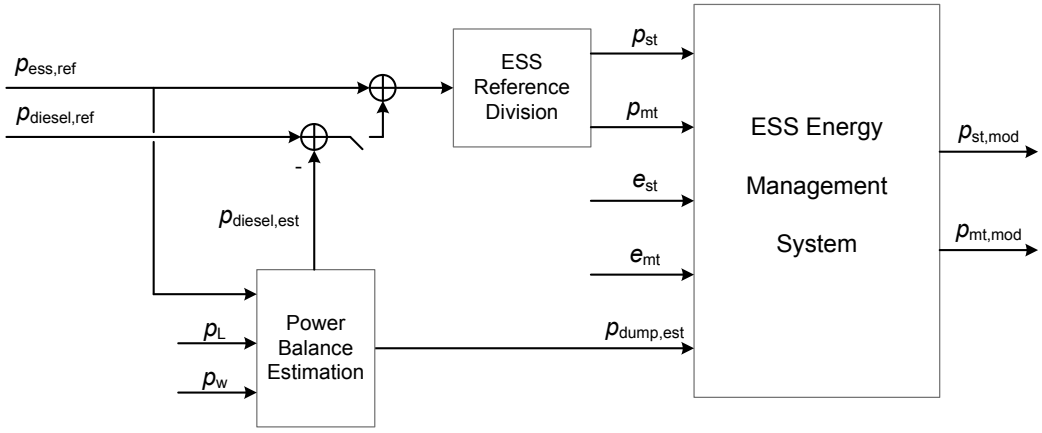

Fig. 5.5 High level overview of two-level energy storage system controller

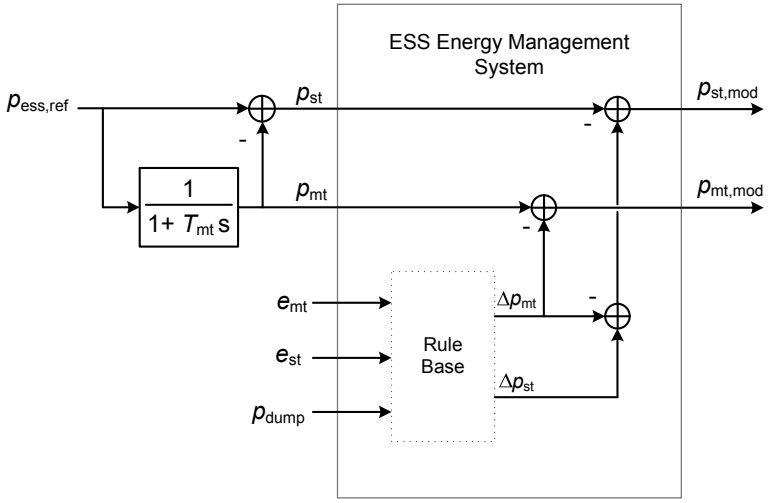

Fig. 5.6 Two-level energy storage system controller for wind-diesel systems

tions, defining rules for modifications to the power references, and then selecting optimum thresholds using parametric analysis. The performance metrics previously defined were used to assess the merits of a given set of thresholds.

The resulting table is given for the case where e_{st}, e_{mt}, and $p_{\mathrm{dump,est}}$ are used as inputs, Table 5.1. It was constructed with the objective of maintaining the overall ESS power reference, $p_{\mathrm{ess,ref}}$ ($p_{\mathrm{ess,k}}$), under as many conditions as possible by transferring portions of

the power reference between the two levels, if one or the other approaches its upper or lower energy limit. Moreover, with $p_{\text{dump,est}}$ included as a supplemental signal, the power references may also be adjusted to minimize the dumped power, assuming sufficient capacity exists.

If there are capacity issues with either of the storage devices, rules 2-7 together with Fig. 5.5 are used to reschedule the ESS. For the first of the two objectives, the power reference of the short-term device is increased as it approaches its upper limit while the reference of medium-term device is decreased by the same amount to maintain the overall power reference. In contrast, if the short-term device is nearly discharged, its reference is curtailed with the medium-term being augmented in like manner.

For the objective of reducing dumped power, the short-term device is favoured to accept it as an additional load but the medium-term device may be used in the event the former does not have sufficient capacity (rules 8-15). In the event there is no dump load, the power references of the two-levels remains unchanged (rule 1).

Together the table captures a number of separate objectives and the constraints associated with each device. However, additional details related to the diesel plant and its operation are required before proceeding to the evaluation of the various control modes.

Diesel Plant Control

The diesel plant is normally the grid forming agent—it sets the frequency and voltage of the system. It does this through its governor control and control of its dc field current, respectively. These two controls indirectly result in supply of real and reactive power to the system. The details of these two controllers will not be provided since they are well covered in the literature, [81,88]. Instead, the management of power within the system will be of interest; the dynamics of the system are not under consideration.

The overall diesel plant control system, as well as possible modes are given in Fig. 5.7. The diesel power reference is set by the output of its governor control, which monitors the change in frequency or equivalently the mechanical speed of the generator. The dump load also represents an integral part of the control in that it is engaged to maintain the diesel at its minimum loading. First, recalling that residual load is given by:

$$p_{\text{res}} = p_{\text{L}} - p_{\text{w}} \tag{5.5}$$

Table 5.1 Rule base for ESS energy management system for use with wind-diesel systems[1]

Rule	$p_{\text{dump,est}}$	e_{mt}	e_{st}	Δp_{mt}	Δp_{st}
1	0	$[0.05, 0.95]$	$[0.3, 0.7]$	0	0
2	0	$[0.05, 0.95]$	0.05	1	0
3	0	$[0.05, 0.95]$	0.95	-1	0
4	0	0	X	-1	X
5	0	1	X	1	X
6	0	X	0	X	-1
7	0	X	1	X	1
8	$\neq 0$	$[0.05, 0.95]$	$[0.3, 0.7]$	0	$-p_{\text{dump,est}}$
9	$\neq 0$	$[0.05, 0.95]$	0.05	1	$-p_{\text{dump,est}}$
10	$\neq 0$	$[0.05, 0.95]$	0.95	-1	$-p_{\text{dump,est}}$
11	$\neq 0$	0	$[0.05, 0.95]$	-1	$-p_{\text{dump,est}}$
12	$\neq 0$	1	$[0.05, 0.95]$	1	$-p_{\text{dump,est}}$
13	$\neq 0$	X	0	X	$-p_{\text{dump,est}}$
14	$\neq 0$	$[0, 0.95]$	1	$-p_{\text{dump,est}}$	1
15	$\neq 0$	1	1	1	1

1. Storage powers changes and energies are expressed in per unit, on a base corresponding to their respective ratings.

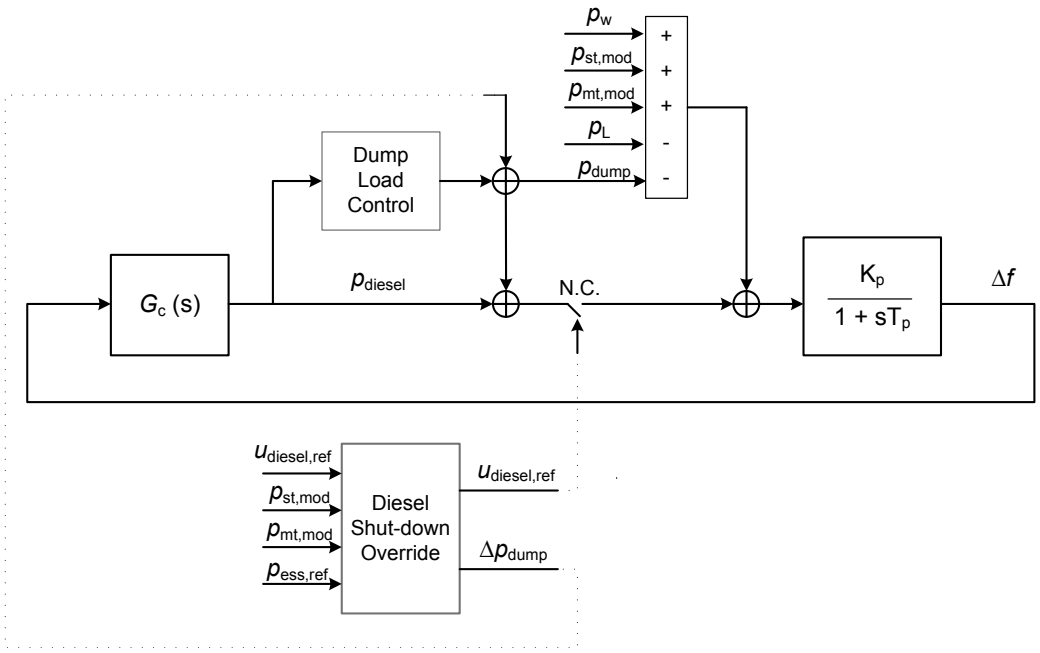

Fig. 5.7 Block diagram of diesel plant control

The equations for dump load under the different operating modes are then defined by:

$$p_{\text{dump}} = \begin{cases} 0 & p_{\text{res}} - p_{\text{ess}} \geq P_{\text{diesel,min}}, \\ P_{\text{diesel,min}} + p_{\text{ess}} - p_{\text{res}} & p_{\text{res}} - p_{\text{ess}} \leq P_{\text{diesel,min}}. \end{cases} \tag{5.6}$$

Under continuous operation, the rest of the schematic is fairly self-explanatory. However, additional details are required when the diesel plant is shutdown ($u_{\text{diesel,k}} = 0$). Specifically, what is the role of the dump load in this mode of operation and what is the process of overriding the shutdown order.

For the diesel shutdown override, one must consider the level of energy in the medium-term storage. As was seen in the previous section, the medium-term device will support the short-term device when the latter has neared one of its limits. However, when the medium-term device reaches one of its limits, a critical situation has been reached. This scenario is indicated by the difference between the initial power reference coming from the power balance and the sum of the short-term and medium-term ESS powers ($p_{\text{ess,ref}} -$

Table 5.2 Rules for generation of diesel scheduling and changes to dump load for cases where shutdown is signalled

State of ESS	$p_{\text{ess,ref}} - p_{\text{mt,mod}} - p_{\text{st,mod}}$	$u_{\text{diesel,ref}}$ [1]	$u_{\text{diesel,mod}}$	Δp_{dump}
Normal	0	0	0	0
Overcharged	> 0	0	0	$p_{\text{ess,ref}} - p_{\text{mt,mod}} - p_{\text{st,mod}}$
Undercharged	< 0	0	1	0

1. These are used only for cases where a shut-down is signalled and are not used in any way for setting of these variables when the diesel is scheduled on, i.e. $u_{\text{diesel,ref}} = 1$.

$(p_{\text{mt,ref}} + p_{\text{st,ref}})$). Whether it is overcharged or undercharged depends on the the sign of this difference.

Table 5.2 presents the rules for generation of the dump load power and for signalling a shutdown override, when the diesel is shutdown. As mentioned the difference between the initial power reference and the total power delivered by the two ESS levels indicates which of the cases, and thereby dictates the appropriate actions. If the ESS's are overcharged then the dump load can be used to dissipate additional energy and an override condition is not required. However, if both levels are completely discharged then one has no choice, apart from shedding load, but to issue an override signal.

5.3 Controller Performance Testing

The general control structure for the two-level was then tested using both simulation of the system and its hardware-in-the-loop (HIL) real-time simulation (RTS) representation to validate results and ensure that it functions adequately in real-time. First, the different control modes tested are defined. Then the performance metrics used to compare the different control modes are defined before presenting the results.

5.3.1 Test Cases

The different test cases are really just combinations of the different features of the two-level ESS control previously discussed. They are numbered and defined in Table 5.3. Control mode 1 is the general structure of Fig. 5.5 with $p_{\text{ess,ref}}$ modified by the difference between $p_{\text{diesel,ref}}$ and $p_{\text{diesel,est}}$. The rule base that coordinates the two levels is not included. Control mode 2 includes only the estimated dumped energy as inputs to the rule base; the energy

Table 5.3 Wind-diesel and two-level ESS control mode test cases

No.	Control mode	Description
1	min Δp_{diesel}	Minimization of deviations of p_{diesel} from its hourly reference
2	min p_{dump}	Minimization of intrahour dumped energy
3	ESS coordinate	Coordination of two ESS levels to maximum utilization of combined energy ratings
4	23	Combination of control modes 2 and 3
5	13	Combination of control modes 1 and 3
6	123	Combination of all three control modes
7	Base case	Divide $p_{\text{ess,ref}}$ between two levels using low-pass filter only
8	No ESS	Storage power and energy ratings are set to '0'

levels are presumed to be at 0.5 per unit and therefore do not impact the decision making process. Control mode 3 includes the coordination between the two ESS levels, but does not consider $p_{\text{dump,est}}$ as an input. Mode 4–6 are simply combinations of the other three modes.

In addition to the 6 modes described, two additional cases are included to serve as reference points. The first is the simple division of the ESS power reference using the low-pass filter, represented by Fig. 5.2a. As the power references are constant this reduces to the case of maintaining the dispatch orders given by the results of the ANN controller or the off-line optimization approach. Finally, the case of no ESS is again included to define the baseline, as a minimum level of performance that all ESS control modes should surpass.

The ratings of the ESS is as used in the previous chapters, those resulting from the results of the ESS sizing for the two modes of diesel operation, at the optimum penetration level, $r_{\text{wl,p}}$. A representative week from WR 1 was used, but some processing of the hourly data was required to render it intrahour data, sampled at a frequency of 5 Hz. The rationale and assumptions made are relegated to Appendix C.

5.3.2 Performance Metrics

Once again, two of the main metrics that will be used measure the performance of the various control modes will be the cost of energy and the amount of dumped energy, E_{dump}. The intrahourly cost of energy will be calculated as follows, again normalized using the energy of the load over the period to give an amount in \$/kWh:

$$C_{\text{intra}} = \frac{1}{E_{\text{load}}} \left[n_{\text{d}} \left(\pi_{\text{ess,e}} \, E_{\text{ess}} + \pi_{\text{ess,p}} \, P_{\text{ess}} \right) + \frac{K}{I} \sum_{i=1}^{I} \left(\pi_{\text{e}} \, p_{\text{diesel},i} + \pi_{\text{w}} \, p_{\text{w},i} \right) \right] \tag{5.7}$$

where n_{d} is the number of days over which the simulation is carried out, I is the total number of intrahour samples, and K is the number of hourly dispatches. An important caveat is that the cost for these simulations will be skewed depending on the final energy state of the ESS, E_{T}. As the period is fairly short, control modes that lead to a fully charged storage would be related to higher C_{intra}. Likewise, those that fully discharged storage would give lower costs, due to use of the initially stored energy, which is essentially free. For the longer simulations this effect is less pronounced and can be neglected, whereas for the present simulations one should refer more to E_{dump} as an indicator of performance.

Three additional measures are defined to help assess the impact of the control mode on the way in which diesel power changes relative to its dispatch, Δp_{diesel}:

$$\Delta p_{\text{diesel},i} = p_{\text{diesel,ref}} - p_{\text{diesel,i}} \tag{5.8}$$

The control modes will be compared using the maximum Δp_{diesel}, its mean, and standard deviation, the latter two being given by:

$$\mu \left(\Delta p_{\text{diesel}} \right) = \frac{1}{I} \sum_{i} \Delta p_{\text{diesel},i}, \qquad i = 1, \ldots, I \tag{5.9}$$

And:

$$\rho \left(\Delta p_{\text{diesel}} \right) = \sqrt{\frac{1}{I} \sum_{i} \left[\Delta p_{\text{diesel},i} - \mu \left(\Delta p_{\text{diesel}} \right) \right]^2}, \qquad i = 1, \ldots, I \tag{5.10}$$

5.3.3 Simulation Results

Procedure

To evaluate the performance of the different control modes required a representative profile of intrahourly wind data. To this end, the 5 Hz data from [110] was adapted for use with one week of the hourly data from WR 1. Appendix C provides details of this procedure. Figure 5.8 gives the resulting wind power and load profiles, which were used in the subsequent

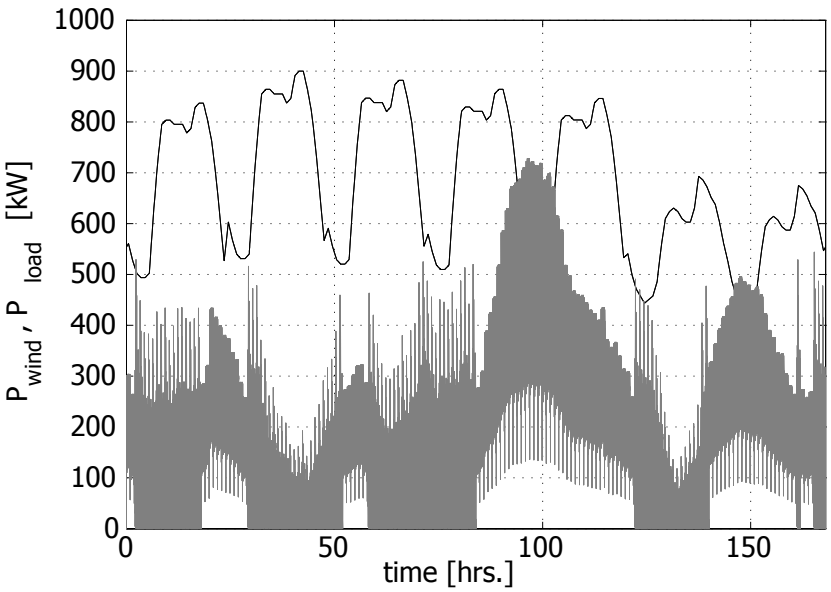

Fig. 5.8 Plot of wind (grey) and load (black) profiles for evaluation of two-level ESS controllers.

cases considered. It was assumed that intrahour wind power variations are more important than load variations. The intrahour load variations were modeled by interpolating linearly between the two hourly averages.

Different controllers were simulated over the selected week, including continuous diesel operation and with diesel shutdown permitted. Performance metrics were calculated for the eight different control modes. Due to the fact that the system is only run over a week, the cost of energy is somewhat less representative since the amount of stored energy at the end of the period will impact to a much larger extent the cost of energy. When the ESS is nearly fully charged, this results in larger diesel consumption and consequently, higher costs, even if the dumped energy is lower. As a result, the dumped energy over the period is more indicative of the value brought to the system. Unfortunately, this affects our ability to gauge the role of ESS capital costs; but, given that sizing is not the focus of this chapter, this is acceptable.

In addition, the time domain data was also plotted to better illustrate how the different components in the system were used under the different control modes. Data was plotted for the two ESS levels, the diesel plant power, and the dump load, over the 168 hours of operation, for control modes 1, 2, 3, and 6 (combination of the first three modes). Power

and energy scatter plots, together with time domain representations were again used to visualize the operation of the ESS levels. Diesel plant power was given as a time series and was also presented by its discrete probability distribution function. The wind and load data was common to all cases, as given in Fig. 5.8.

Analysis - Parallel Operation

The performance indices are given for the eight control modes in Table 5.4. The dumped energy is highest in the case of no ESS, which is as it should be. The control modes that have minimizing the dumped energy as objectives—modes 2, 4, and 6 (combination of the first three modes)—exhibit the lowest dumped of energy as well. This is supported to a certain extent by the cost of energy, but again it is skewed in some cases by the different levels of residual stored energy at the end of the period.

The control mode also has a strong influence on the deviation of the diesel power from its scheduled power. All modes that include the feature of control mode 1 result in smaller standard deviations for ΔP_{diesel}, and smaller values for the maximum deviation from the schedule. The mean values of ΔP_{diesel} are actually largest in these cases but given that the objective is to reduce variations over time, this is acceptable. Interestingly, the best performance from the point of view of $\rho(\Delta P_{\text{diesel}})$ and $max\ |\Delta P_{\text{diesel}}|$ the diesel schedule is achieved when the three modes are combined (mode 6).

The two-level ESS data was plotted using power and energy scatter plots (Figs. 5.9 and 5.10 for the medium-term and short-term devices, respectively) as well as the time domain plots of the two storage level powers, Fig. 5.11. The scatter plots provide the trajectories of the different levels. No longer are there distinct boundaries as existed for the hourly results, due to the fact that the step size is now 0.2 seconds. The trajectories are quite different depending on the control mode.

The most random patterns are observed for cases where minimization of Δp_{diesel} is an objective (modes 1 and 6) as these modes transfer the balance of power function to the ESS. Control mode 3, which only provides coordination between the two-level, only shows moderate variations as it generally follows the dispatched value. Somewhat greater variation is seen in control mode 2 where the schedule is modified in an attempt to minimize the dumped energy.

These results are mirrored in the time domain plots where modes 1 and 6 show the

Table 5.4 Performance data of different two-level ESS operation strategies

Control Mode	Description	E_{dump} [pu]	Simulated Cost, C_{intra} [$/kWh]	Mean Δp_{diesel} [pu]	Std. Dev. Δp_{diesel} [pu]	Maximum Δp_{diesel} [pu]
1	min. ΔP_{diesel}	0.04479	0.5727	-0.03196	0.0745	0.3414
2	min. E_{dump}	0.03410	0.5585	-0.01598	0.1153	0.4283
3	E_{st}, E_{mt} coordination	0.04291	0.5630	-0.02109	0.1195	0.4283
4	2 and 3	0.02941	0.5580	-0.01543	0.1151	0.4283
5	1 and 3	0.04404	0.5716	-0.03080	0.0723	0.3388
6	1, 2 and 3	0.03413	0.5699	-0.02885	0.0644	0.3388
7	Base case	0.04293	0.5631	-0.02122	0.1199	0.4283
8	no ESS	0.05561	0.5652	-0.02357	0.1215	0.4283

greatest activity, a moderate level of activity with mode 2 and only limited activity in case 3. Referring back to the wind and load profiles, the greatest source of variation is from the wind power, which is reflected in the two most active modes. Periods of charging and discharging with controller 2 coincide with periods of high wind and low load, indicating the control is performing its desired function. The ESS associated with controller 3 remains relatively inactive as it more or less follows the hourly schedules, oblivious to the intrahour variations.

Diesel power is presented in terms of its power density function, Fig. 5.12 and by its time series, Fig. 5.13, for the four control modes. When ESS is not re-scheduled to accept more of the power balance variations (modes 2 and 3), the diesel must handle the majority of the fluctuations introduced by the wind. Also, there seems to be a tendency to operate at lower loadings, although mode 3 shows the lowest frequency of operation at minimum loading. When the ESS is rescheduled to respect the diesel schedule (modes 1 and 6), the *pdf* shows more random behaviour (more constant probabilities across loadings). When the objective is to minimize dumped energy (modes 2 and 6) the diesel operates more often at its minimum loading, an unexpected consequence.

The time series of the dumped energy for the different control modes, Fig. 5.14, supports the observations from the other results. From these figures many of the trends previously discussed are apparent. Remaining faithful to the original schedule (mode 3) results in the highest frequency of dumped load, whereas when dump load minimization is an objective of

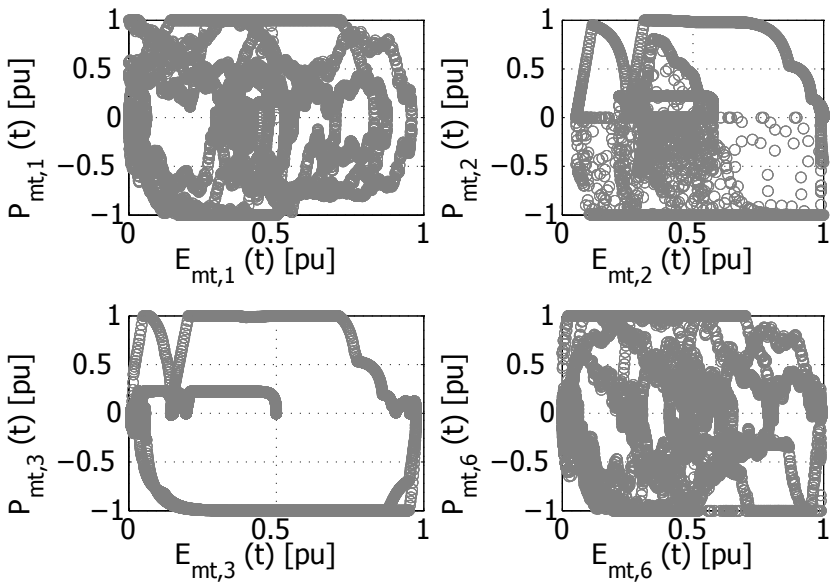

Fig. 5.9 Plot of medium-term ESS power and energy states for a representative week, with continuous diesel operation, given for different control modes.

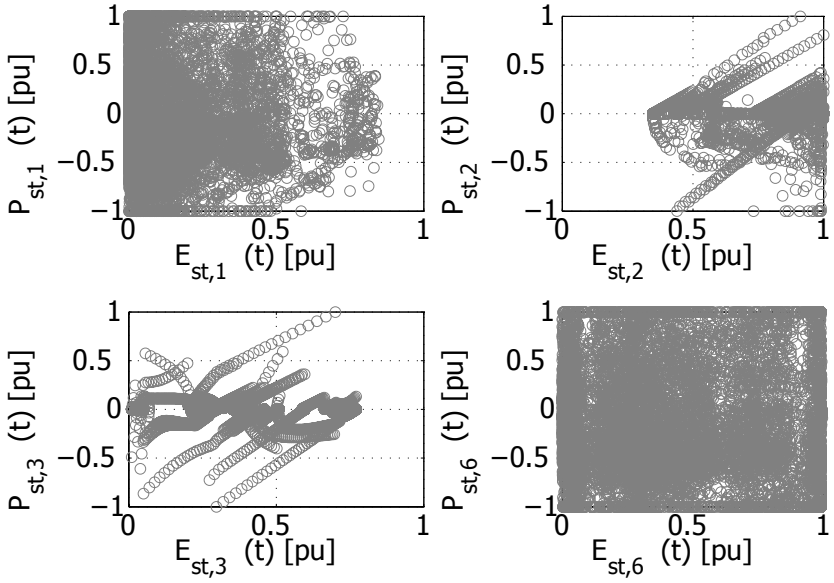

Fig. 5.10 Plot of short-term ESS power and energy states for a representative week, with continuous diesel operation, given for different control modes.

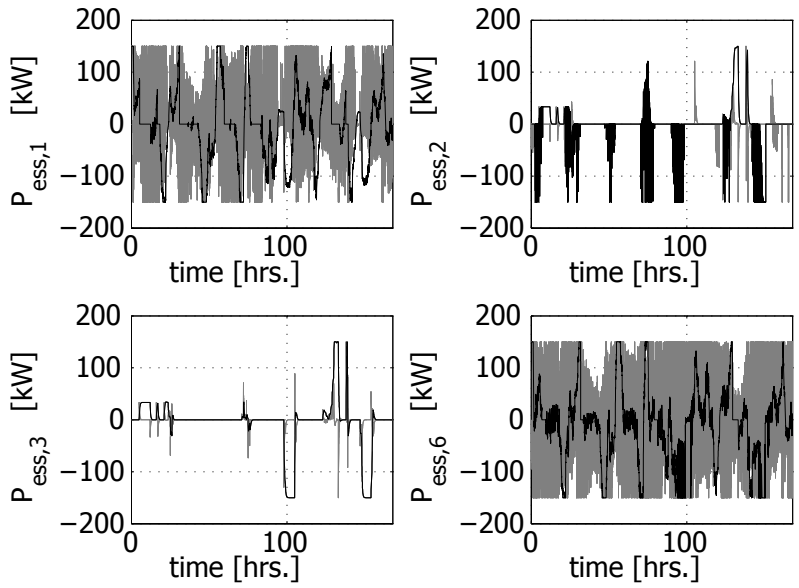

Fig. 5.11 Plot of time series of medium-(black) and short-term (grey) ESS powers, for control mode 6, for a representative week, with continuous diesel operation.

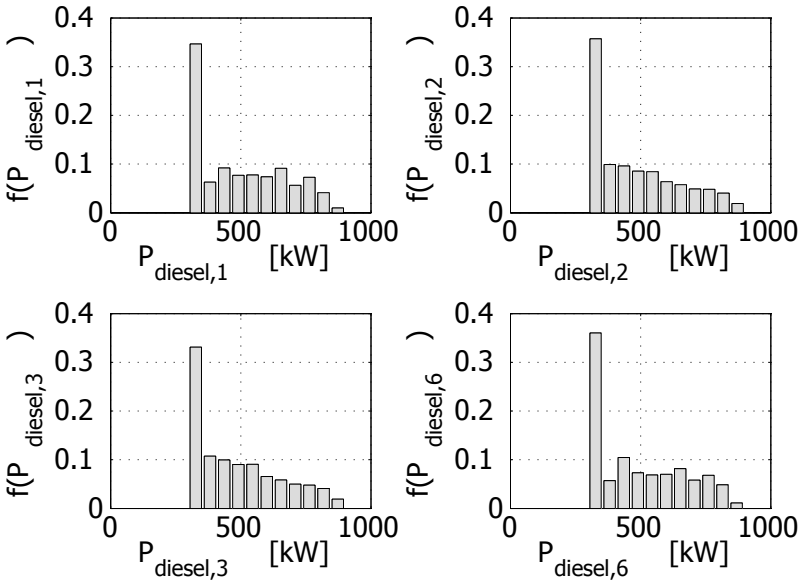

Fig. 5.12 Plot of diesel power discrete probability functions for different ESS control modes, for a representative week, with continuous diesel operation.

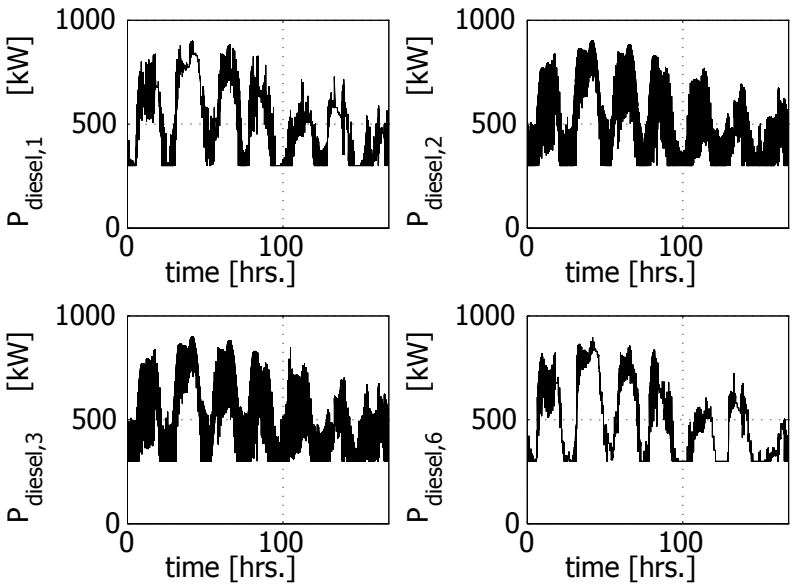

Fig. 5.13 Plot of time series of diesel power for control mode 6 for a representative week, with continuous diesel operation.

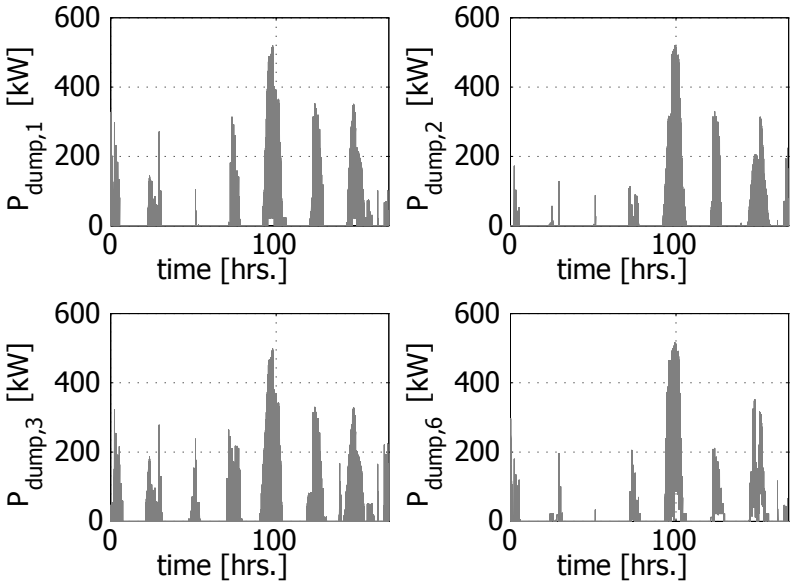

Fig. 5.14 Plot of time series of dump load for control mode 6 for a representative week, with continuous diesel operation.

the instantaneous control, many instances are eliminated. During period of high dumped energy (e.g. hours 100, 125, 150), although not completely eliminated, the amount of dumped energy is greatly reduced. Interestingly, a desirable but indirect consequence of reducing fluctuations of diesel power is reduced dump load, albeit to a lesser extent than when limiting dumped energy is more explicitly embedded in the control algorithm.

Analysis - Diesel Shutdown Operation

The results were again repeated for diesel shutdown operation, the performance metrics for the different control modes are given in Table 5.5. Once again the cost of energy does not necessarily coincide with what is expected in that the case of no ESS shows a lower C_{intra} than some of its contemporaries. This is due again to the different SOCs at the end of the interval. Those that result in a predominantly discharged ESS will be associated with lower costs of energy. Contrarily, the dumped energy is highest in the case with no ESS, following what one would expect.

As for the continuous case, control modes that incorporated the objective of minimizing E_{dump} by deviating from predefined schedules (modes 2, 4, and 6) lead to reduced dumped energy. However, unlike the continuous case mode 4 resulted in the lowest E_{dump} in place of mode 6. This is perhaps due to the fact that when the diesel is ordered to shutdown, making it more difficult under mode 6 to meet both objectives of minimizing E_{dump} and deviations from the diesel schedules.

The deviations from the diesel schedules also exhibited similar trends as for the continuous case. The standard deviation and maximum values of ΔP_{diesel} were lowest in cases 1, 5 and 6. Once again, the advantage of this control mode is most clearly illustrated in the time domain plots, where the balancing of high frequency fluctuations is transferred to the short-term ESS.

The data for the two-levels were once again plotted using the power and energy scatter plots (Figs. 5.15 and 5.16, for the medium- and short-term ESS, respectively) and the time domain plots of their powers, Fig. 5.17. Again the activity of the two ESS levels is greatest when minimizing diesel power fluctuations is the goal (modes 1 and 6) and to a lesser extent when the objective is to minimize dumped energy (control mode 2).

In comparison with the continuous diesel operation results, there is a greater spread of points, probably due to the inclusion of shutdown periods. In these instances the ESS must

Table 5.5 Performance data of different two-level ESS operating strategies

Control Mode	Description	E_{dump} [pu]	Simulated $Cost, C_{\text{intra}}$ [$/kWh]	Mean Δp_{diesel} [pu]	Std. Dev. Δp_{diesel} [pu]	Maximum Δp_{diesel} [pu]
1	min. ΔP_{diesel}	0.03092	0.5623	-0.05232	0.1059	0.3324
2	min. E_{dump}	0.02590	0.5503	-0.03763	0.1389	0.3870
3	E_{st}, E_{mt} coordination	0.03246	0.5534	-0.04046	0.1415	0.4283
4	2 and 3	0.02260	0.5500	-0.03763	0.1391	0.3807
5	1 and 3	0.02975	0.5617	-0.05196	0.1059	0.3669
6	1, 2 and 3	0.02550	0.5622	-0.05106	0.1034	0.2996
7	Base case	0.03216	0.5529	-0.04025	0.1414	0.4283
8	no ESS	0.04184	0.5570	-0.03972	0.1418	0.4283

meet the power balance equation, accepting the entire variability of the wind. The time domain results show some similarities to the continuous diesel operating case but differ during high dump periods due to the shutdown of the diesel plant and the resulting greater involvement of the ESS. This is particularly evident for the cases of control modes 2 and 3.

The *pdf* and time domain plots of diesel power for the different control modes are given, respectively in Figs. 5.18 and 5.19. The areas of shutdown occur during hours of minimum load that are correlated with high wind periods, specifically in the vicinity of hours 100 and 150. There are a number of shutdown and start-up instances during these intervals, rather than shutdown being maintained for a complete hour, as would be preferred.

Due to repeated cycling of the diesel plant between *on* and *off* states, it might be desirable to incorporate a minimum shutdown constraint somehow into the problem. This cycling results directly from the intrahour wind fluctuations, and indicates that further investigation is required to understand the conditions under which it is favourable for diesel shutdown to occur. It does not seem to be as simple as counting on the scheduling from the offline optimization or NN controller to dictate the shutdown schedule.

Similar trends as for continuous diesel operation are observed for the dump energy when considering the different control modes, Fig. 5.20. Modes 2 and 6 eliminate large periods of dumped energy. Interestingly, the shutdown periods are generally accompanied by large amounts of dumped energy, likely to maintain the shutdown order when the storage has reached its full storage capacity. In the control structure, maintaining a shutdown

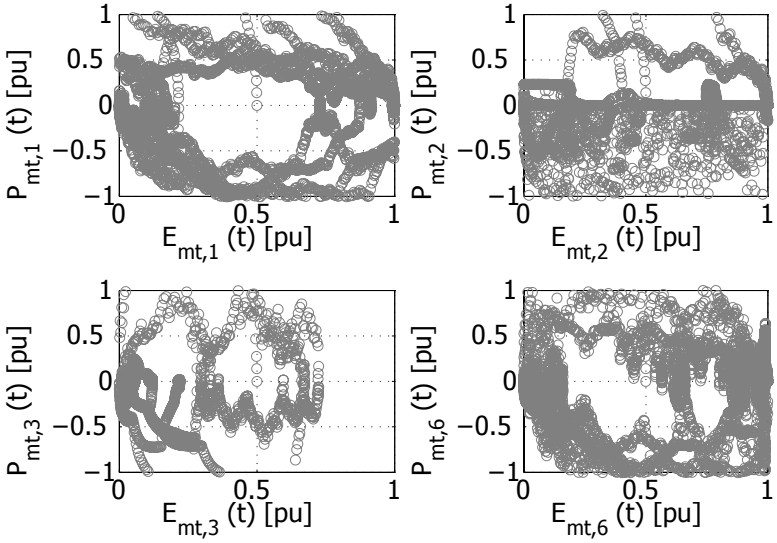

Fig. 5.15 Plot of medium-term ESS power and energy states for representative week of operation with diesel shut-down permitted, given for different control modes.

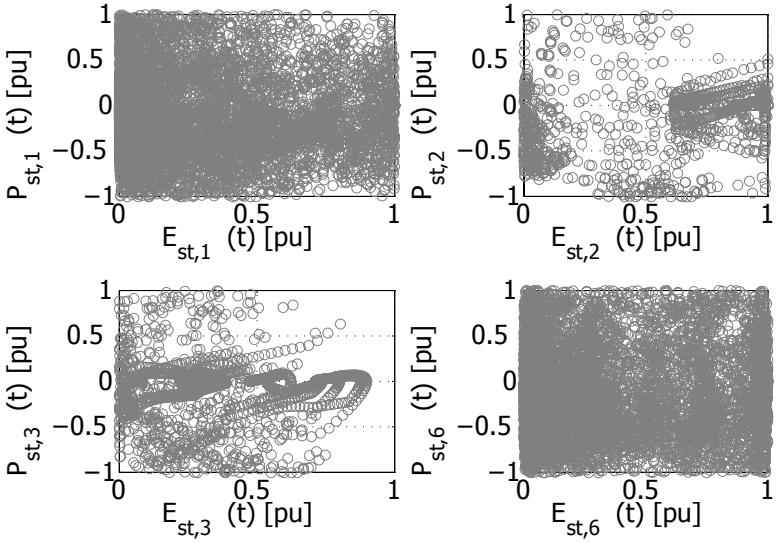

Fig. 5.16 Plot of short-term ESS power and energy states for representative week of operation with diesel shut-down permitted, given for different control modes.

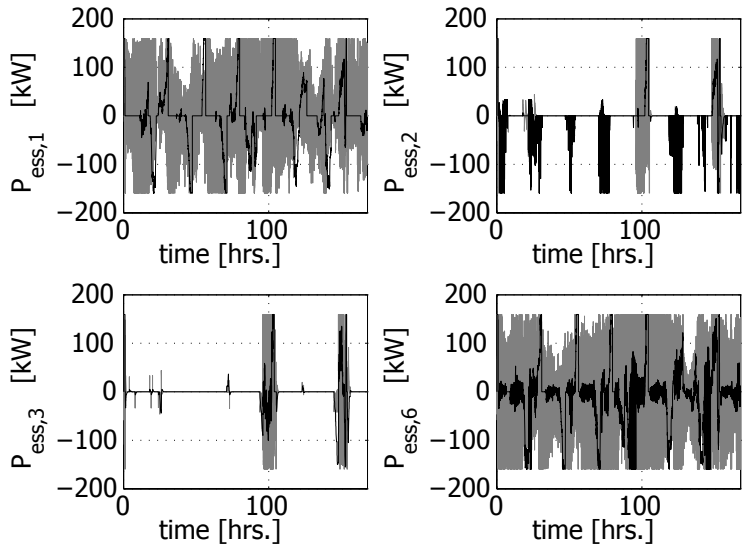

Fig. 5.17 Plot of time series of medium- (black) and short-term (grey) ESS powers, for control mode 6, for representative week of operation with diesel shut-down permitted.

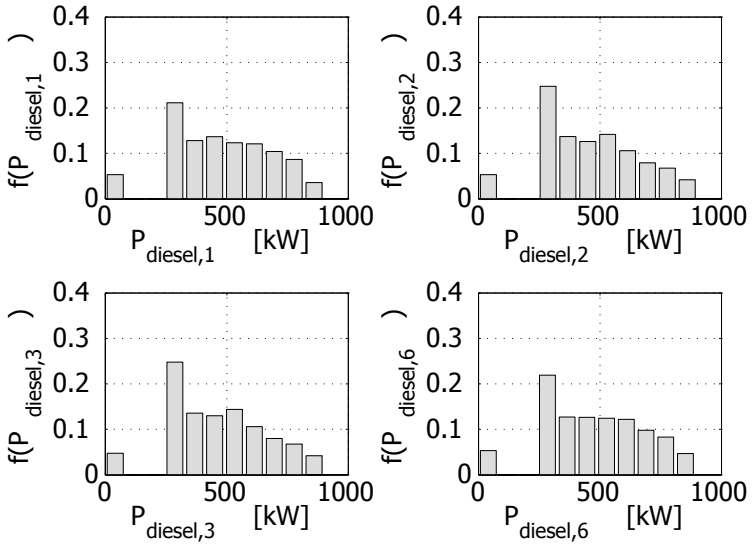

Fig. 5.18 Plot of diesel power discrete probability density functions for different ESS control modes, for a representative week of operation, with diesel shutdown permitted.

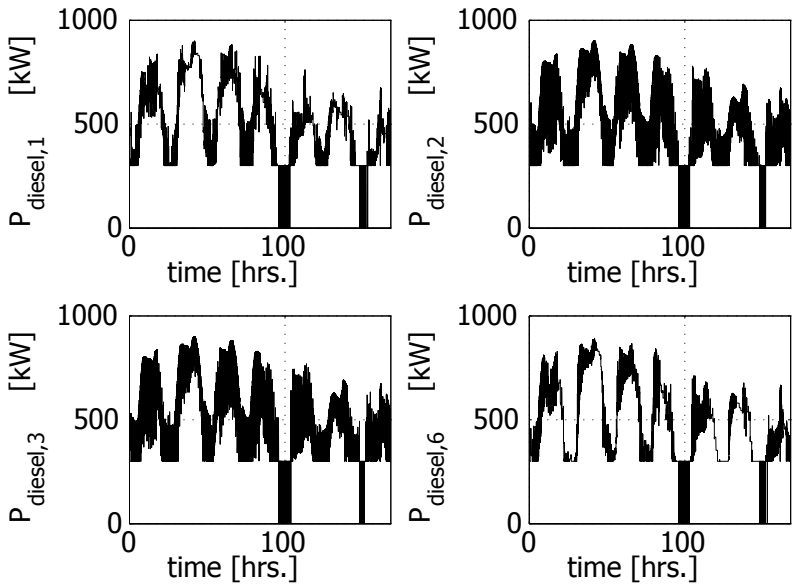

Fig. 5.19 Plot of time series of diesel power for different ESS control modes, for a representative week of operation, with diesel shutdown permitted.

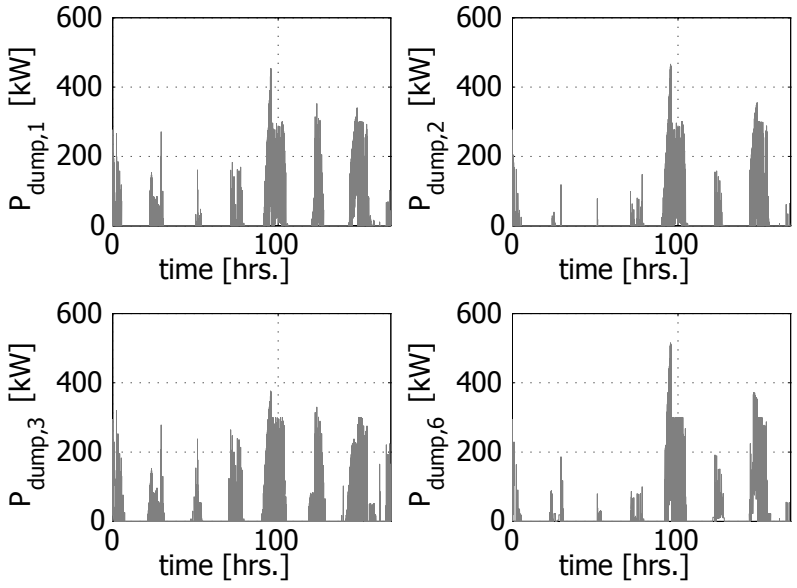

Fig. 5.20 Plot of time series of dump load power for different ESS control modes, for a representative week of operation, with diesel shutdown permitted.

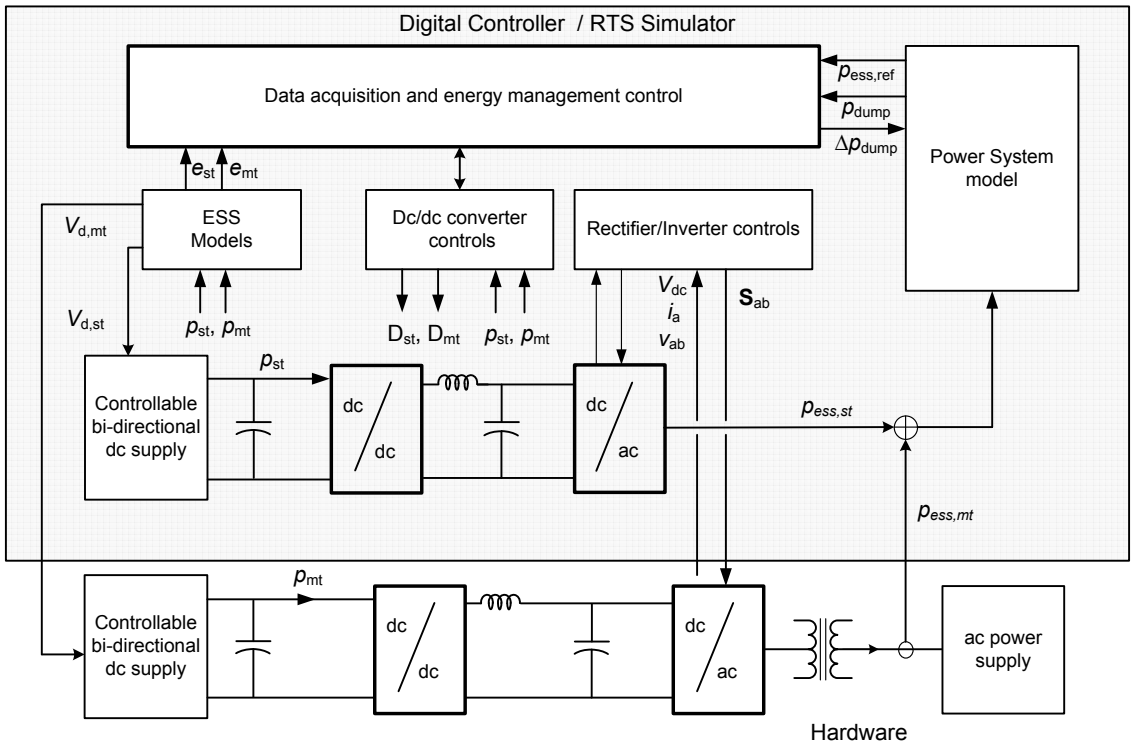

Fig. 5.21 Real-time simulation set-up of two-level energy storage system

order using the dumped load is given priority to minimizing dumped load since no diesel fuel is used during these periods. This justifies why we observe the highest magnitude of dumped load power for control mode 6 (occurring during a shutdown interval), even though minimizing dumped energy is one of the main objectives.

5.3.4 Experimental Results

As full scale validation of the system was not possible, HIL real-time simulation was used in order to validate some of the simulation results. The main intent of the HIL-RTS was to confirm that the controller could be implemented and run in real-time.

The HIL real-time simulation representation is shown in Fig. 5.21. In this case, the medium-term ESS is represented partly in hardware. The dc voltage from a vanadium-redox flow batterty (VRB) model, detailed in [107], was supplied as dc voltage reference to a controllable rectifier. Likewise, any other battery model, [111–114], or ESS charging

schemes, [96, 115, 116], could be used in the set-up.

Various power converter topologies can be used for integration of ESS, [117–121]. Here a bidirectional dc/dc converter was coupled to this emulated battery voltage through an inductor, permitting control of power to or from the dc source. A two-phase controllable inverter/rectifier was used to regulate the high side dc voltage and facilitate flow of power to or from the emulated battery.

The measured dc current was then fed back into the power system model, as a dc current source on the ESS converter dc bus. This dc bus sources the supercapacitor storage through its dc/dc converter, and through an inverter/rectifier provides the connection to the grid, which includes wind, load, and the diesel plant. The two-level ESS controller was realized on the same real-time simulator, and provides gating signals to the power converters. Details on the hardware components are contained in Appendix E.

Procedure

As the primary intent of the HIL results was to confirm that the controller could work on-line, only one hour of the weekly profile was used. Hour 150 was chosen as it occurred during one of the weekend days with high wind. In this way, the ESS was active and there was greater possibility of driving one of the levels to its limits. The ESS levels were initialized according to the hourly scheduling results, as were the set-points for $p_{\text{ess,ref},k}$ and $p_{\text{diesel},k}$.

Control modes 4-6 were run using the HIL set-up and using the simulation representation of the model. The previously defined performance metrics were tabulated for all cases and time domain results were generated for the HIL system using control mode 6. Only continuous operation of the diesel plant was tested using the experimental set-up.

Analysis

Comparison of the performance metrics shows good agreement between the HIL and simulation results, Table 5.6. Small differences do exists due to the non-ideal characteristics introduced by the power electronic converters, and possibly due to small differences between the ESS models in the HIL set-up (VRB and supercapacitors) and those used in simulation (generic short- and medium-term storage device with constant efficiency η). The results are sufficiently similar in order to be confident that the results obtained by simulation are

Table 5.6 Performance metrics of hardware-in-the-loop and simulation results for hour 150

Control Mode	Model Type	E_{dump} [pu]	Mean C_{intra} \$/kWh]	Mean Δp_{diesel} [pu]	Std. Dev. Δp_{diesel} [pu]	Maximum Δp_{diesel} [pu]
4	Sim.	0.1146	0.7605	0.028	-0.0097	0.292
	HIL	0.1096	0.7591	0.029	-0.0102	0.297
5	Sim.	0.2227	0.7477	0.0052	-0.0004	0.142
	HIL	0.2097	0.7723	0.0051	-0.0010	0.149
6	Sim.	0.0915	0.7478	0.0052	-0.0004	0.142
	HIL	0.0905	0.7489	0.0058	-0.0011	0.155

representative.

Time domain results using control mode 6 are given for the HIL set-up, Figs. 5.22–5.24. As can be noted, the diesel is driven to near or at its minimum loading for the majority of the hour. This leads to mostly charging by the medium-term ESS, while the short-term ESS absorbs the fast fluctuations introduced by the wind power. Energy states of both levels exhibit charging from the initial state to slightly higher levels, with the short-term device showing greater fluctuations.

Measured traces of the inverter/rectifier output current, converter output voltage, and line voltages are given, Fig. 5.25. As can be noted, the output current is 180 degrees out-of-phase with the voltages, as the ESS is charging. This is reflected in the dc current, Fig. 5.26, that has a negative average value. The dc inductor voltage is produced by the switching of the dc/dc converter, voltages dictated by the differences between the dc bus voltage (300 V) and the emulated VRB voltage (roughly 225 V at that particular state-of-charge), Fig. 5.27.

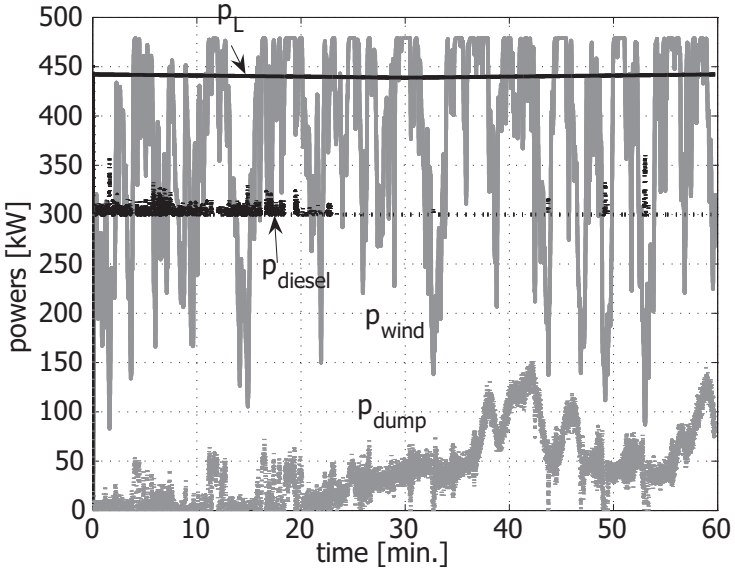

Fig. 5.22 Plot of wind power, diesel power, dump load, and load profile from HIL simulation for hour 150 of weekly wind power and load profile, using control mode 6

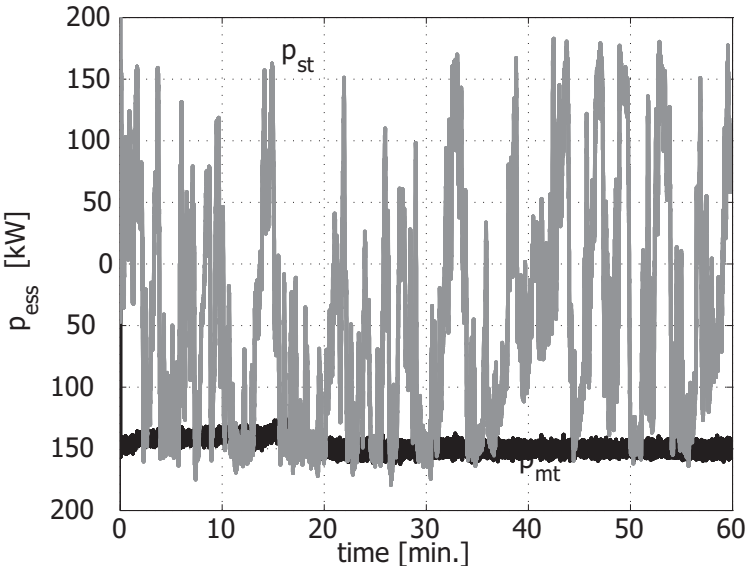

Fig. 5.23 Plot of short-term (grey) and medium-term (black) powers from HIL simulation for hour 150 of weekly wind power and load profile, using control mode 6

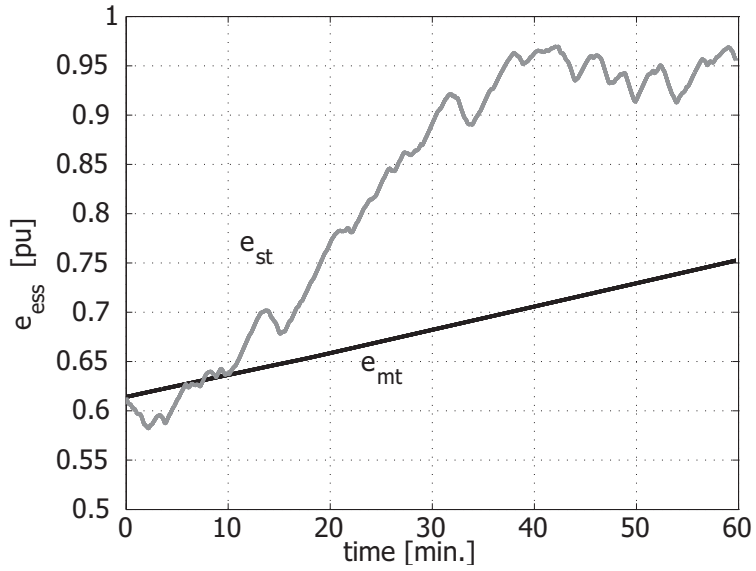

Fig. 5.24 Plot of short-term (grey) and medium-term (black) energies from HIL simulation for hour 150 of weekly wind power and load profile, using control mode 6

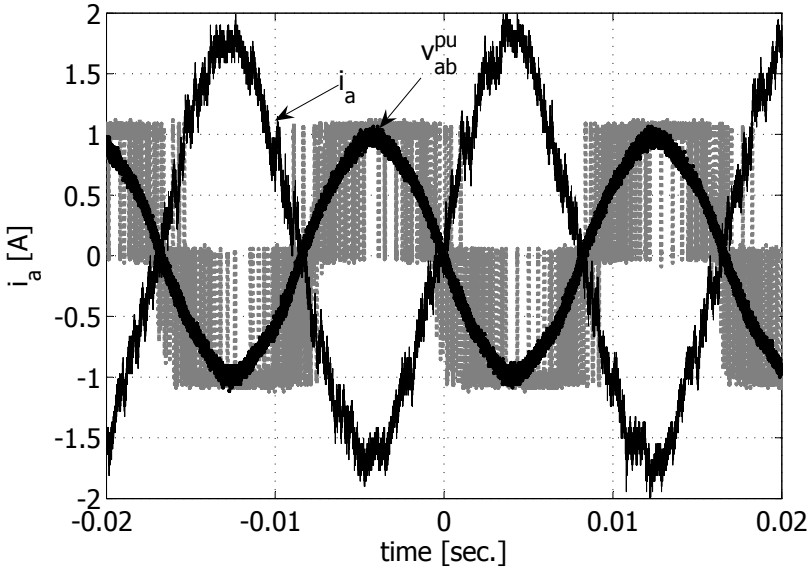

Fig. 5.25 Plot of converter output current and normalized output voltage and normalized system line voltage for battery charging.

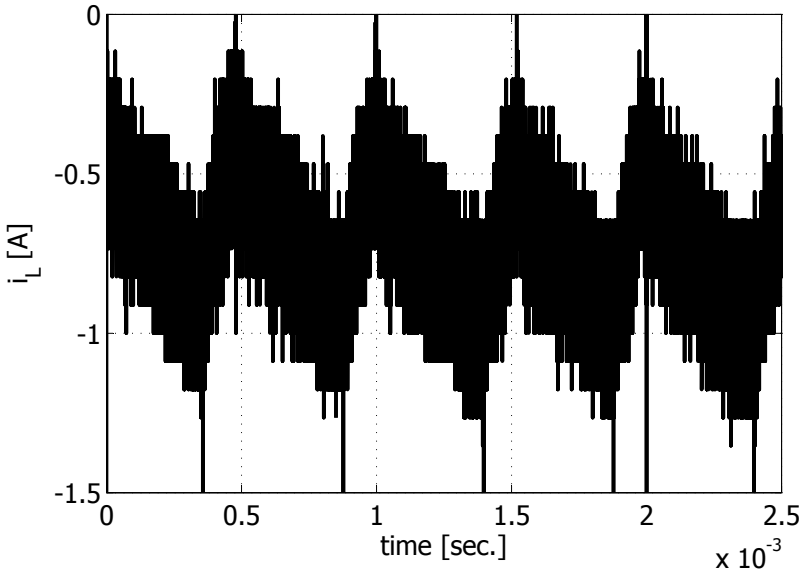

Fig. 5.26 Plot of dc current for battery charging.

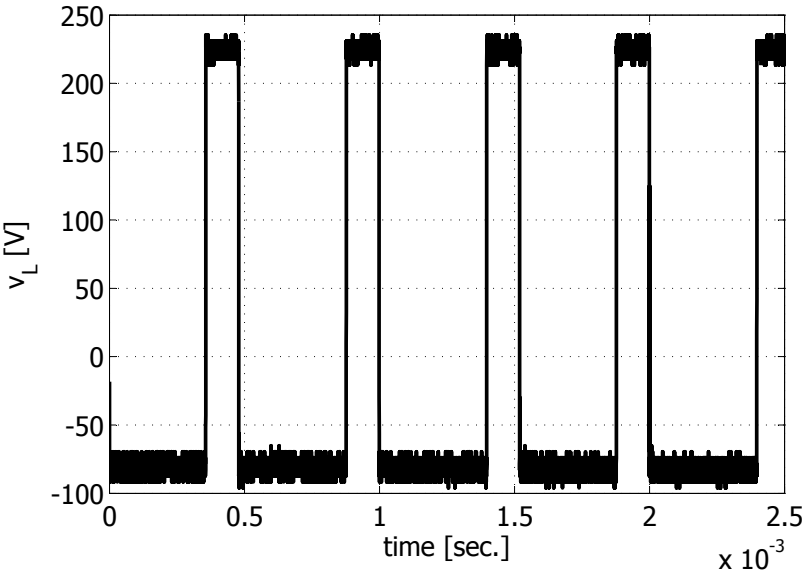

Fig. 5.27 Plot of dc inductor voltage for battery charging.

5.4 Conclusions

This chapter consider the implications of operating the ESS in real-time. This included the extension of the idealized ESS to a two-level ESS by complementing the high energy rated medium-term device with a fast-acting short-term ESS to respond to high frequency variations due to wind power fluctuations. A general control structure was developed for multi-level ESS systems. Then specific real-time control functionalities were defined for the wind-diesel system, that work on variations to the hourly set-points established by the higher level controls, developed in previous chapters. The different control modes were simulated and selected results were validated using a HIL real-time simulation implementation of the system.

From the ESS design point-of-view, the inclusion of a two-levels results in an energy rating that is higher than that required from a single level. This fact needs to be somehow incorporated into the sizing study, possibly in a first instance by simply scaling the per unit value of fixed costs associated with ESS energy capacity. The different energy costs associated with the short-term and medium-term technologies would need to be factored in, using the assumed proportions due to the value of T_{mt} used.

Although included as a performance metric for the results, the cost of energy was less indicative of the value that ESS brings to the system due to the residual energy that might remain at the end of the period considered. This effect was only important due to the shorter simulation periods relative to the previous investigations. As the analysis was focused more on the utilization of assets, the relative dumped energy and deviation of the diesel from its schedule, Δp_{diesel} were more useful indicators.

Control modes that attempted to absorb the fluctuations imposed on the diesel generator were successful at transferring short-term variations from the diesel to the ESS. This was predominantly absorbed by the short-term device but slower variations were handled by the medium-term device. In combination with other control functions, the benefit is enhanced, likely due to the improved ability in managing the energy within the two levels.

There is a clear benefit in deviating from the hourly schedule in order to minimize dumped energy. Short-term variations in the expected set-points due to differences between the average hourly wind power and the instantaneous power can cause instances of dumped energy than can be better handled if concessions exist in the two-level storage control to adjust power references accordingly. Again these can be combined with other control

functions and successfully meet the different objectives.

When diesel shutdown occurs there are often a number of transitions between the *on* and *off* states, something that is likely undesirable over the long-term. Ultimately this fact needs to be considered in greater detail and potentially propose some mitigating strategy, either through the use of minimum on- and offtime constraints, higher ESS energy ratings, or other. Obviously, this will undoubtedly impact all previous analyses, including hourly operation and ESS sizing. Most probably, cost reductions associated with this mode of operation are likely optimistic.

Large amounts of dumped energy coincide with shutdown period. The ESS charges quickly but also the power capacity is often limited at which point the dump load must be activated in order to maintain shutdown of the diesel. The wind then drops and the diesel is scheduled on after a short while once the ESS is discharged. Power limits of the ESS also prevent meeting of the power balance even though sufficient energy stores may be in place. These volatile wind power periods are poorly handled by the ESS since it has been sized for much more constant wind powers.

The intrahour variations of load were not modeled but it is anticipated that the variations would not be as extreme as those of wind power. Also, the approach to modeling of wind likely leads to poorer performance than would be observed in the field. The nature of wind power and load profiles dictate the frequency of this cycling between *on* and *off* states. The availability of high resolution data would help to improve confidence in these results and implications on results from the other chapters.

The real-time simulation representation although time consuming to design, implement and debug, remains an incremental step towards full implementation of the entire system. The small differences in results observed were minor but given the same proportion of the overall system that was represented in hardware, this was anticipated. Nonetheless the HIL set-up results did validate the ability of the system to work in real-time and of the set-points to be realized by the controls of the power electronic converters. Extension of the concepts developed here for validation and prototyping ESS systems and associated controls are worth the additional effort. As one can hope for in an interesting research field, the answers obtained here are greatly outweighed by the additional number of questions.

Chapter 6

Conclusions

> The fact is that all writers create their precursors. Their work modifies our conception of the past, just as it is bound to modify the future.
>
> *Jorge Luis Borges* (1899 - 1986)

6.1 Thesis Summary

In this thesis, a general methodology for ESS optimization and control for the integration of wind energy. The specific example of a remote wind-diesel power system served as the basis for the proposed ESS sizing methodology and was used throughout to investigate issues of scheduling and real-time control of the ESS. The thesis considers the pairing of these two technologies—energy storage systems and wind power—from a long-term planning point of view down to operation on a second-to-second basis. The problem was formulated for the specific case of wind-diesel system but the methodology could readily be extended to other power system applications. Moreover, it is also amenable to technologies other than ESS for balancing power and optimizing energy use.

Chapter 2

The long-term planning problem of ESS sizing was rigorously defined as a stochastic optimization problem for continuous diesel operation and operation allowing shutdown of the diesel plant. Various probabilistic models to characterise the wind and load relationship were evaluated. Sensitivity analysis was performed on a number of important parameters, including the wind resource, ESS characteristics, and energy costs. The role of energy storage under different fuel price scenarios showed that fairly realistic price increase scenarios translated to greatly improved business cases for the ESS.

Chapter 3

The ESS sizing optimization problem was extended to hourly scheduling of the ESS, considering a 24-hour sliding window approach. Variations of the original formulation were considered in order to incorporate methods for controlling the frequency of deep discharges, in the form of different penalizing terms. The role of imperfect wind and load forecasting was also evaluated; persistence as a prediction approach resulted in only modest reductions in performance relative to the ideal case. The scheduling algorithm was also used to evaluate the performance of the different sizing approaches by comparing the expected costs and energy usage from the long-term planning studies with those resulting from operation of the system.

Chapter 4

Artificial neural networks were used in an effort to translate the scheduling results using off-line optimization to an on-line approach. Numerous ANN architectures and input variables were evaluated, for both continuous diesel operation and with shutdown permitted. The results were compared for the training data (one year of wind and load data) and for 19 additional years, the latter being independent of the training data set. Preferred structures emerged and the ANN was sufficiently general in that performance over all years was maintained. However, none were able to satisfactorily approach the level of performance achieved in the off-line optimization results.

Chapter 5

Finally, the entire system was implemented using a two-level ESS system consisting of a supercapacitor and vanadium redox flow battery. To coordinate the two storage levels on an intrahourly timeframe, an on-line controller was proposed as part of an overall hierarchical control structure. The control generated modification to the hourly scheduled in an effort to meet the objectives of dump load minimization, limiting diesel ramp rates and maximizing overall ESS capacity utilization. The performance of the various control modes was compared using clearly defined metrics. Selected simulation results were validated using a hardware-in-the-loop representation of the system and the feasibility of the control for on-line implementation was confirmed.

6.2 Conclusions

In research one begins with a definition of the problem, then methodologies or tools are proposed in order to investigate further or, if it is the intent, to find a solution. In some cases, the proposed approach exceeds expectations whereas in others the results are disappointing. In both cases greater insight is achieved. Here, we conclude on the contributions of the thesis and point out any shortcomings of the methodologies proposed.

ESS Sizing

The problem of design of power and energy ratings of an energy storage system in order to minimize the cost of energy delivered to a wind-diesel system was solved using stochastic optimization. The methodology provided many interesting results and when compared with operating results was shown to be accurate in assessing the feasibility of ESS. However, the accuracy depended on the type of probabilistic model of wind and load used. Using the model consisting of two random variables, the results were very promising whereas the ARMA models of residual load did not lead to good prediction of the true costs.

Results showed that, apart from obvious conclusions (such as higher costs of energy lead to larger ESS capacities), when the diesel is allowed to shut-down the cost of energy is greatly reduced and storage becomes quite attractive. In continuous diesel operation, even when the optimal design includes ESS, the value it brings is insufficient to practically justify its inclusion into the power system design. The role of the wind resource characteristics

is only partly understood. Obviously load and wind that are negatively correlated on a daily basis are more attractive for ESS but the relationship with the probability density functions of the two random variables needs further consideration.

ESS Scheduling using Optimization

The scheduling algorithm based on optimization using a 24-hour sliding window for energy storage system realized two main contributions: i) a methodology for determining the optimal ESS schedule given a defined ESS capacity and ii) a tool for auditing the ESS sizing methodologies. This tool was used to evaluate the performance of different sizing methodologies, something that is generally not done in cost-benefit analyzes. This general methodology could greatly facilitate optimization of long-term planning methodologies, not only for ESS sizing but other power system applications as well.

The scheduling algorithm was also modified in order to investigate the impact of penalizing term for low SOCs as well as to look at the impact of imperfect wind power and load profile predictions. Using the penalizing term one can in fact shape the *pdf* of the ESS energy state. The thesis did not provide recommendations as to what the ideal shape of the *pdf* should be, as this would require greater knowledge of the battery technologies. Using a persistence method for prediction, while it degraded performance, the difference was marginal and hardly merits mention. Why this is the case was not determined. Perhaps it lies in the fact the current hour is more important than future events.

ESS Scheduling using Artificial Intelligence

The optimization results were used as training data in an attempt to define an energy storage system scheduling approach based on artificial neural networks. The methodology, although potentially a good application of this tool, failed to produce results that satisfactorily reproduced the training data, even after numerous architectures and input data combinations were attempted. Quite possibly the input-output relationship was too complicated to map using ANN or the important input information was somehow not included. The ANN did prove to be sufficiently general in that performance was maintained for the 19 years independent of the training data set. However, the performance was not good enough to realize the benefits anticipated by the ESS sizing methodology.

On-line Control of Two-level ESS

Implementation of a two-level ESS system was realized in simulation and hardware. A generalized two-level ESS control structure was proposed and applied, with some variations, to the wind-diesel system. The results highlighted the fact that the intrahour variations are important and suggest that an hourly base for ESS sizing may not be entirely appropriate. However, as only a week of operation was simulated using high precision data, this point need to be substantiated. Also, given that the intrahour data used was generated using various assumptions the conclusions would carry greater weight had actual intrahour data for an entire year been available.

Different control modes were proposed and evaluated. The combination of the three control modes—dump load minimization, diesel ramp rate limiting and ESS capacity optimization—demonstrated that the control was able to rationalize the three objectives, yielding good performance, as measured by defined metrics. The value of diesel ramp rate limiting was not quantified and warrants greater consideration.

A hardware-in-the-loop test bench for emulation of two-level ESS was constructed and used to evaluate the ESS control with the wind-diesel system. The hardware results demonstrated that the control could be operated on-line. This test bench was limited in that it did not employ real ESS technologies and the ESS as a grid forming agent was not validated for diesel shutdown. Nonetheless, the set-up has the potential to be used in a multitude of other ESS applications and power conversion topologies.

6.3 Recommendations for Future Work

The thesis has made a contribution in terms of defining a methodology for assessing the overall role of ESS in the integration of wind power. However, there are a number of avenues for future work that could build on the contributions of this thesis. In many cases, these are refinements of some of the specific contributions in each of the chapters, whereas modification of the overall methodology for use in the design and operation of microgrids could also be considered. We will first discuss recommendations for future work related to the different aspects of the thesis and close with a discussion on the extension of the overall methodology to other power system applications.

ESS Sizing

The ESS sizing problem itself could be revisited from a number of different angles. Comparison of the stochastic optimization approach to sizing using a Monte Carlo approach would be interesting. In this case, the daily wind and load profiles would be developed according to the probability density functions and an optimal sizing would be determined in each case, resulting in $pdfs$ for the ESS power and energy ratings. Presumably, the optimal ratings would then be the expected values as calculated from the $pdfs$.

The use of the ARMA model or some variation thereof could also be considered in more detail. Although the models treated in the thesis did not yield desirable results, refined ARMA models could lead to better performance and more interesting insights. For instance, the assumption of one ARMA model for all different levels of residual load may not have been valid. Instead, different ARMA models could be used for different ranges of the daily average residual load.

As well, the solution was shown to be quite sensitive to the expected yearly increases in the price of diesel fuel. As this variable is known to be quite volatile, defining it as a third random variable, to be incorporated into the stochastic optimization problem, might help to better model its contribution. The drawback would be that this increases the number of scenarios and consequently the dimensions of the problem, perhaps necessitating scenario reduction techniques. Related to energy prices, the concept of risk could also be better integrated rather than relying solely on the discount rate as indicator of risk tolerance.

The sizing methodology could also benefit from a finer analysis of the relationship between the wind resource characteristics and the difference between expected costs and simulated (true) cost resulting from the sliding window approach to scheduling. This could consist of analysis of the power density spectrums of wind and load and the resulting performance. A better understanding of when performance is degraded would help to refine the model in order to render it more generalized. Many of the practical aspects, such as low SOC penalty (if relevant), and higher energy capacity due to the need for two or more ESS levels, should be reflected in the ESS sizing formulation. To facilitate this analysis a parametric study using different fixed ESS ratings and the sliding window operating approach could be used as a brute force approach in determining the *true* optimal design. This would then enable one to compare different sizing methodology with the actual optimal design.

ESS Scheduling and Control

The use of ANN to capture the inherent rules in the data from the off-line optimization approach to scheduling fell far short of meeting expectations. As such, other artificial intelligence based tools should be evaluated in an effort to improve performance. Knowledge-based expert systems (KBES) combined with data mining might be better suited for extracting knowledge from the results. Without being able to achieve comparable performance to the optimization approach, the ESS sizing would be overly optimistic as the expected benefits would never fully be realized.

As previously mentioned the intrahour results somehow need to be reflected in the formulation of the sizing problem. Costs associated with two-level ESS somehow needs to be factored into the cost of ESS rating, possibly through appropriate scaling of the power and energy fixed costs. The costs associated with the two technologies should be weighted with their assumed proportions in the final design, based on the value of the T_{mt}.

The intrahour results also showed that many of the intrahour variations are important, calling into question the validity of ESS sizing based on hourly schedules. Obviously performing sizing based on wind and load profiles at 5 Hz is not practical but considering 10 or 15 minute data could be a reasonable compromise. Either way, the impact of this assumption merits further evaluation.

The HIL set-up essentially validated the ability of the controller for continuous diesel operation to operate in realtime; only a limited part of the system was realized in hardware. Future work could entail extending the range of the hardware or at least representing different portion of the system in hardware. For example, interchanging the short-term and medium-term ESS devices would provide a third set of results with only moderate effort. An even more ambitious work would be to include representation of the voltage seen by the loads and ESS interface converter by a controllable voltage source. For shutdown operation this would allow testing of grid tied and grid forming controls for the ESS inverter / rectifier, beyond the scope of this thesis but interesting research nonetheless. This would lead to a closer approximation of the true response of the system and would require one to also consider diesel start-up and shutdown dynamics.

Sustainability and Energy Management

Each of these above considerations discuss specific elements within each of the chapters, however, the overall methodology could also be applied to other ESS power system applications or for design and operation of microgrids, either remote microgrids or those as part of a distribution system. The concept of storage could also be thought of more generally, encompassing both wind curtailing as well as demand-side management. Demand should extend beyond electrical demand as well, including both heat and power.

The overall methodology presented provides the framework for a more holistic approach to design and optimization of community energy production and usage. While this philosophy will take away from the ESS business case, it would undoubtedly lead to a reduction in the cost of energy and probably to a more sustainable engineering approach to design of power systems. Cost of energy should be considered beyond the cost of the commodity. Greenhouse gas credits or penalties and reliability should also be quantified and monetized. Especially in microgrids that could separate from the main grid, the reliability improvement would be of particular importance in making a business case that included islanding.

In closing, it is worth mentioning that many of these endeavors will require cross-disciplinary research collaborations, between university departments or with external organizations. This ensures that duplication or re-engineering is avoided and in the end improves the overall value of the contribution. If done correctly, the pay off is worth the additional effort.

Appendix A

Wind-Load Models and Scenario Generation in ESS Sizing

This appendix provides greater detail on the different approaches used to model the relationship between the wind and load profiles. The developed models were used in the ESS sizing analysis of Chapter 2 and their performance in developing economically feasible designs was evaluated in Chapter 3.

A.1 Correlation Coefficient and Energy Penetration

In wind-diesel systems, dumped energy occurs during periods of low load and high wind. As such, two random variables were chosen to model the frequency of occurrence of these periods. Namely, the ratio of wind energy to load on a given day and the correlation between the two profiles, were chosen as a first attempt at probabilistic modeling of the wind and load characteristics of a given system.

A.1.1 Model Description

The correlation of the two profiles provides an indication of when the peak of the wind power occurs relative to the load peak. It is given by:

$$\rho_{\mathrm{wl}} = \sum_{t=1}^{T} \frac{(p_{\mathrm{w},t} - \bar{p}_{\mathrm{w}})(p_{\mathrm{L},t} - \bar{p}_{\mathrm{L}})}{(T-1)s_{p_{\mathrm{w}}} s_{p_{\mathrm{L}}}} \tag{A.1}$$

Where the time period, T, is the length of each of the scenarios. Generally, 24 hour scenarios were considered but week long periods (168 hours) were also considered. The energy penetration was also calculated for the same period length:

$$r_{\mathrm{wl,e}} = \frac{E_{\mathrm{w}}}{E_{\mathrm{L}}} \tag{A.2}$$

Thus, for a year's worth of wind power and load data points, a vector for each of the random variables was generated, each of a length of 365, assuming $T = 24$. Each element of these vectors was calculated for a given day, using the corresponding twenty-four hours from the wind and load data sources. These vectors were then used to generate the discrete *pdf*s for the two random variables.

A.1.2 Scenario Generation

The distributions of ρ_{wl} and $r_{\mathrm{wl,e}}$ were divided into discrete divisions, the number depending on the total number of scenarios to be modeled. Obviously, the greater number of scenarios used the closer the results approximate the true data, the tradeoff being computational efficiency. The number of variables increases with the number of scenarios so some analysis is required to determine appropriate number, as explained in Chapter 2.

The actual wind profile used for each scenario was generated by multiplying a base load profile by $r_{\mathrm{wl,e}}$ and then time shifting to achieve the desired ρ_{wl}. The procedure is illustrated in Fig. A.1, for negatively correlated wind with an energy penetration of 75%.

It is important to note that the resulting wind profile is not unique, as there are an infinite number of wind profiles that could be used to obtain the required $r_{\mathrm{wl,e}}$ and ρ_{wl}. However, this is the method used in Chapter 2 and its validity was assessed in Chapter 3.

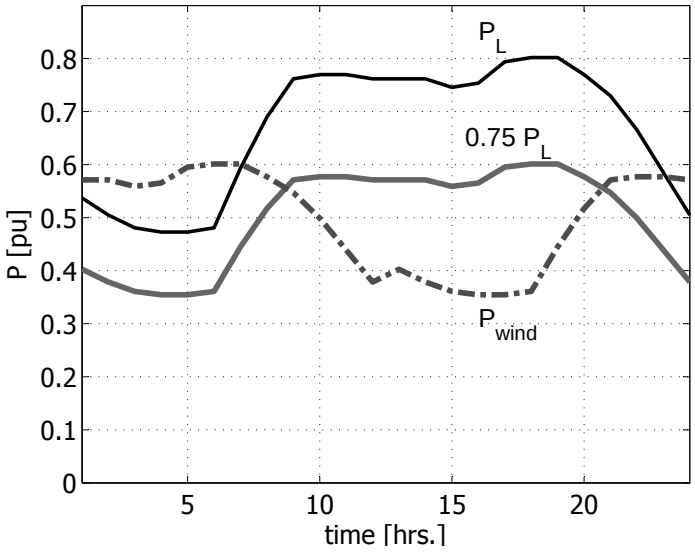

Fig. A.1 Original daily load profile and resulting wind power profile for ρ_{wl} = 0.75 and $r_{\mathrm{wl,e}}$ = -1

A.2 ARMA Model of Residual Load

The previous model yields a daily wind profile that is identical in frequency content to the load profile. This limitation may prevent the model from adequately characterizing the features that allow one to estimate the dumped energy and accordingly, the feasibility of energy storage. Thus, an alternate model was proposed, based on an autoregressive moving average (ARMA) model of the time series data.

A.2.1 Model Description

ARMA models are often used to characterize a given time series, $\mathbf{x}$. Here the theory of ARMA models is briefly reviewed before presenting its application to the wind-load data.

First one can define the L^i lag operator, which operates on x_t to product the $(t-i)^{th}$ element of the time series given by $\mathbf{x}$:

$$L^i \, x_t = x_{t-i} \tag{A.3}$$

An $ARMA(p,q)$ model consists of p autoregressive terms and q moving average terms. Its

general form is given by, [99]:

$$\left(1+\sum_{i=1}^{p}\phi_i L^i\right)x_t = \left(1+\sum_{i=1}^{q}\theta_i L^i\right)\varepsilon_t \tag{A.4}$$

Where ε_t is a normal white noise process with zero mean and a variance of σ. The ARMA parameters (ϕ, θ, and σ) can be obtained using various iterative algorithms, such as the non-linear least squares approach. The pre-defined function available in the MATLAB System Identification toolbox was used for determination of the ARMA model.

The residual load, p_{res}, was generated using the wind power and load data. From this the discrete *pdf* for the daily average residual mean, $\overline{p}_{\text{res}}$ was generated. The average daily residual load mean was then subtracted from the residual load profile and the resulting profile was used to construct an ARMA model.

A.2.2 Scenario Generation

Again, scenarios were generated by first selecting a particular portion of the probability density function, but this time using the daily average residual load as random variable, Fig. A.2. The daily residual load profile used for the scenario in question was taken as the sum of the daily average and the output of the ARMA model over the period, such that for time t the residual is given by:

$$p_{\text{res,t}} = \overline{p}_{\text{res}} + ARMA(p,q)_t \tag{A.5}$$

A possible variation to the model would be to generate ARMA models for different ranges of $\overline{p}_{\text{res}}$. Especially at higher wind speeds (negative values of p_{res}), the profile may be more volatile than at lower wind speeds. A number of ARMA models might lead to better overall modeling of the characteristic. In the thesis only a single ARMA was used.

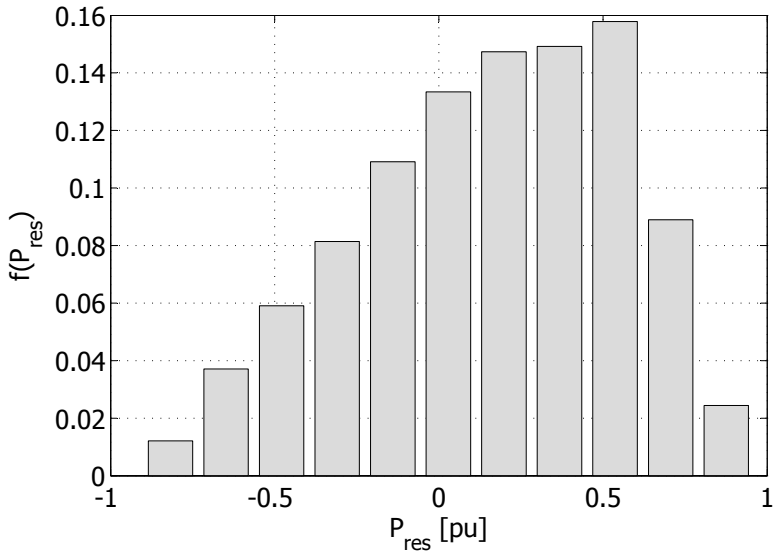

Fig. A.2 Discrete probability density function of average daily residual load for wind resource 1.

Appendix B

Hourly Wind Power Data Sources

This Appendix describes the two sources of hourly wind power data and data processing performed prior to their use in the ESS sizing studies (Chapter 2) and the ESS scheduling problems (Chapters 3 and 4). The probabilistic characteristics of the 12 wind resources are presented at the end of the Appendix.

B.1 Data Sources and Calculations

B.1.1 Kansas Electric Utilities Research Program

The Kansas Electric Utilities Research Program (KEURP) with support from the Utility Wind Interest Group (UWIG) and the U.S. Department of Energy (DOE) collected wind data for 12-months at six sites in Kansas as part of an assessment of the wind potential in the state. The data was made available publicly through the website in [92]. Unfortunately, it was recently relocated to an unknown location.

The wind speeds from one of the site was converted to wind power using the wind power curve from the Entegrity 50 kW wind turbines, [122], and given in table form in Table B.1. The simple wind park model applies a scaling factor for the number of turbines, neglecting array losses and forced outage rates, such that the resulting wind park

$$p_{\mathrm{w}} = \frac{P_{\mathrm{w}}}{P_{\mathrm{WTG}}} p_{\mathrm{WTG}} \tag{B.1}$$

Table B.1 Entegrity 50 kW Wind Turbine Generator Power Curve

v_w [m/s]	0	4.6	11.5	12.5	13	14	20	22.4
p_{WTG} [kW]	0	0	50	56	60	63	63	0

The wind power from this site tends to peak in the winter months with lulls in the late spring and summer. The seasonal correlation gives a general idea of how the two are matched. Daily correlation as shown was an important factor in determining the dumped energy.

B.1.2 Ontario Power Authority

In 2007, the Ontario Power Authority contracted AWS Truewind LLC to produce 20 years of simulated hourly wind generation data for 60 prospective wind project sites in Ontario. The sites were then aggregated, grouping them into 11 different regions and the data was made available through the OPA website, [123]. Details of how the data was generated are given in the associated report but the main features are summarized here.

The company used a mesoscale weather model of the southern half of the province of Ontario that was built using observed wind speed from a number of tall towers, at a height of 80 m, the typical hub height for large wind turbines. The model generated the predicted wind speed, direction, temperature, and surface pressure in hourly intervals at each point of a 20 km grid point, at several heights. Some scaling was performed to match expected mean speeds from the Ontario Wind Atlas.

The speed, direction, and density data were then combined with a 3 MW wind turbine generator power curve. The wind park model took into consideration wind plant losses, including wake losses, blade soiling, high-wind control hysteresis, turbine availability, and electrical losses. On average these factors contributed to a net production that was 14% lower than the gross production as predicted by the power curve. The spatial averaging of fluctuations in large wind projects was also modeled by filtering the resulting data.

In this thesis, the time series wind power from the OPA study were modified in order to adjust the rated capacity to that of the remote wind park. The wind power used in the

various studies was calculated from the raw data according to:

$$p_{\mathrm{w},jkl} = \frac{P_{\mathrm{w}}}{P_{\mathrm{park},j}} p_{\mathrm{OPA},jkl} \tag{B.2}$$

Where $P_{\mathrm{park},j}$ is the rating of the wind park j and $p_{\mathrm{park},jkl}$ is the wind power from the wind park j, in hour k, of year l.

B.2 Wind Resource Characteristics

The two sources of data are different and explain some of the differences noted in the sizing study. The Kansas data provides only raw wind speeds and the wind park model was quite basic, leading to more volatile wind power than for the OPA data. On the other hand the OPA data was constructed with large wind parks in mind and consequently leads to less volatile wind output, reducing the attractiveness of energy storage. Here the mean and standard deviation of the random variables from Chapter 2 are plotted for each WR, along with the *pdf*s for selected WRs.

B.2.1 Energy Penetration

The energy penetration is given for each of the wind resources, assuming a rated wind park capacity of 900 kW. These graphs show that the Kansas data (WR 12) has a much higher energy penetration (higher mean) and volatility (larger standard deviation. The wind park model likely plays an important role, as losses were modeled in the OPA data.

B.2.2 Wind-Load Correlation Coefficient

Looking at the daily correlation coefficient, the Kansas data in fact has one of the highest mean values (only slightly negative). Other WRs, especially WR 2 and 3 are quite negatively correlated. The standard deviations are all quite similar, with WR 12 have the small standard deviation. From this figure, it would be expected that the Kansas data would be less amenable to ESS, contrary to what was observed in Chapter 2.

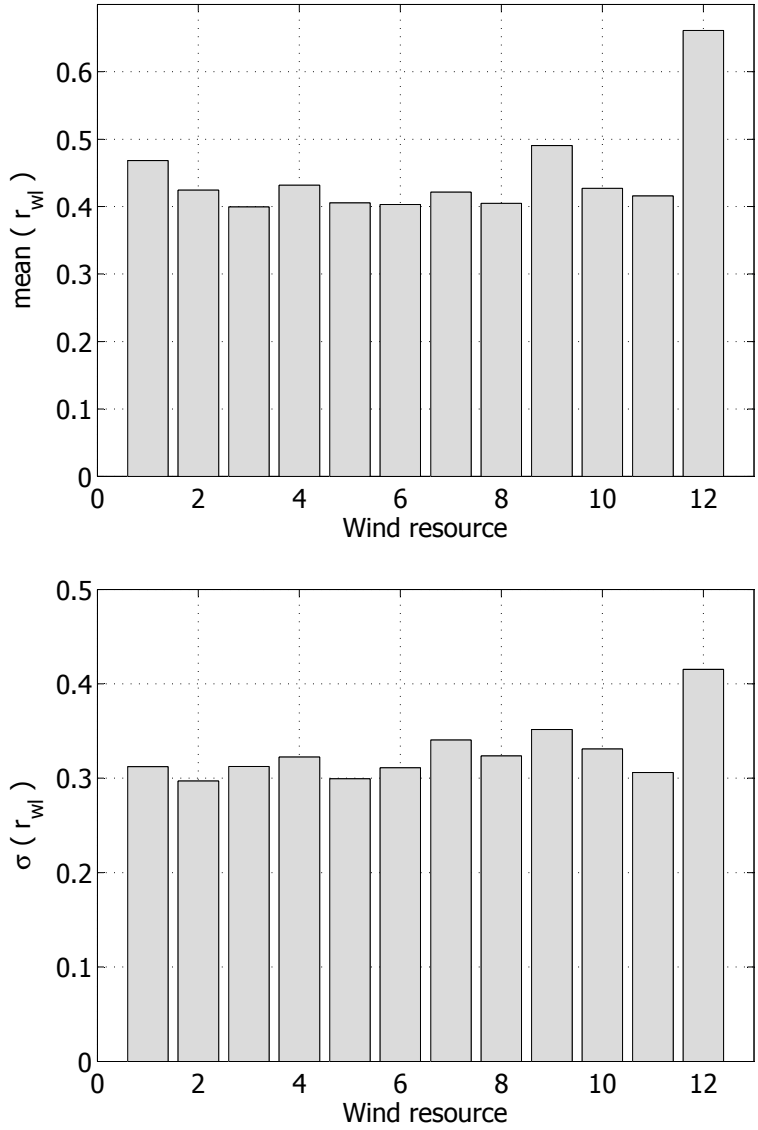

Fig. B.1 Mean and standard deviation of energy penetration, r_{wl}, for wind resources under investigation, $r_{\mathrm{wl,p}} = 0.9$.

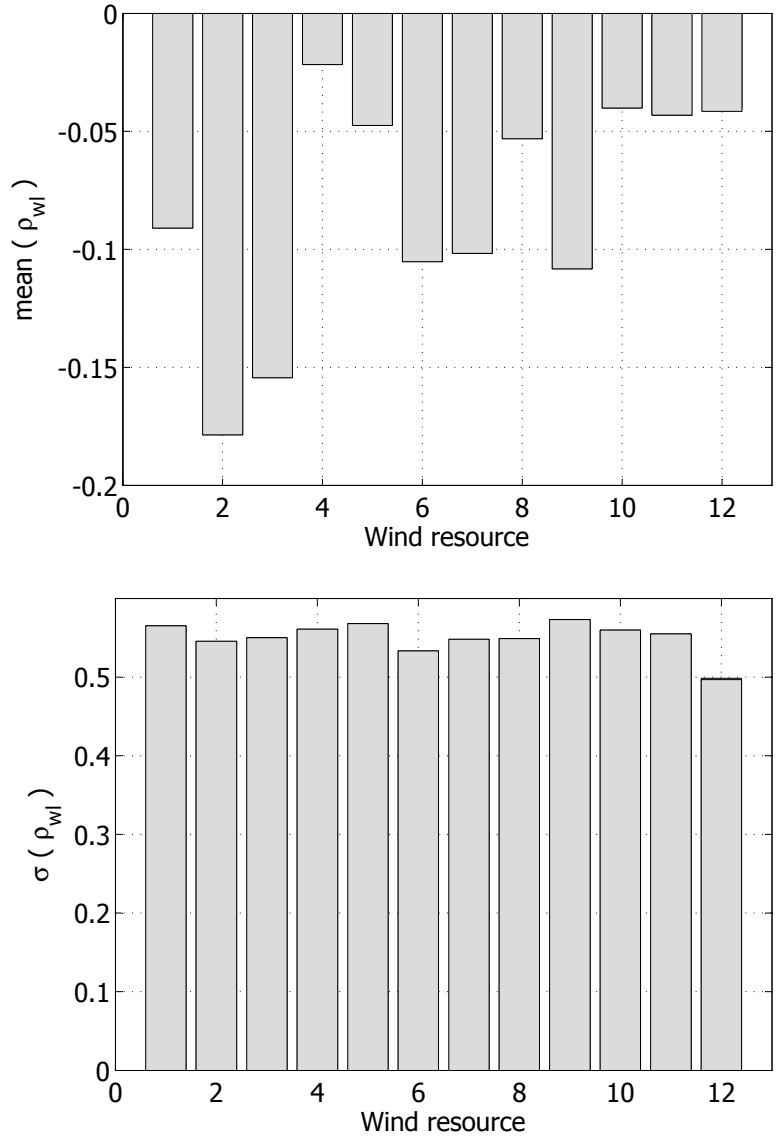

Fig. B.2 Mean and standard deviation of wind-load correlation coefficient, $\rho_{\mathrm{wl,e}}$, for wind resources under investigation, $r_{\mathrm{wl,p}} = 0.9$.

B.2.3 Discrete Probability Density Function

As the mean and standard deviation of the correlation coefficient are not sufficient to explain the results seen in Chapter 2, the full *pdf*s were plotted for the two random variables, for selected WRs, Figs. B.3 and B.4. These plots would be used in generating the scenarios and associated probabilities for the stochastic optimization results.

These plots are revealing in that they show quite different shapes for the two data sources. The *pdf* of the Kansas data is quite flat whereas in the case of the OPA data, the probabilities are grouped more to one end. This is important when one recalls that the sizing study is based on different scenarios corresponding to combination of these two profiles. While the OPA data is more negatively correlated with load on average, many of these instances will be with low energy penetration. A large capacity ESS cannot be justified based on a one or two very attractive scenarios but rather must be taken together with the high probability of very poor scenarios.

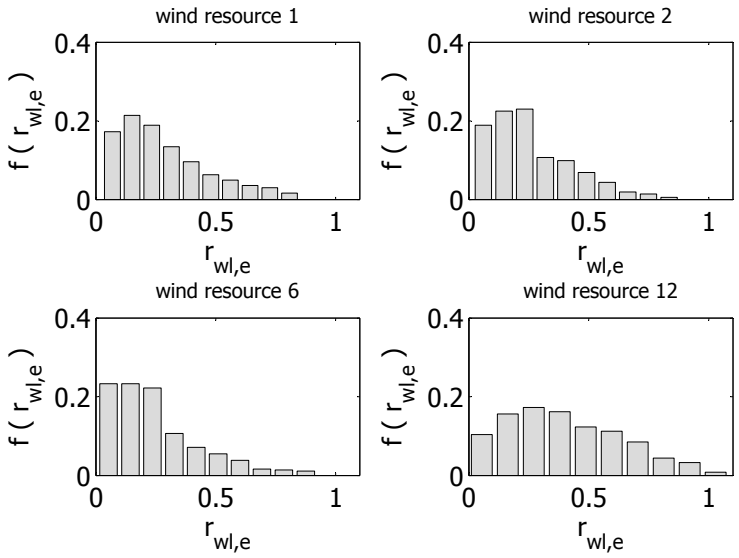

Fig. B.3 Discrete probability density function of energy penetration for WRs 1, 2, 6, and 12.

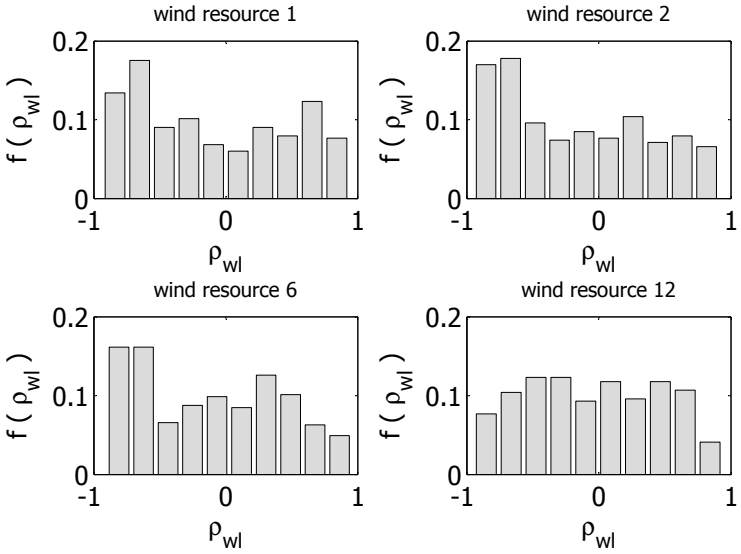

Fig. B.4 Discrete probability density function of daily wind-load correlation coefficient for WRs 1, 2, 6, and 12.

Appendix C

Intrahour Wind-Load Data

This Appendix discusses the generation of the intrahour wind power data. The procedure described here was used to generate wind power every 0.2 seconds for a corresponding hourly average wind power data points in Appendix B. This data was used in Chapter 5. The source of a generic wind speed data, sampled at 5 Hz is first discussed followed by the procedure for generation of the intrahour data for a given hourly average wind power.

C.1 Wind Speed Data

As the wind data sources presented in Appendix B were hourly averages, they were not appropriate for the studies conducted in Chapter 5. As such, higher resolution wind speed data was obtained from a website that offers this service free of charge for a select number of sites, [110]. The wind speed data is organized in terms of different hours, sampled at 5 Hz. Hours are available for different average wind speeds and turbulence. Data was taken from the site named San Gorgonio, in the USA. Three different hours were selected: one with a low average wind speed, medium, and high. These were used together with the data from Appendix B to generate a week long wind power profile, sampled at 5 Hz.

C.2 Wind Power Calculation

Here the procedure for generation of the week long wind power profile is described. As mentioned three different high resolution hourly profiles were selected. The intrahour wind

speed profile used for a given hour was selected according to the value of the average wind power for that hour:

$$v_{\mathrm{w,i}} = \begin{cases} v_{\mathrm{low,i}} & p_{\mathrm{w,k}} \leq 200kW \\ v_{\mathrm{med,i}} & 200kW < p_{\mathrm{w,k}} \leq 800kW \\ v_{\mathrm{high,i}} & p_{\mathrm{w,k}} > 800kW \end{cases} \tag{C.1}$$

The wind power was then derived using the wind speed and the Entergrity power curve, Fig. B.1. The resulting wind power, $p_{\mathrm{Entw,i}}$ was then filtered using a discrete time filter to account for the turbine inertia:

$$p_{\mathrm{Entwf,i}} = \frac{b}{a}\ p_{\mathrm{Entw,i}}(v_{\mathrm{w,i}}) \tag{C.2}$$

Where the parameters $a = 1 - T_{\mathrm{s}}/(T + T_{\mathrm{s}})$ and $b = T/(T + T_{\mathrm{s}})$, with sample time $T = 0.2$ secs. and WTG time constant $T_{\mathrm{s}} = 2$ seconds. Finally, in order for the average wind power for the hour in question to equal that from the hourly data, a scaling factor, based on the mean of the time series resulting from C.2, was applied:

$$p_{\mathrm{w},i} = \frac{I}{\sum_i p_{\mathrm{i}}} p_{\mathrm{w}} \tag{C.3}$$

In this way the high resolution wind power time series has the identical hourly average values as the hourly time series data.

Appendix D

Simulation Tools

This Appendix describes the simulation tools used in the research.

D.1 GAMS

The solution of the ESS sizing problem required a solver capable of handling mixed integer linear programming. The continuous diesel operating problem only requires an LP solver but the diesel shut-down mode introduces binary variables.

The General Algebraic Modeling System (GAMS) is a modeling system for mathematical programming and optimization, [91, 124]. Its advantage over other tools is in its high-performance solvers, which are particularly stable and can handle binary variables. It has been used in numerous optimization problem related to power systems, for example, [125].

GAMS complements well the ability of MATLAB to represent matrices and perform matrix manipulations. As such the problem was formulated in MATLAB and then passed to the GAMS solver through an interface made available by power lab colleague, Jose Restrepo.

D.2 MATLAB

MATLAB®was used in all parts of the thesis in some capacity. MATLAB m-files were used for formulating the optimization problem, handling input/output data and generating graphs. In addition, a number of toolboxes were used for different parts of the thesis, which are described below.

D.2.1 MATLAB Toolboxes

The System Identification Toolbox was used in the development of the ARMA model, as described in Appendix A. The built in function were use to solve for the autoregressive and moving average terms, using the daily residual load profiles.

The Neural Network Toolbox was used in Chapter 4 of the thesis for training of the different neural network architecture and their simulation. The built-in functions were used for this purpose. This enabled application of the theory with very little development as the functions were called directly from the m-files. Example cases were used as templates, adding code to coordinate the input and output files.

D.2.2 Simulink/SimPowerSystems

Simulink®was used as the basis for the two-level energy management system and for representation of the wind-diesel system. The wind power described in Appendix C was interfaced as a `.mat` file as was the load data. The system was represented as a power flow model, updated every 0.2 seconds. The dynamics of the diesel plant were not considered; it was assumed the governor control would maintain it at nominal frequency. Likewise, during shutdown periods, it was assumed that the power electronic interface of the ESS would handled voltage and frequency control.

The *SimPowerSystems*™ Toolbox was used for representation of the converter controls and, and the supercapacitor and battery models of Chapter 5. The system was tested in simulation before applying the controls to the hardware set-up. The different components of the hardware set-up are reviewed in Appendix E.

Appendix E

Experimental Set-up

This Appendix discusses the various components of the experimental set-up for the hardware-in-the-loop, real-time simulation used in Chapter 5. Other test benches have been proposed in the literature, [126,127], however the current set-up was developed with the ability to emulate energy storage systems in mind. Chapter 5 defined the real and simulated components of the test bench. Here, the discussion is restricted to the specific hardware components.

Figure E.1 provides an overview of the hardware components. The Semikron Miniskiip product was used to realize the power electronic converters. One of the two MiniSkiip served as a three-phase inverter/rectifier; the second as a two-phase controlled inverter/rectifier, with the third leg serving as the bidirectional dc/dc converter. A $Y_g - Y$ transformer was used to couple the three-phase converter. This served to step-down the voltage and also to isolate the grounds of the two converters, allowing independent control of the two dc bus voltages. All data processing and control was performed by the RT-LAB MX Station, a real-time simulator and digital controller.

E.1 RT-LAB MX Station

The RT-LAB MX Station is a real-time simulation product offered by OPAL-RT Technologies Inc., [128]. It consists of a compact PC and input/output components for prototyping and real-time simulation of engineering systems. It is integrated with Simulink, Real-Time Workshop and the SimPowerSystem Blockset, making the transition from simulation models to real-time simulation quite simple. The computation targets run on RedHawk Linux RTOS, and integrate the measured voltages and currents, and provide converter gating

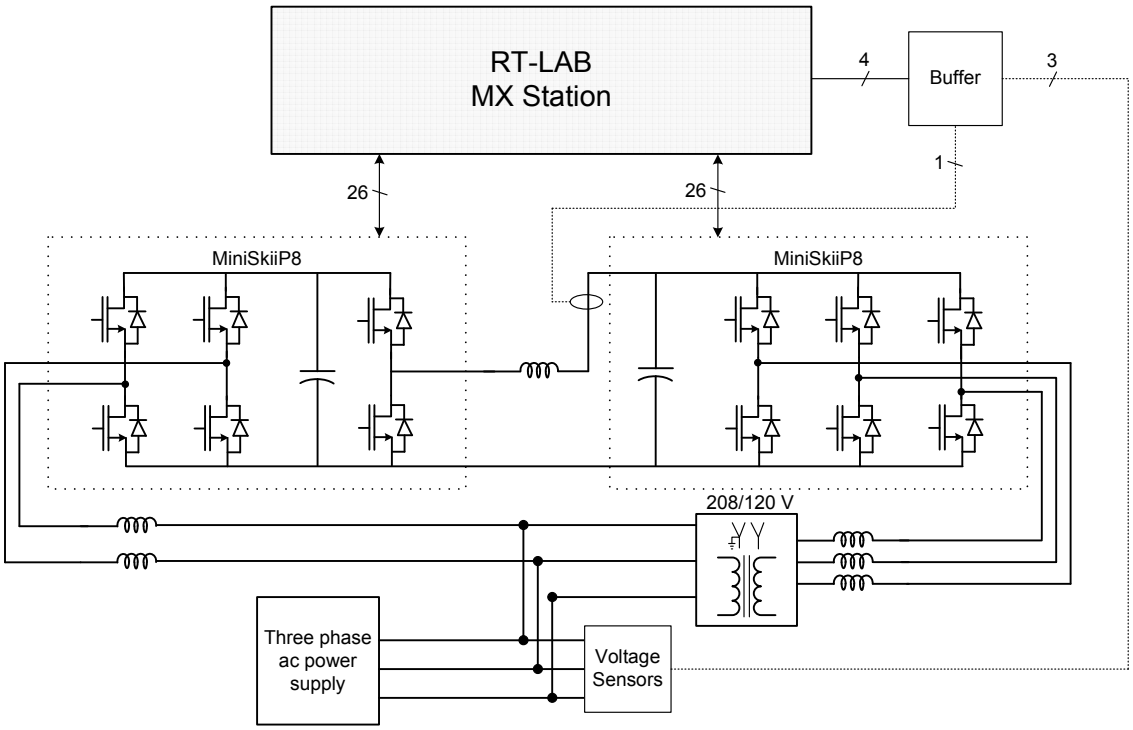

Fig. E.1 Hardware components and set-up for testing of two-level .

signals through the analog output channels.

E.2 Power Electronic Converters

The Miniskiip 8 Three-Phase Inverter is an integrated power electronic converter that allows realization of a number of different power converter topologies, [129]. The inverter contains an 800 V DC Link, 1500uF of dc link capacitance, three leg IGBT bridge, driver circuitry, heat sink and fans. The converter is capable of sourcing up to 50 A of current continuously. There are a number of integrated sensors including temperature sensor, closed loop current sensors, dc bus voltage, as well as fault monitoring and protection circuitry.

The inputs and outputs are provided through a 26-pin connector. Gate drive signals for each of the 6 switches require a voltage between +5V and +15V for turn-on, compatible with the MX Station output channel capabilities. The integrated sensors provide current measurements as a normalized voltages. The values of the measured currents were obtained

according to the scaling factor given in the data sheet:

$$I_{\text{out}}(A) = 125A \, \frac{I_{\text{analog,out}}(V)}{8V} \tag{E.1}$$

In a similar manner the dc bus voltage was obtained according to:

$$U_{\text{dc}}(V_{dc}) = 100 \, U_{\text{analog,out}}(V) \tag{E.2}$$

E.3 Data Acquisition

In addition to the integrated sensor from the MiniSkiip, various other measurements were made, using sensors designed and constructed by colleague Johan Guzman. Voltage sensors were used to extract the phase angle at the point of connection and a current sensor was used to measure the dc current. Both sensors first convert the measured signal to a current that is proportional to the magnitude of the measured signal. The currents were then converted back to voltages using a buffer stage, whose outputs were then fed directly into the MX Station analog input channels. Amplifier stages are used to calibrate the sensor outputs. All components were realized using discrete component and connected using printed circuit boards.

E.3.1 Voltage Sensors

The voltage sensors consist of four stages, Fig. E.2. First the voltage is dividing in order to be compatible with the operational amplifier input. The input is then passed through the differential amplifier and filtered. Finally it is converted to a current signal in order to reduce noise as the signal is transmitted to the buffer stage. Three of these sensors were used to measure the three phase to ground voltages, and were used in synchronization.

E.3.2 Current Sensors

The current sensor was designed with a similar philosophy as the voltage sensor, Fig. E.3. The current is first converted to a voltage as an output of the hall probe. The number of turns through the hall probe can be selected, depending on the anticipated current range. The resulting voltage is then amplified and filtered. Finally, the voltage is again converted

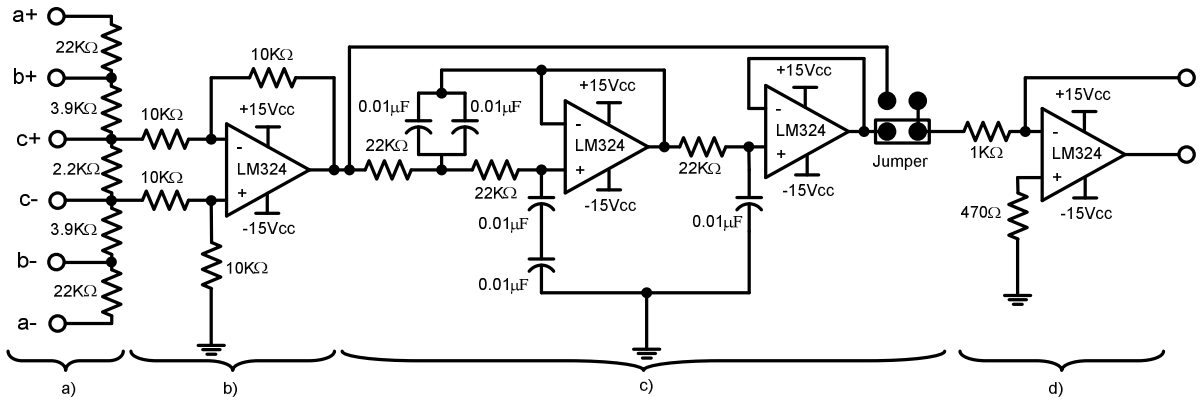

Fig. E.2 Voltage sensor circuit: (a) voltage divider, (b) differential amplifier, (c) filter, (d) voltage to current interface.

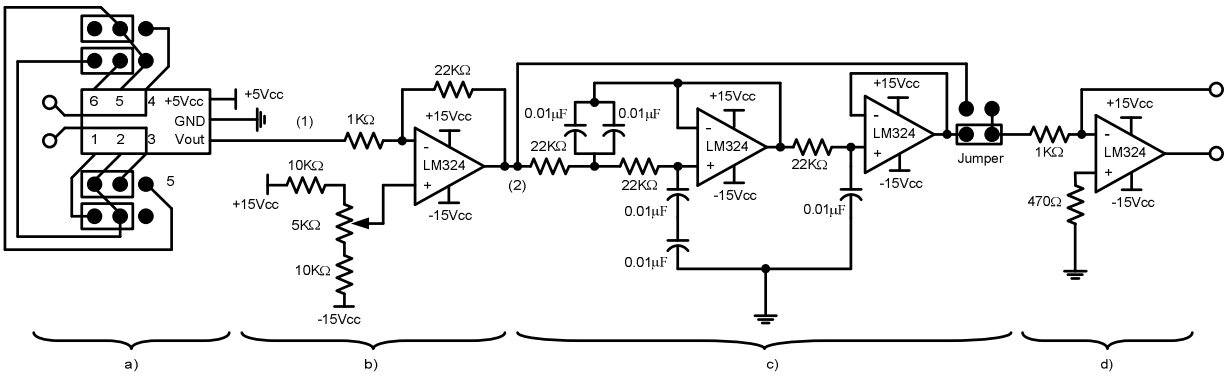

Fig. E.3 25A current sensor circuit: (a) turn number selector, (b) amplifier, (c) filter, (d) voltage to current interface.

to a current signal and sent to the buffer stage. The current sensor was used only in measurement of the dc current between the two converters.

E.3.3 Buffers

The buffer stage was used to convert the current signals back to voltage before providing them as inputs to the MX Station. The current is first converted to a voltage and then is passed through two amplifier stages, Fig. E.4. Voltage clipping was employed at the output to limit the voltage to +5V, as the original design was intended for a digital signal

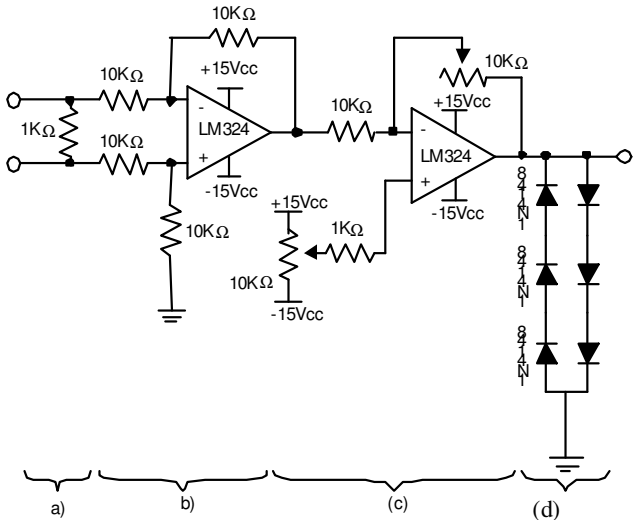

Fig. E.4 Current to voltage interface (single channel): (a) conversion of current to voltage, (b) differential amplifier, (c) amplifier and (d) voltage clipper.

processor (DSP) that could only handle small input voltages. Four buffers channels were used corresponding to the three phase-to-ground voltages and the dc current.

References

[1] Y. Makarov, V. Reshetov, A. Stroev, and I. Voropai, "Blackout prevention in the United States, Europe, and Russia," *Proc. IEEE*, vol. 93, no. 11, pp. 1942–1955, Nov. 2005.

[2] U.S.-Canada Power System Outage Task Force. (April, 2004) Final Report on the August 14, 2003 Blackout in the United States and Canada: Causes and Recommendations. [Online]. Available: http://www.nerc.com

[3] (2006) Final Report System Disturbance on 4 November 2006, Union for the Co-ordination of Transmission of Electricity (UCTE). [Online]. Available: http://www.ucte.org

[4] (2008) Smartgrids: European Technology Platform for the Electricity Networks of the Future. [Online]. Available: http://www.smartgrids.eu/

[5] (2008) Galvin Electricity Initiative. [Online]. Available: http://www.galvinpower.org/

[6] (2008) Gridwise Alliance. [Online]. Available: http://www.gridwise.org/

[7] J. Hughes, "IntelliGrid architecture concepts and IEC61850," in *Proc. IEEE PES Transmission and Distribution Conference and Exhibition*, 2005/2006, pp. 401–404.

[8] A. Apostolov, "Multi-agent systems and IEC 61850," in *Proc. IEEE Power Engineering Society General Meeting*, Montréal, 18-22 June 2006.

[9] R. Mackiewicz, "Overview of IEC 61850 and benefits," in *Proc. IEEE PES Transmission and Distribution Conference and Exhibition*, 2005/2006, pp. 376–383.

[10] J. Gillerman, H. Falk, and R. Mackiewicz, "Focus on IEC TC 57 - power system reliability and profitability," *IEEE Power Energy Mag.*, vol. 3, no. 4, pp. 66–67, July-Aug. 2005.

[11] (2008) International Electrotechnical Commission. [Online]. Available: www.iec.ch/

[12] "IEEE Standard for Interconnecting Distributed Resources with Electric Power Systems," *IEEE Std. 1547-2003*, pp. 1–16, 2003.

[13] (2008) Electric Power Research Institute. [Online]. Available: http://my.epri.com/

[14] (2008) CIGRE International. [Online]. Available: www.cigre.org/

[15] (2008) Enabling Tomorrow's Electricity System: Report of the Ontario Smart Grid Forum. [Online]. Available: http://www.ieso.ca/imoweb/marketsandprograms/

[16] G. Venkataramanan and C. Marnay, "A larger role for microgrids," *IEEE Power Energy Mag.*, vol. 6, no. 3, pp. 78–82, May-June 2008.

[17] E. Barklund, N. Pogaku, M. Prodanovic, C. Hernandez-Aramburo, and T. Green, "Energy management in autonomous microgrid using stability-constrained droop control of inverters," *IEEE Trans. Power Electron.*, vol. 23, no. 5, pp. 2346–2352, Sept. 2008.

[18] C. Marnay, G. Venkataramanan, M. Stadler, A. Siddiqui, R. Firestone, and B. Chandran, "Optimal technology selection and operation of commercial-building microgrids," *IEEE Trans. Power Syst.*, vol. 23, no. 3, pp. 975–982, Aug. 2008.

[19] F. Katiraei, R. Iravani, N. Hatziargyriou, and A. Dimeas, "Microgrids management," *IEEE Power Energy Mag.*, vol. 6, no. 3, pp. 54–65, May-June 2008.

[20] I. Bae and J. Kim, "Reliability evaluation of customers in a microgrid," *IEEE Trans. Power Syst.*, vol. 23, no. 3, pp. 1416–1422, Aug. 2008.

[21] B. Kroposki, R. Lasseter, T. Ise, S. Morozumi, S. Papatlianassiou, and N. Hatziargyriou, "Making microgrids work," *IEEE Power Energy Mag.*, vol. 6, no. 3, pp. 40–53, May-June 2008.

[22] F. Katiraei, M. Iravani, and P. Lehn, "Micro-grid autonomous operation during and subsequent to islanding process," *IEEE Trans. Power Del.*, vol. 20, no. 1, pp. 248–257, Jan. 2005.

[23] C. Hernandez-Aramburo, T. Green, and N. Mugniot, "Fuel consumption minimization of a microgrid," *IEEE Trans. Ind. Appl.*, vol. 41, no. 3, pp. 673–681, May-June 2005.

[24] A. Tsikalakis and N. Hatziargyriou, "Centralized control for optimizing microgrids operation," *IEEE Trans. Energy Convers.*, vol. 23, no. 1, pp. 241–248, March 2008.

[25] S. Durand and D. Slagle, "United States Coast Guard hybrid system experience on Kodiak Island, Alaska," in *Proc. IEEE Photovoltaic Specialists Conference, 1996*, 13-17 May 1996, pp. 1223–1225.

[26] R. Billinton, "Incorporating reliability index distributions in small isolated generating system reliability performance assessment," *Generation, Transmission and Distribution, IEE Proceedings-*, vol. 151, no. 4, pp. 469–476, 2004.

[27] M. Devine, E. Baring-Gould, and B. Petrie, "Wind-diesel hybrid options for remote villages in Alaska," in *Proc. AWEA Annual Conference*, Chicago, 2004.

[28] F. Katiraei and C. Abbey, "Diesel plant sizing and performance analysis of a remote wind-diesel microgrid," in *Proc. IEEE Power Engineering Society General Meeting*, Tampa Bay, USA, 24-28 June 2007.

[29] P. Lautier, M. Prévost, and P. Martel, "Off-Grid Diesel Power Plant Efficiency Optimization and Integration of Renewable Energy Sources," in *Proc. IEEE Canada Electrical Power Conference*, Montréal, Canada, Oct. 2007.

[30] M. Elnashar, M. Kazerani, R. El-Shatshat, and M. Salama, "Comparative evaluation of reactive power compensation methods for a stand-alone wind energy conversion system," in *IEEE Power Electronics Specialists Conference, 2008.*, June 2008, pp. 4539–4544.

[31] K. El-Arroudi, G. Joos, I. Kamwa, and D. McGillis, "Intelligent-based approach to islanding detection in distributed generation," *IEEE Trans. Power Del.*, vol. 22, no. 2, pp. 828–835, April 2007.

[32] F. Katiraei, C. Abbey, and R. Bahry, "Analysis of voltage regulation problem for a 25 kv distribution network with distributed generation," in *Proc. IEEE Power Engineering Society General Meeting*, Montréal, Canada, 18-22 June 2006.

[33] J. W. Smith, J. A. Taylor, D. L. Brooks, and R. C. Dugan, "Interconnection studies for wind generation," in *Proc. Rural Electric Power Conference*, May 2004, pp. C3 1–8.

[34] (2008) Demand-response research plan to reflect the needs of the California Independent System Operator (CAISO). [Online]. Available: http://www.energy.ca.gov/publications

[35] J. H. R. Enslin, J. Knijp, C. P. J. Jansen, and P. Bauer, "Integrated approach to network stability and wind energy technology for on-shore and offshore applications," in *Proc. Power Quality*, May 2003, pp. 182–192.

[36] T. Ackermann, *Wind Power in Power Systems.* John Wiley and Sons, 2005.

[37] U. Hassan and D. Sykes, *Wind Energy Conversion Systems.* Englewood Cliffs, NJ: Prentice-Hall, 2001.

[38] F. Galiana, F. Bouffard, J. Arroyo, and J. Restrepo, "Scheduling and pricing of coupled energy and primary, secondary, and tertiary reserves," *Proc. IEEE*, vol. 93, no. 11, pp. 1970–1983, Nov. 2005.

[39] E. Hirst, "Integrating wind output with bulk power operations and wholesale electricity markets," *Wind Energ.*, vol. 5, pp. 19–36, 2002.

[40] G. N. Bathurst, J. Weatherill, and G. Strbac, "Trading wind generation in short term energy markets," *IEEE Trans. Power Syst.*, vol. 17, no. 3, Aug. 2002.

[41] H. Holttinen, "Impact of hourly wind power variations on the system operation in the Nordic countries," *Wind Energ.*, vol. 8, pp. 197–218, 2005.

[42] ——, "Optimal electricity market for wind power," *Energy Policy*, vol. 33, pp. 2052–2063, 2005.

[43] P. Erikson, T. Ackermann, H. Abildgaard, P. Smith, W. Winter, and J. R. Garcia, "System operation with high wind penetration," *IEEE Power Energy Mag.*, pp. 65–74, Nov./Dec. 2005.

[44] J. Matevosyan and L. Soder, "Minimization of imbalance cost trading wind power on the short-term power market," *IEEE Trans. Power Syst.*, vol. 21, no. 3, pp. 1396–1404, Aug. 2006.

[45] C. Luo, H. Banakar, B. Shen, and B. Ooi, "Strategies to smooth wind power fluctuations of wind turbine generator," *IEEE Trans. Energy Convers.*, vol. 22, no. 2, pp. 341–349, June 2007.

[46] H. Banakar, C. Luo, and B. Ooi, "Impacts of wind power minute-to-minute variations on power system operation," *IEEE Trans. Power Syst.*, vol. 23, no. 1, pp. 150–160, Feb. 2008.

[47] R. de Almeida, E. Castronuovo, and J. Lopes, "Optimum generation control in wind parks when carrying out system operator requests," *IEEE Trans. Power Syst.*, vol. 21, no. 2, pp. 718–725, May 2006.

[48] R. de Almeida and J. Lopes, "Participation of doubly fed induction wind generators in system frequency regulation," *IEEE Trans. Power Syst.*, vol. 22, no. 3, pp. 944–950, Aug. 2007.

[49] F. Kanellos and N. Hatziargyriou, "Control of variable speed wind turbines in islanded mode of operation," *IEEE Trans. Energy Convers.*, vol. 23, no. 2, pp. 535–543, June 2008.

[50] C. Abbey and G. Joos, "Supercapacitor energy storage for wind energy applications," *IEEE Trans. Ind. Appl.*, vol. 43, no. 3, pp. 769–776, May-june 2007.

[51] M. Molinas, A. S. Jon, and T. Undeland, "Low voltage ride through of wind farms with cage generators: STATCOM versus SVC," *IEEE Trans. Power Electron.*, vol. 23, no. 3, pp. 1104–1117, May 2008.

[52] J. Ekanayake and N. Jenkins, "Comparison of the response of doubly fed and fixed-speed induction generator wind turbines to changes in network frequency," *IEEE Trans. Energy Convers.*, vol. 19, no. 4, pp. 800–802, Dec. 2004.

[53] J. Morren, S. de Haan, W. Kling, and J. Ferreira, "Wind turbines emulating inertia and supporting primary frequency control," *IEEE Trans. Power Syst.*, vol. 21, no. 1, pp. 433–434, Feb. 2006.

[54] J. McDowall, "High power batteries for utilities - the world's most powerful battery and other developments," in *Proc. IEEE Power Engineering Society General Meeting, 2004*, vol. 2, June 6-10, 2004, pp. 2034–2037.

[55] B. Roberts and J. McDowall, "Commercial successes in power storage," *IEEE Power Energy Mag.*, vol. 3, no. 2, pp. 24–30, March-April 2005.

[56] L. Mears and H. Gotschall, *EPRI-DOE Handbook of Energy Storage for Transmission and Distribution Applications*. EPRI and the U.S. DOE, 2003.

[57] (2008) Electricity storage association website. [Online]. Available: http://electricitystorage.org

[58] T. Lee, "Operating schedule of battery energy storage system in a time-of-use rate industrial user with wind turbine generators: A multipass iteration particle swarm optimization approach," *IEEE Trans. Energy Convers.*, vol. 22, no. 3, pp. 774–782, Sept. 2007.

[59] Bagen and R. Billinton, "Incorporating well-being considerations in generating systems using energy storage," *IEEE Trans. Energy Convers.*, vol. 20, no. 1, March 2005.

[60] X. Wang, D. Mahinda Vilathgamuwa, and S. Choi, "Determination of battery storage capacity in energy buffer for wind farm," *IEEE Trans. Energy Convers.*, vol. 23, no. 3, pp. 868–878, Sept. 2008.

[61] M. Black and G. Strbac, "Value of bulk energy storage for managing wind power fluctuations," *IEEE Trans. Energy Convers.*, vol. 22, no. 1, pp. 197–205, March 2007.

[62] J. Paatero and P. Lund, "Effect of energy storage on variations in wind power," *Wind Energ.*, vol. 8, pp. 421–441, 2005.

[63] J. P. Barton and D. G. Infield, "Energy storage and its use with intermittent renewable energy," *IEEE Trans. Energy Convers.*, vol. 19, no. 2, pp. 441–448, Jun. 2004.

[64] B. Ummels, E. Pelgrum, and W. Kling, "Integration of large-scale wind power and use of energy storage in the netherlands' electricity supply," *IET Renewable Power Generation*, vol. 2, no. 1, pp. 34–46, March 2008.

[65] L. Ran, J. R. Bumby, and P. J. Tavner, "Use of turbine inertia for power smoothing of wind turbines with a DFIG," in *Proc. 11th International Conference on Harmonics and Quality of Power*, vol. 63, Sep. 2004, pp. 106–111.

[66] P. Keung, P. Li, H. Banakar, and B. Ooi, "Kinetic energy of wind-turbine generators for system frequency support," *IEEE Trans. Power Electron.*, vol. 24, no. 1, pp. 279–287, Feb. 2009.

[67] M. Korpas and A. Holen, "Operation planning of hydrogen storage connected to wind power operating in a power market," *IEEE Trans. Energy Convers.*, vol. 21, no. 3, pp. 742–749, 2006.

[68] E. D. Castronuovo and J. A. P. Lopes, "On the optimization of the daily operation of a wind-hydro power plant," *IEEE Trans. Power Syst.*, vol. 19, no. 3, pp. 1599–1606, 2004.

[69] E. Koutroulis, D. Kolokotsa, A. Potirakis, and K. Kalaitzakis, "Methodology for optimal sizing of stand-alone photovoltaic/wind-generator systems using genetic algorithms," *Solar energy*, vol. 80, no. 9, pp. 1072–1088, 2006.

[70] Power Systems Engineering Committee, "Reliability indices for use in bulk power supply adequacy evaluation," *IEEE Trans. Power App. Syst.*, vol. PAS-97, no. 4, pp. 1097–1103, July 1978.

[71] C. Abbey and G. Joos, "A stochastic optimization approach to rating of energy storage systems in wind-diesel isolated grids," *IEEE Trans. Power Syst.*, vol. 24, no. 1, pp. 418–426, Feb. 2009.

[72] C. Abbey, J. Chahwan, and G. Joos, "Energy storage and management in wind turbine generator systems," *EPE-European Power Electronics and Drives Journal*, vol. 17, no. 4, pp. 6–12, 2007.

[73] C. Abbey, K. Strunz, and G. Joos, "A knowledge-based approach for control of two-level energy storage for wind energy systems," *IEEE Trans. Energy Convers.*, vol. 24, no. 2, pp. 539–547, June 2009.

[74] C. Abbey and G. Joos, "Coordination of distributed storage with wind energy in a rural distribution system," in *Proc. IEEE Industry Applications Conference, 2007*, Sept. 23-27, 2007, pp. 1087–1092.

[75] ——, "Short-term energy storage for wind energy applications," in *Proc. IEEE Industry Applications Conference, (IAS '05)*, vol. 3, Hong Kong, 2005, pp. 2035–2042.

[76] ——, "Sizing and power management strategies for battery storage integration into wind-diesel systems," in *Industrial Electronics, 2008. IECON 2008. 34th Annual Conference of IEEE*, 2008, pp. 3376–3381.

[77] R. Hunter and G. Elliot, *Wind-Diesel Systems: A Guide to the Technology and Its Implementation*. Cambridge University Press, 1994.

[78] L. Ning, J. Chow, and A. Desrochers, "Pumped-storage hydro-turbine bidding strategies in a competitive electricity market," *IEEE Trans. Power Syst.*, vol. 19, no. 2, pp. 834–841, May 2004.

[79] M. Korpaas, A. Holen, and R. Hildrum, "Operation and sizing of energy storage for wind power plants in a market system," *Electrical Power Energ. Syst.*, vol. 25, pp. 599–606, 2003.

[80] M. Muselli, G. Notton, and A. Louche, "Design of hybrid-photovoltaic power generator, with optimization of energy management," *Solar Energy*, vol. 65, no. 3, p. 143, 1999.

[81] R. S. Garcia and D. Weisser, "A wind-diesel system with hydrogen storage: Joint optimisation of design and dispatch," *Renewable energy*, vol. 31, no. 14, pp. 2296–2320, 2006.

[82] A. Prasad and E. Natarajan, "Optimization of integrated photovoltaic–wind power generation systems with battery storage," *Energy*, vol. 31, no. 12, pp. 1607–1618, 2006.

[83] E. Ma and S. Shaahid, "Optimal sizing of battery storage for hybrid (wind + diesel) power systems," *Renewable Energy*, vol. 18, no. 1, pp. 77–86, 1999.

[84] M. P. Nowak and R. W., "Stochastic lagragian relaxation applied to power scheduling in a hydro-thermal system under uncertainty," *Annals of Operations Research*, vol. 100, no. 1, pp. 251–272, Dec. 2000.

[85] V. Pappala and I. Erlich, "Management of distributed generation units under stochastic load demands using particle swarm optimization," in *Proc. IEEE Power Engineering Society General Meeting*, Tampa Bay, USA, June 24-28, 2007.

[86] (2008) RETScreen Clean Energy Project Analysis Software. [Online]. Available: www.retscreen.net

[87] (2008) HOMER: The Optimization Model For Distributed Power. [Online]. Available: https://analysis.nrel.gov/homer/

[88] L. Mahon, *Diesel Generator Handbook*. Newnes, 1992.

[89] O. M. I. Nwafor, G. Rice, and A. I. Ogbonna, "Effect of advanced injection timing on the performance of rapeseed oil in diesel engines," *Renewable Energy*, vol. 21, no. 3-4, pp. 433 – 444, 2000.

[90] J. Birge and F. Louveaux, *Introduction to Stochastic Programming*. Springer, 1997.

[91] (2008) GAMS website. [Online]. Available: http://www.gams.com/

[92] (2008) The Kansas Electric Utilities Wind Program, Kansas Electric Utilities Research Program (KERUP), Wind Energy in Kansas. [Online]. Available: http://www.agroplastics.com/kswind

[93] C. Grigg, P. Wong, P. Albrecht *et al.*, "The IEEE Reliability Test System-1996. A report prepared by the Reliability Test System Task Force of the Application of Probability Methods Subcommittee," *IEEE Trans. Power Syst.*, vol. 14, no. 3, pp. 1010–1020, 1999.

[94] (2008) Survey of the small wind (300 W to 300 kW) turbine market in Canada. [Online]. Available: http://www.smallwindenergy.ca

[95] J. Garcia-Gonzalez, R. de la Muela, L. Santos, and A. Gonzalez, "Stochastic joint optimization of wind generation and pumped-storage units in an electricity market," *IEEE Trans. Power Syst.*, vol. 23, no. 2, pp. 460–468, May 2008.

[96] M. Coleman, C. K. Lee, C. Zhu, and W. Hurley, "State-of-charge determination from EMF voltage estimation: Using impedance, terminal voltage, and current for lead-acid and lithium-ion batteries," *IEEE Trans. Ind. Electron.*, vol. 54, no. 5, pp. 2550–2557, Oct. 2007.

[97] I. Moghram and S. Rahman, "Analysis and evaluation of five short-term load forecasting techniques," *IEEE Trans. Power Syst.*, vol. 4, no. 4, pp. 1484–1491, Nov 1989.

[98] G. Giebel, R. Brownsword, and G. Kariniotakis, "The State-of-the-Art in Short-Term Prediction of Wind Power–A Literature Overview," *Risoe National Laboratory*, 2003.

[99] G. Box and G. Jenkins, *Time Series Analysis, Forecasting and Control*. Holden-Day, Incorporated, 1990.

[100] A. Ferreira, J. Pomilio, G. Spiazzi, and L. de Araujo Silva, "Energy management fuzzy logic supervisory for electric vehicle power supplies system," *IEEE Trans. Power Electron.*, vol. 23, no. 1, pp. 107–115, Jan. 2008.

[101] L. Leclercq, A. Davigny, A. Ansel, and B. Robyns, "Grid connected or islanded operation of variable speed wind generators associated with flywheel energy storage systems," in *Proc. EPE-PEMC 2004*, vol. 63, 2003, pp. 271–280.

[102] L. Leclercq, C. Saudemont, B. Robyns, G. Cimuca, and M. Radulescu, "Flywheel energy storage system to improve the integration of wind generators into a grid," *Electromotion*, vol. 10, no. 3–4, 2003.

[103] L. Leclercq, B. Robyns, and J. Grave, "Control based on fuzzy logic of flywheel energy storage system associated with wind and diesel generators," *Math. Comp. Simul.*, vol. 63, pp. 271–280, 2003.

[104] H. Nguyen and E. Walker, *A First Course in Fuzzy Logic*. Chapman & Hall/CRC, 2006.

[105] K. Strunz and E. K. Brock, "Stochastic energy source access management: Infrastructure-integrative modular plant for sustainable hydrogen-electric co-generation," *Journal of Hydrogen Energ.*, vol. 31, pp. 1129–1141, 2006.

[106] T. Ise, M. Kita, and A. Taguchi, "A hybrid energy storage with a SMES and secondary battery," *IEEE Trans. Appl. Supercond.*, vol. 15, no. 2 Part 2, pp. 1915–1918, 2005.

[107] W. Li and G. Joos, "A power electronic interface for a battery supercapacitor hybrid energy storage system for wind applications," June 2008, pp. 1762–1768.

[108] J. Bauman and M. Kazerani, "A comparative study of fuel-cell-battery, fuel-cell-ultracapacitor, and fuel-cell-battery-ultracapacitor vehicles," *IEEE Trans. Veh. Technol.*, vol. 57, no. 2, pp. 760–769, March 2008.

[109] K. Strunz and E. K. Brock, "Hybrid plant of renewable stochastic source and multilevel storage for emission-free deterministic power generation," in *Proc. Quality and Security of Electric Power Delivery Systems, CIGRÉ/IEEE PES International Symposium*, Montréal, Canada, 2003, pp. 214–218.

[110] (2006) Database on wind characterisitics. [Online]. Available: http://www.winddata.com/

[111] M. Chen and G. Rincon-Mora, "Accurate electrical battery model capable of predicting runtime and I-V performance," *IEEE Trans. Energy Convers.*, vol. 21, no. 2, pp. 504–511, June 2006.

[112] L. Gao, S. Liu, and R. Dougal, "Dynamic lithium-ion battery model for system simulation," *IEEE Trans. Compon. Packag. Technol.*, vol. 25, no. 3, pp. 495–505, Sep 2002.

[113] A. Mason, D. Tschirhart, and P. Jain, "New ZVS phase shift modulated full-bridge converter topologies with adaptive energy storage for sofc application," *IEEE Trans. Power Electron.*, vol. 23, no. 1, pp. 332–342, Jan. 2008.

[114] Z. M. Salameh, M. A. Casacca, and W. A. Lynch, "A mathematical model for lead-acid batteries," *IEEE Trans. Energy Convers.*, vol. 7, no. 1, pp. 93–98, 1992.

[115] E. Koutroulis and K. Kalaitzakis, "Novel battery charging regulation system for photovoltaic applications," *IEE Proceedings Electric Power Applications*, vol. 151, no. 2, pp. 191–197, 2004.

[116] P. Rong and M. Pedram, "Battery-aware power management based on markovian decision processes," *IEEE J. Technol. Comput. Aided Design*, vol. 25, no. 7, pp. 1337–1349, July 2006.

[117] F. Blaabjerg, A. Consoli, J. Ferreira, and J. van Wyk, "The future of electronic power processing and conversion," *IEEE Trans. Power Electron.*, vol. 20, no. 3, pp. 715–720, May 2005.

[118] J. Carrasco, L. Franquelo, J. Bialasiewicz, E. Galvan, R. Portillo-Guisado, M. Prats, J. Leon, and N. Moreno-Alfonso, "Power-electronic systems for the grid integration of renewable energy sources: A survey," *IEEE Trans. Ind. Electron.*, vol. 53, no. 4, pp. 1002–1016, June 2006.

[119] S. Inoue and H. Akagi, "A bidirectional dc-dc converter for an energy storage system with galvanic isolation," *IEEE Trans. Power Electron.*, vol. 22, no. 6, pp. 2299–2306, Nov. 2007.

[120] W. Li, G. Joos, and C. Abbey, "A parallel bidirectional dc/dc converter topology for energy storage systems in wind applications," in *Proc. IEEE Industry Applications Conference, 2007*, 23-27 Sept. 2007, pp. 179–185.

[121] N. Stretch and M. Kazerani, "A stand-alone, split-phase current-sourced inverter with novel energy storage," *IEEE Trans. Power Electron.*, vol. 23, no. 6, pp. 2766–2774, Nov. 2008.

[122] (2008) Entegrity Wind Systems Inc. EW15 Specifications. [Online]. Available: http://www.entegritywind.com

[123] (2008) A Report to the Ontario Power Authority (OPA): Wind Generation Data. [Online]. Available: http://www.powerauthority.on.ca/

[124] A. M. A. Brooke, D. Kendrick, *GAMS—A user's guide*, GAMS Development Corporation, 2005.

[125] D. Chattopadhyay, "Application of general algebraic modeling system to power system optimization," *IEEE Trans. Power Syst.*, vol. 14, pp. 15–22, Feb. 1999.

[126] V. Dinavahi, M. Iravani, and R. Bonert, "Real-time digital simulation of power electronic apparatus interfaced with digital controllers," *IEEE Trans. Power Del.*, vol. 16, no. 4, pp. 775–781, Oct 2001.

[127] G. Parma and V. Dinavahi, "Real-time digital hardware simulation of power electronics and drives," *IEEE Trans. Power Del.*, vol. 22, no. 2, pp. 1235–1246, April 2007.

[128] (2008) OPAL-RT Technologies Inc. [Online]. Available: http://www.opal-rt.com

[129] (2008) Semikron MiniSkiip®. [Online]. Available: http://www.semikron.com/